

**MATHEMATICAL MODELS FOR THE EFFECT OF TOTAL
NITROGEN ON MANGROVE FOREST**



**A THESIS SUBMITTED IN PARTIAL FULFILLMENT
OF THE REQUIREMENTS FOR
THE DEGREE OF MASTER OF SCIENCE
(APPLIED MATHEMATICS)
FACULTY OF GRADUATE STUDIES
MAHIDOL UNIVERSITY
2007**

COPYRIGHT OF MAHIDOL UNIVERSITY

Copyright by Mahidol University

Thesis
Entitled

**MATHEMATICAL MODELS FOR THE EFFECT OF TOTAL
NITROGEN ON MANGROVE FOREST**



Wichuta Sae-jie
Miss Wichuta Sae-jie
Candidate

Kornkanok Bunwong
Dr. Kornkanok Bunwong,
Ph.D.(Mathematics)
Major Advisor

Chontita Rattanakul
Asst. Prof. Chontita Rattanakul,
Ph.D.(Mathematics)
Co-Advisor

M.R. Jisnuson Svasti
Prof. M.R. Jisnuson Svasti,
Ph.D.
Dean
Faculty of Graduate Studies

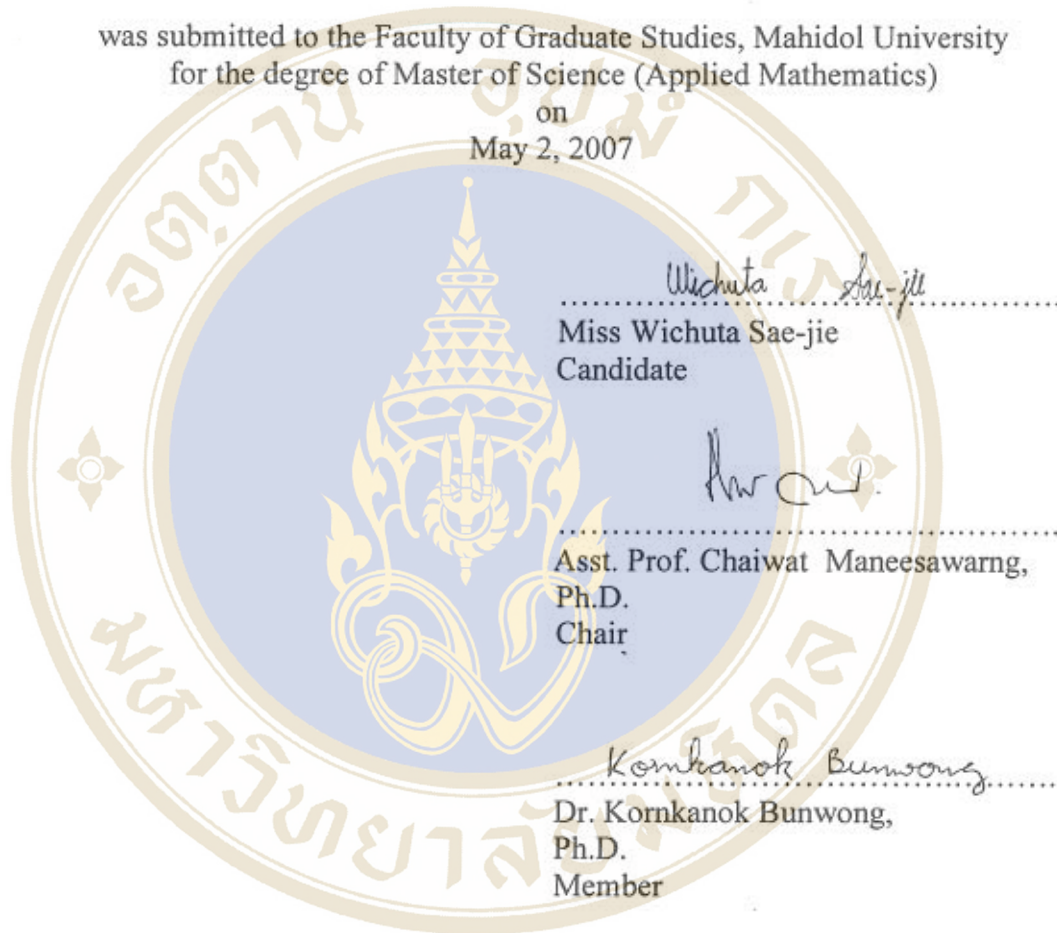
Chaiwat Maneesawarn
Asst. Prof. Chaiwat Maneesawarn,
Ph.D.(Mathematics)
Chair
Master of Science Programme in
Applied Mathematics
Faculty of Science

Thesis
Entitled

**MATHEMATICAL MODELS FOR THE EFFECT OF TOTAL
NITROGEN ON MANGROVE FOREST**

was submitted to the Faculty of Graduate Studies, Mahidol University
for the degree of Master of Science (Applied Mathematics)

on
May 2, 2007



Wichuta Sae-jie
.....
Miss Wichuta Sae-jie
Candidate

Chaiwat Manee
.....
Asst. Prof. Chaiwat Maneesawang,
Ph.D.
Chair

Kornkanok Bunwong
.....
Dr. Kornkanok Bunwong,
Ph.D.
Member

Elvin J. Moore
.....
Dr. Elvin J. Moore,
Ph.D.
Member

Chontita Rattanakul
.....
Asst. Prof. Chontita Rattanakul,
Ph.D.
Member

M.R. Jisnuson Svasti
.....
Prof. M.R. Jisnuson Svasti,
Ph.D.
Dean
Faculty of Graduate Studies
Mahidol University

Amaret Bhumiratana
.....
Prof. Amaret Bhumiratana,
Ph.D.
Dean
Faculty of Science
Mahidol University

ACKNOWLEDGEMENTS

I would like to express my appreciation to my major advisor, Dr. Kornkanok Bunwong, for her advice and constant encouragement that enabled me to complete this thesis successfully. She was never lacking in kindness and support. My appreciation is also expressed to my co-advisor, Asst. Prof. Dr. Chontita Rattanakul and my chair for thesis defence examination, Asst. Prof. Dr. Chaiwat Maneesawarn for their helpful comments, guidance and advice concerning this thesis.

A special gratitude is expressed to Prof. Dr. Kasem Chunkao from Kasetsart University (KU) and Prof. Dr. Sanit Aksornkoe from Thailand Environment Institute, for their expert and excellent guidance and their useful comments about the research. My sincere gratitude also goes to Dr. Elvin Moore from King Mongkut's Institute of Technology North Bangkok, who is serving an external committee member for my thesis defence examination, for his advice and comments as well as his kindness and understanding throughout the study.

I am particularly indebted to the Commission on Higher Education and Prince of Songkla University for granting a scholarship under the Commission on Higher Education Staff Development Project for financial support which has enabled me to undertake this study at Mahidol University.

I would like to thank the staff at Department of Mathematics, Faculty of Science, Mahidol University, and the staff at College of Environment, KU and the King's Royally Initiated Laem Phak Bia Environmental Research and Development Project (LERD) for their help and providing facilities during my study.

I wish to thank my friends for their help and genuine friendship. Also many special thanks are due to all my teachers who gave me much knowledge and whose support and encouragement helped me to finish my education.

Finally, I am greatly thankful to my family, who have brought me up with their power of love, given me great expectations for my life that have kept me going through hard times.

Wichuta Sae-jie

MATHEMATICAL MODELS FOR THE EFFECT OF TOTAL NITROGEN ON MANGROVE FOREST

WICHUTA SAE-JIE 4736852 SCAM/M

M.Sc. (APPLIED MATHEMATICS)

THESIS ADVISORS: KORNGANOK BUNWONG, Ph.D. (MATHEMATICS),
CHONTITA RATTANAKUL, Ph.D. (MATHEMATICS)**ABSTRACT**

Mangrove wetlands are useful for purifying domestic wastewater. In this research, a nonlinear differential equations model is described for the relationship between mangrove biomass concentration and the total nitrogen (TN) concentration in wastewater and in soil solution.

There are four different models. The first model is a two-dimensional model which describes the mangrove biomass concentration and TN concentration in the source (wastewater and soil). The second model is similar to the first model except that the wastewater input is assumed to be a periodic function of time. The third model is a three-dimensional model which separates the TN concentration into wastewater and soil solution components. The fourth model is similar to the third model except that a modified function is used for uptake of TN from the soil into the mangrove biomass.

For each model, the existence of steady-state solutions is determined and the local stability of the steady-state solutions is analyzed. A Liapunov function is also found for the first and third models and used to determine the global stability of the models. It can be found that a periodic solution exists for the second model. A limit cycle and Hopf bifurcation exists in the fourth model.

**KEY WORDS: MATHEMATICAL MODEL / MANGROVE / TOTAL NITROGEN
/ SOIL SOLUTION / LIAPUNOV FUNCTION**

98 pp.

ตัวแบบทางคณิตศาสตร์แสดงผลกระทบของปริมาณไนโตรเจนทั้งหมดต่อป่าชายเลน
(MATHEMATICAL MODELS FOR THE EFFECT OF TOTAL NITROGEN ON
MANGROVE FOREST)

วิชาตา แซ่เจีย 4736852 SCAM/M

วท.ม. (คณิตศาสตร์ประยุกต์)

คณะกรรมการควบคุมวิทยานิพนธ์ : กรกนก บุญวงษ์, Ph.D. (Mathematics), ชนม์ทิศา รัตนกุล,
Ph.D. (Mathematics)

บทคัดย่อ

พื้นที่ชุ่มน้ำชายเลนมีประโยชน์ในการกรองน้ำเสียชุมชน ในการวิจัยนี้ ตัวแบบที่นำมาใช้อธิบายความสัมพันธ์ระหว่างความเข้มข้นของมวลชีวภาพและความเข้มข้นของไนโตรเจนทั้งหมดในน้ำเสียรวมทั้งในสารละลายดิน เป็นสมการอนุพันธ์ไม่เชิงเส้น

ตัวแบบทางคณิตศาสตร์ที่สร้างขึ้นมาเพื่อพิจารณามีทั้งหมด 4 แบบด้วยกัน แบบแรกจะกล่าวถึงสมการในระบบ 2 มิติ ที่ใช้อธิบายความสัมพันธ์ ระหว่างความเข้มข้นของมวลชีวภาพและความเข้มข้นของไนโตรเจนทั้งหมดทั้งในน้ำและในสารละลายดิน แบบที่สองคล้ายกับแบบแรกยกเว้นอัตราการนำน้ำเสียเข้าสู่ระบบเปลี่ยนเป็นการนำเข้าไปในลักษณะของฟังก์ชันคาบ แบบที่สามเกิดจากการพัฒนาระบบแรกโดยแบ่งแหล่งของไนโตรเจนทั้งหมดเป็น 2 ส่วนคือในน้ำและในสารละลายดิน แบบสุดท้ายคล้ายกับแบบที่สามยกเว้นฟังก์ชันการดูดซับความเข้มข้นไนโตรเจนทั้งหมดของมวลชีวภาพ

ในแต่ละตัวแบบทางคณิตศาสตร์ได้มีการพิจารณาหาผลเฉลยที่สมมูลและการเสถียรเฉพาะที่ของผลเฉลยที่สมมูล ฟังก์ชันไลปูนอฟได้ถูกนำมาใช้ในตัวแบบทางคณิตศาสตร์ที่หนึ่งและสามเพื่อใช้ศึกษาเสถียรภาพของระบบในวงกว้าง ผลการศึกษาสามารถสรุปได้ว่า ตัวแบบทางคณิตศาสตร์ที่สองให้ผลเฉลยที่มีลักษณะเป็นคาบ ลิมิตไซเคิลและมีไบเฟอเคชันของฮอฟเกิดขึ้นที่ตัวแบบทางคณิตศาสตร์ที่สี่

98 หน้า

CONTENTS

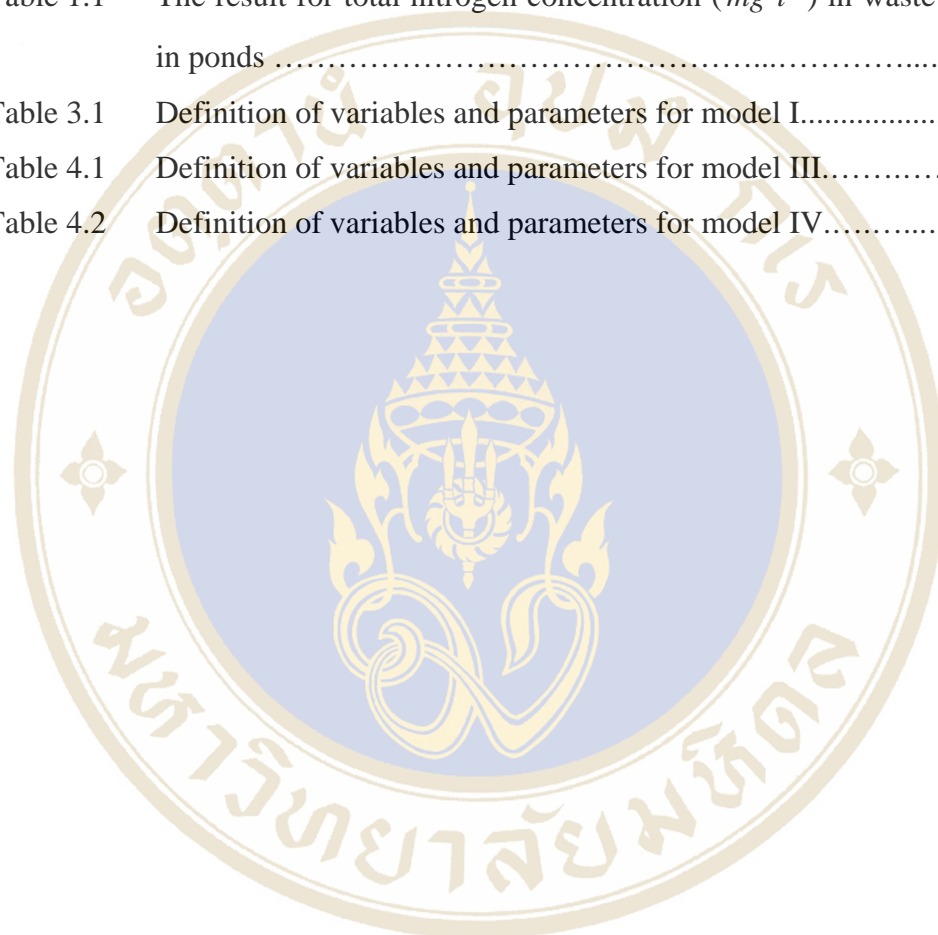
	Page
ACKNOWLEDGEMENTS	iii
ABSTRACT	iv
LIST OF TABLES	viii
LIST OF FIGURES	ix
CHAPTER	
1 INTRODUCTION	1
1.1 Biological Concepts.....	1
1.1.1 Mangrove Forest	2
1.1.2 Plant Nutrition	5
1.1.3 The Nitrogen Cycle	5
1.1.4 The Nitrogen Cycle in Mangrove Mud.....	6
1.1.5 Wastewater and Nitrogen.....	7
1.1.6 Human Impact on the Nitrogen Cycle.....	8
1.2 Literature Review.....	8
1.2.1 Research Based on Experiment.....	8
1.2.2 Research Based on Analysis of Mathematical Models.....	10
1.3 Objectives.....	12
1.4 Expected Benefits.....	12
1.5 Organization of the Study.....	13
2 THEORETICAL BACKGROUND	14
2.1 Introduction to Systems of ODEs.....	14
2.2 Liapunov Function.....	25
2.3 Local and Global Maxima and Minima	25
2.4 Hopf Bifurcation Theorem.....	27

CONTENTS (continued)

	Page
3 MODEL ANALYSIS I	30
3.1 Two-Dimensional Model: Constant Input.....	32
3.1.1 Local Stability Analysis.....	35
3.1.2 Global Stability Analysis.....	42
3.2 Two-Dimensional Model: Periodic Input.....	48
4 MODEL ANALYSIS II	53
4.1 Three-Dimensional Model: Linear Uptake Function.....	53
4.1.1 Local Stability Analysis.....	57
4.1.2 Global Stability Analysis.....	67
4.2 Three-Dimensional Model: Monod Uptake Function (Limiting Growth).....	71
4.2.1 Local Stability Analysis.....	74
5 CONCLUSIONS AND DISCUSSION	85
REFERENCES	90
APPENDIX	93
BIOGRAPHY	98

LIST OF TABLES

	Page
Table 1.1 The result for total nitrogen concentration ($mg\ l^{-1}$) in wastewater in ponds	9
Table 3.1 Definition of variables and parameters for model I.....	32
Table 4.1 Definition of variables and parameters for model III.....	53
Table 4.2 Definition of variables and parameters for model IV.....	72



LIST OF FIGURES

	Page
Figure 1.1 <i>R. mucronata</i> trees and their stilt roots [4].....	2
Figure 1.2 <i>A. marina</i> tree has the horizontal root system which is extensive and gives rise to a forest of vertical pencil-like pneumatophores [4].....	3
Figure 1.3 Plant zonation [8].....	5
Figure 1.4 Nitrogen cycle [12].....	6
Figure 2.1 Asymptotically stable two-tangent node.....	18
Figure 2.2 Unstable two-tangent node	18
Figure 2.3 Saddle node	18
Figure 2.4 Stellar node (a) Stable (b) Unstable.....	19
Figure 2.5 One-tangent node (a) Stable (b) Unstable	19
Figure 2.6 Spiral node (a) Unstable (b) Stable.....	20
Figure 2.7 Stable limit cycle	21
Figure 2.8 Unstable limit cycle	22
Figure 2.9 Semi-stable limit cycle	22
Figure 2.10 Examples of hyperbolic equilibria in R^3 [24].....	24
Figure 2.11 Examples of non-hyperbolic equilibria in R^2 [24].....	24
Figure 2.12 Supercritical bifurcation: as γ increases from small values through γ^* and up to $\gamma = c$, the steady state changes from a stable node to an unstable node. A stable limit cycle appears at γ^* , and its diameter grows as indicated by the parabolic envelope.....	28
Figure 2.13 Subcritical bifurcation: as γ decreases from values above γ^* and down to $\gamma = d$, the steady state changes from an unstable node to a stable node. An unstable limit cycle appears at γ^* , and its diameter grows as indicated by the parabolic envelope.....	28

LIST OF FIGURES (continued)

		Page
Figure 3.1	Nitrogen transformations in wetlands	31
Figure 3.2	A pond for the experiment of constructed wetland.....	31
Figure 3.3	Flow chart for the transformation of total nitrogen for model I.....	32
Figure 3.4	Numerical solution of the dimensionless model equations (3.2a,b) for mangrove biomass and TN concentration for parameters $m = 0.05, \sigma = 0.5, \phi = 1$	39
Figure 3.5	Phase plane plot of the dimensionless model equations (3.2a,b) for the solution for mangrove biomass and the TN concentration for parameters $m = 0.05, \sigma = 0.5, \phi = 1$	39
Figure 3.6	Numerical solution of the dimensionless model equations (3.2a,b) for mangrove biomass and TN concentration for parameters $m = 0.6, \sigma = 0.5, \phi = 1$	40
Figure 3.7	Phase plane plot of the dimensionless model equations (3.2a,b) for the solution for mangrove biomass and the TN concentration for parameters $m = 0.6, \sigma = 0.5, \phi = 1$	40
Figure 3.8	Numerical solution of the dimensionless model equations (3.2a,b) for mangrove biomass and TN concentration for parameters $m = 0.05, \sigma = 0.5, \phi = 0.001$	41
Figure 3.9	Phase plane plot of the dimensionless model equations (3.2a,b) for the solution for mangrove biomass and the TN concentration for parameters $m = 0.05, \sigma = 0.5, \phi = 0.001$	41
Figure 3.10	Graph of $f(x) = x$ and $f(x) = \ln(x+1)$	45
Figure 3.11	The sketch of the curve $\dot{V}(x, y)$	47
Figure 3.12	Numerical solution of the dimensionless model equations (3.32a,b) for mangrove biomass and TN concentration for the parameters $\frac{\beta Q}{2} = 10, \sigma = \phi = 1$	51

LIST OF FIGURES (continued)

	Page
Figure 3.13 Phase plane plot of the solution of the dimensionless model equations (3.32a,b) for mangrove biomass and the TN for parameters are $\frac{\beta Q}{2} = 10, \sigma = \phi = 1$	51
Figure 3.14 Numerical solution of the dimensionless model equations (3.32a,b) for mangrove biomass and TN concentration for the parameters $\frac{\beta Q}{2} = 10, \sigma = \phi = 1$	52
Figure 3.15 Phase plane plot of the solution of the dimensionless model equations (3.32a,b) for mangrove biomass and the TN for parameters are $\frac{\beta Q}{2} = 10, \sigma = \phi = 1$	52
Figure 4.1 The flow chart for the transformation of total nitrogen for model III.....	54
Figure 4.2 Numerical solution of the dimensionless model equations (4.2a-c) for parameters $m = 0.05, \sigma = 1, \gamma = 0.5, \alpha = 0.5, \phi = 2$	61
Figure 4.3 Phase plane plot of the dimensionless model equations (4.2a-c) for TN concentration in wastewater and concentration of mangrove biomass for parameters $m = 0.05, \sigma = 1, \gamma = 0.5, \alpha = 0.5, \phi = 2$	62
Figure 4.4 Phase plane plot of the dimensionless model equations (4.2a-c) for TN concentration in soil solution and concentration of mangrove biomass for parameters $m = 0.05, \sigma = 1, \gamma = 0.5, \alpha = 0.5, \phi = 2$	62
Figure 4.5 Numerical solution of the dimensionless model equations (4.2a-c) for mangrove biomass concentration, TN concentration in wastewater and soil solution for parameters $m = 5, \sigma = 1, \gamma = 0.5, \alpha = 0.5, \phi = 0.1$	63

LIST OF FIGURES (continued)

	Page
Figure 4.6 Phase plane plot of the dimensionless model equations (4.2a-c) for TN concentration in wastewater and concentration of mangrove biomass for parameters $m=5$, $\sigma=1$, $\gamma=0.5$, $\alpha=0.5$, $\phi=0.1$	64
Figure 4.7 Phase plane plot of the dimensionless model equations (4.2a-c) for TN concentration in soil solution and concentration of mangrove biomass for parameters $m=5$, $\sigma=1$, $\gamma=0.5$, $\alpha=0.5$, $\phi=0.1$	64
Figure 4.8 Numerical solution of the dimensionless model equations (4.2a-c) for mangrove biomass concentration, TN concentration in wastewater and soil solution for parameters $m=0.05$, $\sigma=0.5$, $\gamma=0.4$, $\alpha=0.1$, $\phi=0.001$	65
Figure 4.9 Phase plane plot of the dimensionless model equations (4.2a-c) for TN concentration in wastewater and concentration of mangrove biomass for parameters $m=0.05$, $\sigma=0.5$, $\gamma=0.4$, $\alpha=0.1$, $\phi=0.001$	66
Figure 4.10 Phase plane plot of the dimensionless model equations (4.2a-c) for TN concentration in soil solution and concentration of mangrove biomass for parameters $m=0.05$, $\sigma=0.5$, $\gamma=0.4$, $\alpha=0.1$, $\phi=0.001$	66
Figure 4.11 Plot of $g(z)$	69
Figure 4.12 $\dot{V}(x, y, z)$ is negative for example when $\alpha=0.1$, $\gamma=0.4$, $\sigma=0.5$, $m=0.05$	70
Figure 4.13 Numerical solution of the dimensionless model equations (4.33a-c) for parameters $\beta=2$, $\sigma=1$, $E=1$, $Q=1$, $\Omega=3$, $\gamma=1$, $\phi=0.1$, $C=0.8$, $D=1$	79

LIST OF FIGURES (continued)

	Page
Figure 4.14 Phase plane plot for the solution of the dimensionless model equations (4.33a-c) for parameter $\beta = 2, \sigma = 1, E = 1, Q = 1, \Omega = 3, \gamma = 1, \phi = 0.1, C = 0.8, D = 1$	80
Figure 4.15 Numerical solution of the dimensionless model equations (4.33a-c) in three-dimensions for parameter $\beta = 2, \sigma = 1, E = 1, Q = 1, \Omega = 3, \gamma = 1, \phi = 0.1, C = 0.8, D = 1$	80
Figure 4.16 Numerical solution of the dimensionless model equations (4.33a-c) for parameters $\beta = 2, \sigma = 1, E = 1, Q = 1, \Omega = 3, \gamma = 1, \phi = 0.1, C = 0.076923077, D = 1$	81
Figure 4.17 Phase plane plot for the solution of the dimensionless model equations (4.33a-c) for parameter are $\beta = 2, \sigma = 1, E = 1, Q = 1, \Omega = 3, \gamma = 1, \phi = 0.1, C = 0.076923077, D = 1$	82
Figure 4.18 Numerical solution of the dimensionless model equations (4.33a-c) in three-dimensions for parameter are $\beta = 2, \sigma = 1, E = 1, Q = 1, \Omega = 3, \gamma = 1, \phi = 0.1, C = 0.076923077, D = 1$	82
Figure 4.19 Numerical solution of the dimensionless model equations (4.33a-c) for parameters are $\beta = 2, \sigma = 1, E = 1, Q = 1, \Omega = 3, \gamma = 1, \phi = 0.1, C = 0.001, D = 1$	83
Figure 4.20 Phase plane plot of the dimensionless model equations (4.33a-c) for parameters are $\beta = 2, \sigma = 1, E = 1, Q = 1, \Omega = 3, \gamma = 1, \phi = 0.1, C = 0.001, D = 1$	84
Figure 4.21 Numerical solution of the dimensionless model equations (4.33a-c) in three-dimensions for parameter are $\beta = 2, \sigma = 1, E = 1, Q = 1, \Omega = 3, \gamma = 1, \phi = 0.1, C = 0.001, D = 1$	84

CHAPTER I

INTRODUCTION

1.1 Biological Concepts

The ecosystem has been changed mainly because of population increase. One of the most important factors for human's daily life is water. In the big cities, each person consumes water approximately 200–400 *l/day* [1]. Domestic wastewater is the used water that comes from household, living place, market, hotel etc. It is caused by human activities such as bathing, washing clothes and dishes, and preparing food. In developing countries, 90% of sewage are discharged without any treatment into ground water [2]. Therefore, water pollution has become a hot issue nowadays.

The nitrogen level in domestic wastewater is usually in the range from 20 to 85 *mg/l* [1]. If you think this limit should be acceptable, please consider the following facts. Firstly, 0.01 *mg/l* of ammonia can harm aquatic life and fish. Secondly, the effect of nitrogen can decrease the dissolved oxygen (*DO*) in water during the nitrification reaction. Thirdly, excess nitrogen loading causes eutrophication which is the phenomenon that excess nutrients stimulate excessive plant growth including algae. Consequently, dissolved oxygen in water is reduced and causes living organisms to die. Then water becomes smelly. Finally, infants who suffer from blue baby syndrome have shortness of breath and blue skin because of oxygen shortage. Normally, hemoglobin in blood has the abilities to carry oxygen (O_2) and contain iron. However, when infant receives excess nitrate compound, his body will change the nitrate compound to nitrite (NO_2^-). This substance is the main cause that reduces the hemoglobins ability to capture O_2 by catching hemoglobin itself and becoming methemoglobin, instead.

In Thailand, Phetchaburi has many dessert manufacturers releasing wastewater around 13,500 m^3/day . It contains many forms of nitrogen; i.e. inorganic

(ammonium, nitrite, nitrate), and organic nitrogen. Therefore, nitrogen in wastewater is one of indicators predicting water pollution. If wastewater contains too much nitrogen, this water becomes smelly and cannot be used for consumption. Fortunately, there are four varieties of wastewater treatment systems (i.e. lagoon treatment, grass filtration, constructed wetland, and mangrove filtration) at the King's Royally Initiated Laem Phak Bia Environmental Research and Development Project (LERD). His Majesty the King's idea is to let nature heal nature. At the LERD, native soil with minimum concrete and steel is used while no engine is required. Only large area and air flow are needed.

1.1.1 Mangrove Forest

Mangrove is from Portuguese word "mangue". Mangrove forest or intertidal forest is evergreen forest. It grows on coastal mud flats in low latitude areas around the globe such as India, Southeast Asia, China, Japan, Philippines, Australia, and Papua New Guinea [3]. Its residence is in the areas between land and sea where freshwater and seawater is mixed (i.e. muddy habitat). The soil structure is more like liquid, very fine, and salty. A special characteristic of this forest type is the root system which differs from the root system of normal terrestrial trees. Mangrove has modified roots that are suitable to grow in coastal regions. Many species have developed prop roots, which are more or less a root system splitting off from the trunk above ground rather than below ground.



Figure 1.1 *R. mucronata* trees and their stilt roots [4].

Respiratory roots or aerating roots of mangrove can absorb oxygen directly from atmosphere for metabolism process because underground has inadequate oxygen. For example, the special root of *R. mucronata* is known as the stilt root (see Figure 1.1)

while the special root of *A. marina* is called pneumatophores. This kind of pencil-like root is suitable for the inland area farther away from the shore where the water is not deep (see Figure 1.2).

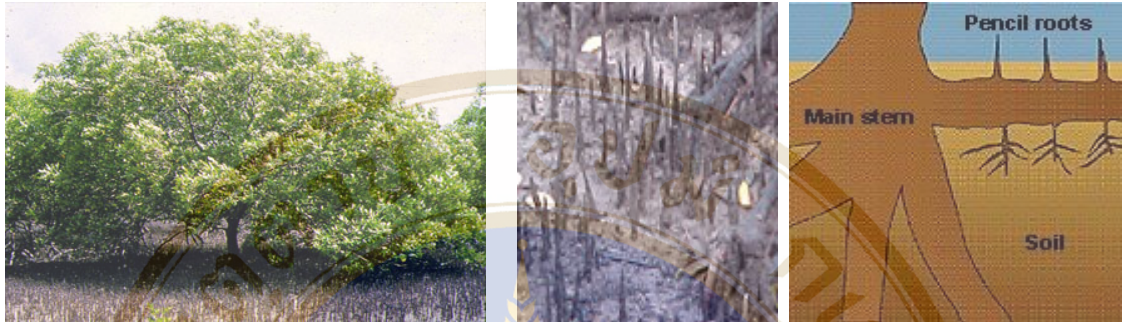


Figure 1.2 *A. marina* tree has the horizontal root system which is extensive and gives rise to a forest of vertical pencil-like pneumatophores [4].

Special root structure is also good at filtration. Therefore, the root can trap fine sediment from the flow of river and tide. This sediment is the suitable home for various bacteria, algae, protozoa, and invertebrates (such as marine worms). Not only are nutrients and heavy metals from wastewaters accumulated in this area, but this enlarged area can also invade the sea in contrast to the area without mangroves. As a conclusion, the important functions of mangrove are to protect the shore from erosion by wind and wave, and to provide home for a variety of organisms including many juvenile species of fish and prawns. Thus mangrove ecosystems have a high biodiversity of plants and animals, thus providing indirect benefit to humans such as fishing, digging crab, etc. Obviously, people who live in this area always gain the advantage. At the present time, the varieties of human activities such as deforestation, shrimp farm, charcoal, and building destroy our intertidal ecosystem.

Factors affecting the distribution of mangroves [5] are

1. **Tide:** the zonation of mangroves is in categories according to tide because each biological species is influenced by the height and the period of tide. Some plants can survive a long time of high tide inundation but some can stand only a short time of inundation. *R. mucronata* is usually found on seashore or in the most inundated areas while *A. marina* lives further inland (see Figure 1.3).

2. **Salinity:** some species have a special salt balance process. The physiology of their leaf has salt glands on the leaf. All *A. marina* can excrete excess salt from its leaves through special salt glands. That is why their surface looks white and tastes salty.

3. **Topography:** mangroves settle in shallow water and calm areas such as gulfs, estuaries behind capes, along coast, etc. Accumulated sedimentation or muddy habitat is an appropriate place.

4. **Climate:** mangroves need strong sunlight. The light intensity required is about 3,000-3,800 *kilocalory/m²/day* [6]. They do not like shadow. Some seedlings die when sunlight is not enough. Normally mangrove forest needs annual rainfall about 1500-3000 *mm.* in 8-10 rainy months. Temperature required is around 37°C. Wind has direct and indirect effect on the mangrove forests. Wind not only increases the strength of waves but also decreases air and water temperatures. Wind also causes erosion along the coast and effects the growth and composition of mangroves. If the wind blows in the same direction as the spring tide, the combined effect brings saline water further inland.

5. **Current:** strong waves not only causes erosion but also builds up sediment, and creates new areas of land over long periods of time. Waves also affect the seedling growth. When they are too young, entire saplings can be wiped out by strong waves. On the other hand, waves spread seeds and increase the area covered by species.

6. **Dissolved Oxygen (DO):** fauna and flora use the oxygen in the water for respiration while bacteria use it for leaf decomposition. The number of plants and animals is limited by the value of *DO*. The value is usually about 3.8-7.8 *ml./litre*. The value of *DO* varies according to daytime and nighttime, season, and density of living creatures.

7. **Soil:** the sediment from the flow of river and tide accumulates around the mangrove forest because its roots slow down the water flow. This sedimentation can extend the area of ground towards the sea.

8. **Nutrient:** except for nitrogen and phosphorus there are enough necessary nutrients in the mangrove forest in both organic and inorganic forms [7]. Thus nitrogen and phosphorus become the limiting factors of mangrove growth.

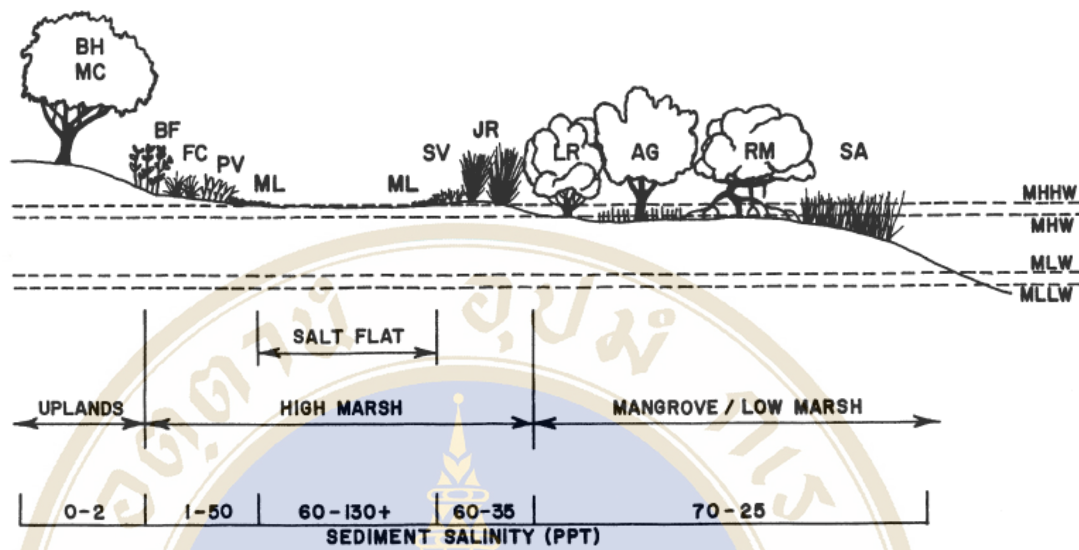


Figure 1.3 Plant zonation [8].

1.1.2 Plant Nutrition

The chemical elements a plant uses to synthesize its own molecules are called plant nutrients. An element is considered an essential plant nutrient if a plant must obtain it to complete its life cycle. There are 17 elements that are essential to all plants and a few others that are essential to certain types of plants. Of the 17 essential elements, 9 including nitrogen are called macronutrients because plants require relatively large amounts of them. Elements that plants need in extremely small amounts are called micronutrients [9].

Nitrogen is one of the principal nutrients, besides phosphorous and potassium. Nitrogen is important for all living things because it is a component of all nucleic acids and proteins. Normally each living cell contains around 16% of biomass of nitrogen [10]. If a plant obtains enough nitrogen, its leave will look green. Otherwise, its growth will be stunted, and it will have slow growth, yellow leaves, and small size flowers and fruits. If a plant consumes too much nitrogen, it can turn yellow [11].

1.1.3 The Nitrogen Cycle

Earth's atmosphere is almost 80% nitrogen gas (N_2). Nitrogen can also be found in soil and the ocean. It is the most limiting nutrient for plant growth. This problem

occurs because most plants can only consume nitrogen in two forms. One form is ammonium ion (NH_4^+) and another form is nitrate ion (NO_3^-) [11]. Most plants need both nitrate and ammonium from the soil solution while animals also need ammonium for metabolism, growth, and reproduction. However, a large concentration of ammonium can be toxic to plant and animal (see Figure 1.4).

In the ecosystem, nitrogen is stored in living and dead organic matter. This organic matter can be converted into inorganic forms and then it settles into the soil. In water and soil, dissolved nitrogen is a part of a biochemical reaction. Such reactions are nitrification, denitrification, and ammonia volatilization. The most important reactions are nitrification and denitrification.

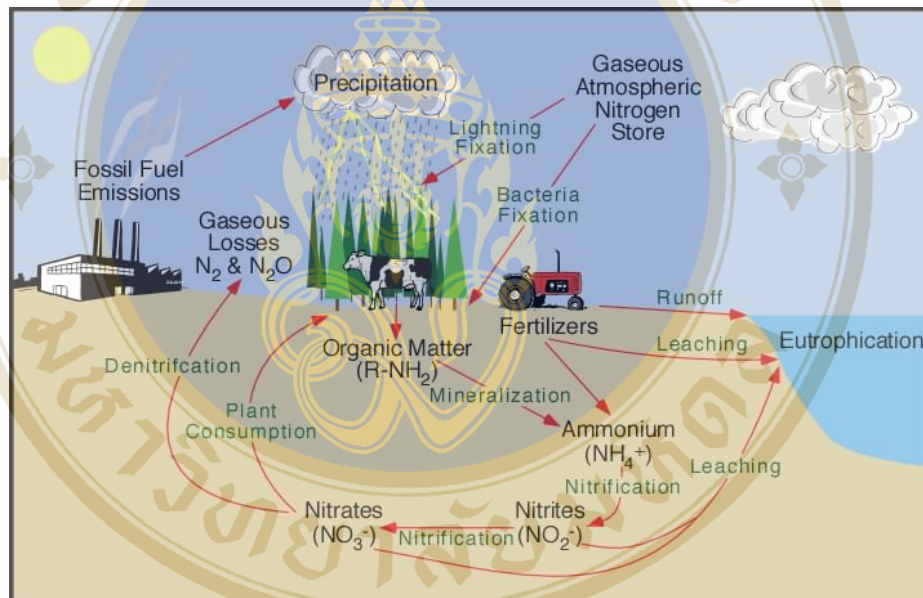


Figure 1.4 Nitrogen cycle [12].

In soil, “nitrogen fixer” bacteria can convert atmospheric N_2 to ammonium while nitrifying bacteria can convert ammonium to nitrates. Ammonium and nitrate are the soil minerals which the roots of plants absorb as a nitrogen source. Finally, the denitrifying bacteria convert soil nitrates to atmospheric N_2 [9].

1.1.4 The Nitrogen Cycle in Mangrove Mud

The availability of nitrogen in mangrove ecosystems depends on a complex pattern of bacterial activity within the anoxic (oxygen-free) mangrove mud, the thin oxic (oxygenated) zone at the visible surface of the mud, and the inner oxic linings of

animal burrows. Bacteria transforms nitrogen in organic material into free ammonium, nitrate, or gaseous nitrogen through three processes: ammonification, nitrification, and denitrification. These processes are closely linked with each other wherever oxic sediment meets anoxic sediment: such conditions occur at some depth below the visible surface of the mangrove mud and around the burrows of mud crabs [13].

The ammonification process is in the oxic and anoxic zone. Particulate organic material (i.e. dead plant and animal matter) is decomposed by bacteria. During the decomposition, nitrogen in the organic material is transformed to ammonium (NH_4^+).

Ammonium in the anoxic sediment is transported to the oxic zone and into the free-flowing burrow water by diffusion. Diffusion is the movement of suspended or dissolved particles from an area of higher concentration to an area of lower concentration as the result of random movement of individual particles. The bulk of ammonium is oxidized by aerobic bacteria, first into nitrite (NO_2^-), and then into nitrate ions (NO_3^-). This process is called nitrification.

Nitrate then diffuses from the oxic layer, back into the anoxic layer. Here its fate depends on circumstances. Nitrate may be taken up by bacteria and mangrove roots and become unavailable. Or it may be reduced by bacteria in anoxic zone of the sediment into either gaseous nitrogen (N_2) or nitrous oxide (N_2O). This process is called denitrification.

The pneumatophore (aerial root) surface of black mangroves is completely colonized by microorganisms, principally N_2 -fixing and non- N_2 -fixing bacteria, diatoms, green microalgae, cyanobacteria, and fungi.

1.1.5 Wastewater and Nitrogen

Wastewater may also contain high level of nutrient (nitrogen and phosphorus) that in certain forms may be toxic to fish and invertebrates at very low concentrations (e.g. ammonia) or that can create nuisance conditions in the receiving environment (e.g. weed or algal growth). Weeds and algae may seem to be an aesthetic issue, but algae can produce toxins, and their death and consumption by bacteria (decay) can deplete oxygen in the water and suffocate fish and other aquatic life [14]. Usually gaseous nitrogen and ammonia can be found in wastewater.

1.1.6 Human Impact on the Nitrogen Cycle

Sewage treatment facilities typically empty large amounts of dissolved inorganic nitrogen compounds into rivers and streams. Farmers routinely apply large amounts of inorganic nitrogen fertilizers, mainly ammonium and nitrate, to cropland. Plants take up some of the nitrogen compounds, and soil bacteria converts some into atmospheric nitrogen (N_2). However, chemical fertilizers usually exceed the soil's natural recycling capacity. The excess nitrogen compounds often enter streams, lakes, and groundwater. In lakes and streams, these nitrogen compounds continue to fertilize, causing heavy growth of algae. Groundwater pollution by nitrogen fertilizers is also a serious problem in many agricultural areas. In the human digestive tract, nitrate in drinking water is converted to nitrites, which can be toxic [9].

1.2 Literature Review

1.2.1 Research Based on Experiment

In 2000, Piyawan Saymanopun [1] studied the growth of seedlings of *R. mucronata* and *A. marina* in municipal sewage treatment with different mangrove soil textures. Her experimental series were set in constructed wetland at the LERD. Twenty-four round cement ponds were placed in order to grow the seedlings of 6-month-old *R. mucronata* and 3-month-old *A. marina*. These two species are dominant in Phetchaburi district. The inner diameter of the cement ponds was 140 cm. Their height was 50 cm. The area was 15,400 cm². The soil level was around 25 cm high. A PVC pipe having holes and covered with cloth was in the middle of each pond in order to protect things passing to the pipe. There were twenty-four seedlings in each pond with dimension 20×20 cm. that had been watered with seawater for 2 months before the experiments started.

At the beginning, wastewater was released into the ponds and kept at its level for 7 days. Then the ponds were drained and kept dry for 2 days before reconditioning by seawater. She repeated the experiment every month for 6 months.

She kept monitoring the total nitrogen concentration in water collected from the PVC pipes on every first and seventh day of each experiment. The collected data are shown in Table 1.1.

Table 1.1 The result for total nitrogen concentration ($mg\ l^{-1}$) in wastewater in ponds.

Month	First day	Seventh day
February	5.60 ± 0.79	1.40 ± 0.40
March	10.36 ± 1.98	1.12 ± 0.00
April	8.12 ± 0.40	1.40 ± 0.40
May	8.12 ± 0.40	4.20 ± 0.40
June	10.92 ± 0.40	3.36 ± 0.79
July	10.92 ± 0.40	6.16 ± 0.00

Table 1.1 show that the concentration level of the total nitrogen in domestic water released and kept in the ponds decreased after seven days.

She also observed that the concentration of the total nitrogen in soil increased from $1.15 - 2.02\ mg\ g^{-1}$ measured before all experiments started to $1.26 - 2.05\ mg\ g^{-1}$ measured after all experiments finish. The biomass also increased around $24.26\ g/tree$. She showed that the rate of nitrogen removal significantly increased by the mangroves.

The biomass can be estimated by the relation of height, diameter of tree and dry mass of some part of the tree in form of allometric relation

$$W = a(D^2H)^b \quad (1.1)$$

where

W is dry weight of leaf, branch or all dry weight (g),

D is diameter at breast height ($cm.$),

H is tree height ($cm.$),

a, b are constant.

In 2003, M.A. Senzia, D.A. Mashauri, and A.W. Mayo [2] studied the suitability of constructed wetlands and waste stabilization ponds for wastewater treatment: to remove and transform. They found that plant growth in the constructed wetlands

related with nutrients. The plants in constructed wetland grow a little faster due to high content of $NH_3 - N$.

1.2.2 Research Based on Analysis of Mathematical Models

In 1979, Gary W. Harrison [15] analyzed the global stability of predator-prey interactions using the following model:

$$\dot{H} = a(H) - f(H)b(P) \quad (1.2a)$$

$$\dot{P} = n(H)g(P) + c(P) \quad (1.2b)$$

where H and P are prey and predator density, respectively. The term $a(H)$ was the intrinsic growth rate of the prey at density H due to all factors except predation, and the term $c(P)$ was the intrinsic rate of increase (or decrease) of the predator.

Assuming $[n(H) - n(H^*)][H - H^*] > 0$ for $H \neq H^*$ and

$$[b(P) - b(P^*)][P - P^*] > 0 \text{ for } P \neq P^*,$$

he constructed a Liapunov function as follows

$$V(H, P) = \int_{H^*}^H \frac{n(x) - n(H^*)}{f(x)} dx + \int_{P^*}^P \frac{b(x) - b(P^*)}{g(x)} dx. \quad (1.3)$$

In 2002, Thomas C. Gard [16] analyzed the following model of a chemostat:

$$\frac{dS}{dt} = (S^{(0)} - S)D - \left(\frac{1}{\gamma}\right) \frac{mSA}{a + S}, \quad (1.4a)$$

$$\frac{dA}{dt} = A \left(\frac{mS}{a + S} - D \right), \quad (1.4b)$$

where S is the density of a substrate and A is the density of a microorganism feeding on the substrate. $S^{(0)}$ is the initial substrate concentration. The parameter D is the common washout rate, γ is a yield constant designating conversion from nutrient to organism and $\frac{mS}{a + S}$ is a Monod (Michaelis-Menten) uptake response function of the substrate by the organism. Gard states that this is the simplest growth functional response model which incorporates the realistic feature of saturation.

Gard analyzed the global stability of his chemostat model using a Liapunov

$$\text{function given by: } V(S, A) = \frac{1}{2}(1 - S - A)^2 + \alpha(a, m)(A - A^* \ln(A/A^*)) \quad (1.5)$$

In 2005, Xuncheng Huang and Lemin Zhu [17] presented a three dimensional chemostat with two microorganisms with quadratic yields for both. They discussed the equilibrium points, the stability of the equilibrium points, the existence of limit cycles, the Hopf bifurcation, and the positive invariant set for their system.

The model was represented by

$$\frac{dS}{dt} = (S_0 - S)Q - \frac{1}{\delta_1} \left(\frac{m_1 S}{k_1 + S} - L \right) x - \frac{1}{\delta_2} \frac{m_2 S}{k_2 + S} y \quad (1.6a)$$

$$\frac{dx}{dt} = x \left(\frac{m_1 S}{k_1 + S} - L - Q \right) \quad (1.6b)$$

$$\frac{dy}{dt} = y \left(\frac{m_2 S}{k_2 + S} - Q \right) \quad (1.6c)$$

where $S(t)$ is the concentration of nutrient in the vessel, $x(t)$ and $y(t)$ are the concentrations of the two organisms, S_0 was the input concentration of nutrient, Q was the washout rate, m_i , the maximal growth rates, k_i , the Michaelis-Menten constants, and $\delta_i, i=1,2$, the yield coefficients. They investigated the system (1.6a-c) with $\delta_1 = A + BS^2, \delta_2 = C + DS^2$, which means that the production of the microbial biomass is more sensitive to the concentration of the nutrient in the vessel than for linear yield coefficients $\delta_1 = A_1 + S, \delta_2 = A_2 + S$.

Huang and Zhu also published a paper [18] in the same year in which the two yield terms are $\delta_1 = A + BS^3$ and $\delta_2 = C + DS^4$.

In 2006, Ling Bai and Ke Wang [19] studied a stage-structured model for a polluted environment. They discussed the existence of equilibrium points, the local stability of the equilibrium points through computing the Jacobian matrices corresponding to each equilibrium and the global stability of the equilibrium points through the Liapunov function. The model contained two stages of population (immature and mature), pollutants in the environment, and pollutants in the body of the immature population.

$$\frac{dN_1}{dt} = \alpha N_2 - \beta N_1 - rN_1 - \eta N_1^2 - r_{11} N_1 U \quad (1.7a)$$

$$\frac{dN_2}{dt} = \beta N_1 - r_2 N_2 \quad (1.7b)$$

$$\frac{dT}{dt} = Q - \delta_0 T + \theta \delta U - \lambda N_1 T \quad (1.7c)$$

$$\frac{dU}{dt} = -\delta U + \theta_0 \delta_0 T + \lambda N_1 T + \gamma N_1 \quad (1.7d)$$

where

N_1 and N_2 are the density (or size, biomass) of the immature and mature subpopulations, respectively,

T is the concentration of pollutant in the environment,

U is the concentration of pollutant in the immature subpopulation.

The parameters $\alpha, \beta, r, \eta, r_{11}, r_2, Q, \delta_0, \delta, \theta_0, \theta, \lambda, \gamma$ were assumed to be positive.

The Liapunov function they use was given by:

$$V(N_1, N_2, T, U) = \sum_{i=1}^2 \alpha_i \left(N_i - N_i^* - N_i^* \ln \frac{N_i}{N_i^*} \right) + \alpha_3 \frac{(T - T^*)^2}{2} + \alpha_4 \frac{(U - U^*)^2}{2}. \quad (1.8)$$

1.3 Objectives

The purpose of this thesis is to obtain fundamental mathematical models representing the total nitrogen dynamic of the constructed wetland and to study the behaviors of these models including the existence of steady states, the stability of the steady states and the existence of Hopf bifurcations.

1.4 Expected Benefits

Using a simplified description of the actual situation, the mathematical models in our work are expected not only to provide a better understanding of the relationship between total nitrogen and mangrove forest but also to reveal modifications to the model that can give a more realistic description of mangrove forests. An understanding of the mangrove forest can be of benefit in construction of wetlands to treat waste water.

The success of mathematical models depends on scientific data from actual field studies. Therefore, the collaboration between field biologists and mathematical modelers is very important. Hopefully, this work may be useful for experimental designers and beginners in mathematical modeling and environmental biology both for studying mangrove forests and for applications to other environmental systems.

1.5 Organization of the Study

This work is organized in five chapters.

In Chapter I, the introduction and literature review describes the relationship between wastewater, mangrove, and nitrogen and includes the most innovative relevant researches and experiments on constructed wetlands and mathematical models.

In Chapter II, we summarize the theoretical background that is necessary for our analysis.

In Chapter III, we analyze two-dimensional models which describe the mangrove biomass concentration and TN concentration in the source (wastewater and soil). The first model is a two-dimensional model. The second model is similar to the first model except that the wastewater input is assumed to be a periodic function of time.

In Chapter IV, we analyze two three-dimensional models which separate the TN concentration into wastewater and soil solution components. The third model is a three-dimensional model which separates the TN concentration into wastewater and soil solution components. The fourth model is similar to the third model except that a modified function is used for uptake of TN from the soil into the mangrove biomass.

In Chapter V, we provide the conclusions and suggestions for future research.

CHAPTER II

THEORETICAL BACKGROUND

2.1 Introduction to Systems of ODEs

The mathematical models for a variety of biological systems regularly involve systems of ordinary differential equations. A system of ordinary differential equations is a collection of n interrelated ordinary differential equations of the form

$$\begin{aligned}\frac{dx_1}{dt} &= f_1(t, x_1, x_2, \dots, x_n) \\ \frac{dx_2}{dt} &= f_2(t, x_1, x_2, \dots, x_n) \\ &\vdots \\ \frac{dx_n}{dt} &= f_n(t, x_1, x_2, \dots, x_n).\end{aligned}\tag{2.1}$$

Here the functions f_1, f_2, \dots, f_n are real-valued functions of the n dependent variables and t the independent variable [20]. Note that the number of equations is equal to the number of dependent variables.

Definition 2.1 The system of equations (2.1) is called autonomous if the functions f_1, f_2, \dots, f_n are independent of t , so that the system has the form

$$\frac{dx_i}{dt} = f_i(x_1, x_2, \dots, x_n) \quad , \quad i = 1, 2, \dots, n.\tag{2.2}$$

Otherwise, it is called non-autonomous [21].

Definition 2.2 The system (2.1) is linear if it has the form

$$\begin{aligned}\frac{dx_1}{dt} &= a_{11}(t)x_1 + a_{12}(t)x_2 + \dots + a_{1n}(t)x_n + b_1(t) \\ \frac{dx_2}{dt} &= a_{21}(t)x_1 + a_{22}(t)x_2 + \dots + a_{2n}(t)x_n + b_2(t) \\ &\vdots \\ \frac{dx_n}{dt} &= a_{n1}(t)x_1 + a_{n2}(t)x_2 + \dots + a_{nn}(t)x_n + b_n(t).\end{aligned}\tag{2.3}$$

Otherwise, it is non-linear.

Definition 2.3 If all the functions b_i are zero, the system is homogeneous. Otherwise it is non-homogeneous.

To simplify notation, the vector notation can be used

$$X = \begin{pmatrix} x_1 \\ \vdots \\ x_n \end{pmatrix}. \tag{2.4}$$

Mathematician often write the vector X as (x_1, x_2, \dots, x_n) to save space [20].

In many realistic situations, nonlinear models are more useful than linear models. For example population’s growth rate looks like a quadratic function rather than a linear function. However, nonlinear equations are difficult to solve analytically. An alternative way to understand the behavior of the system is to look for steady states and to analyze their stability. The lack of stability of a stability of a steady state can suggest the existence of a limit cycle.

Consider a general autonomous vector field

$$\frac{dX}{dt} = f(X) \quad X \in R^n. \tag{2.5}$$

Definition 2.4 An equilibrium solution of (2.5) is a point $X^* \in R^n$ such that $f(X^*) = 0$.

This solution does not change in time. Other terms often substituted for the term “equilibrium solution” are “fixed point”, “stationary point”, “rest point”, or “steady state”.

Once we find any solution of (2.5), it is natural to try to determine if the solution is stable. Let $X^*(t)$ be any solution of (2.5). Then, roughly speaking, $X^*(t)$ is stable if solutions starting “close” to $X^*(t)$ at a given time remain close to $X^*(t)$ for all later times. It is asymptotically stable if nearby solutions actually converge to $X^*(t)$ as $t \rightarrow \infty$. The stability definitions play an important role [22].

Definition 2.5 $X^*(t)$ is said to be stable if, given $\varepsilon > 0$, there exists a $\delta = \delta(\varepsilon) > 0$ such that, for any other solution, $Y(t)$, of (2.5) satisfying $|X^*(t_0) - Y(t_0)| < \delta$, then $|X^*(t) - Y(t)| < \varepsilon$ for $t > t_0, t_0 \in R$.

Definition 2.6 $X^*(t)$ is said to be asymptotically stable if it is stable and if there exists a constant $b > 0$ such that, for any other solution, $Y(t)$, of (2.5) if $|X^*(t_0) - Y(t_0)| < b$, then $\lim_{t \rightarrow \infty} |X^*(t) - Y(t)| = 0$.

Hyperbolic Equilibria in Two-Dimensional Space

For nonlinear systems, linearization is really helpful. Consider a two-dimensional autonomous planar system of the form

$$\frac{dX}{dt} = f_1(X, Y) \quad (2.6a)$$

$$\frac{dY}{dt} = f_2(X, Y) \quad (2.6b)$$

where f_1 and f_2 are nonlinear functions. The equations for the equilibria are found by setting

$$f_1(X, Y) = 0, f_2(X, Y) = 0. \quad (2.7)$$

Suppose that $(X, Y) = (X^*, Y^*)$ satisfies the condition (2.7). To determine the stability of this equilibrium, we introduce new variables that measure the deviation about the equilibrium,

$$X(t) = x^* + x(t) \quad (2.8a)$$

and

$$Y(t) = y^* + y(t). \quad (2.8b)$$

This method is called a perturbation about the equilibrium point. Substituting (2.8a,b) into (2.6a,b), we get

$$\frac{d}{dt}(x^* + x) = f_1(x^* + x, y^* + y) \quad (2.9a)$$

$$\frac{d}{dt}(y^* + y) = f_2(x^* + x, y^* + y). \quad (2.9b)$$

Then, we expand the left hand side derivatives and notice that by definition $\frac{dx^*}{dt} = 0$

and $\frac{dy^*}{dt} = 0$. We also expand the right hand side functions f_1 and f_2 in a Taylor

series about the equilibrium point. Assuming higher order terms are extremely small, we obtain

$$\frac{dx}{dt} = \frac{\partial f_1}{\partial x}(x^*, y^*)x + \frac{\partial f_1}{\partial y}(x^*, y^*)y \tag{2.10a}$$

$$\frac{dy}{dt} = \frac{\partial f_2}{\partial x}(x^*, y^*)x + \frac{\partial f_2}{\partial y}(x^*, y^*)y, \tag{2.10b}$$

and, then define a Jacobian matrix for previous equations

$$J(x^*, y^*) = \begin{bmatrix} a_{11} & a_{12} \\ a_{21} & a_{22} \end{bmatrix} = \begin{bmatrix} \frac{\partial f_1}{\partial x} & \frac{\partial f_1}{\partial y} \\ \frac{\partial f_2}{\partial x} & \frac{\partial f_2}{\partial y} \end{bmatrix}_{(x^*, y^*)}.$$

From Plaats [21], the behavior of the steady state solution depends on the eigenvalues of J . The characteristic equation for the eigenvalues of $J(x^*, y^*)$ is

$$\det(J(x^*, y^*) - \lambda I) = \lambda^2 - a\lambda + b \tag{2.11}$$

where

$$a = \text{trace}(J(x^*, y^*)) = a_{11} + a_{22}, \tag{2.12a}$$

$$b = \det(J(x^*, y^*)) = a_{11}a_{22} - a_{12}a_{21}. \tag{2.12b}$$

There are three possibilities for nonzero eigenvalues of Jacobian matrix J :

- 1) distinct real roots
- 2) repeated real roots
- 3) complex conjugate roots

Case 1: The real and distinct eigenvalues of J can represent three possible behaviors.

- 1.1) If both eigenvalues of J are negative, the steady state will be an asymptotically stable two-tangent node (see Figure 2.1).
- 1.2) If both eigenvalues of J are positive, the equilibrium point will be an unstable two-tangent node (see Figure 2.2).
- 1.3) If an eigenvalues of J is positive and another is negative, the equilibrium point will be an unstable saddle point (see Figure 2.3).

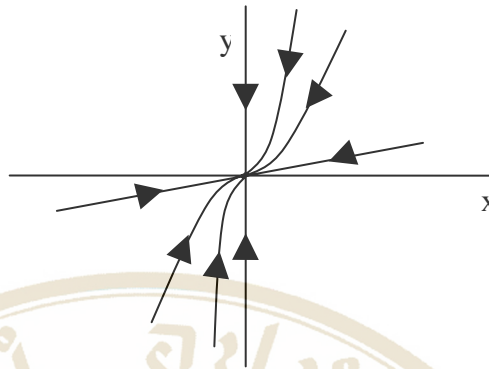


Figure 2.1 Asymptotically stable two-tangent node.

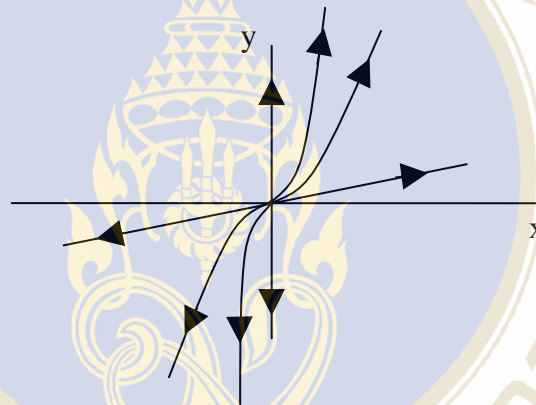


Figure 2.2 Unstable two-tangent node.

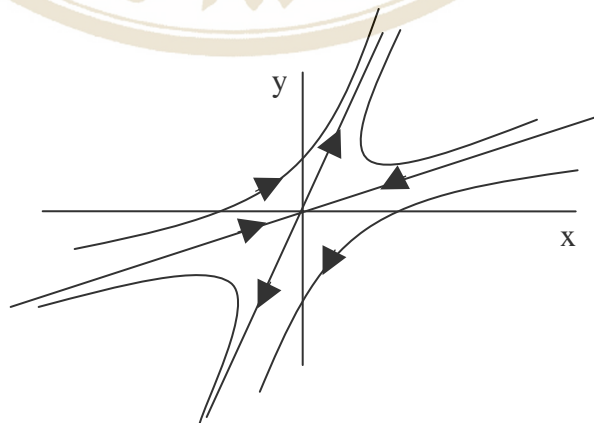


Figure 2.3 Saddle node.

Case 2: The real and repeated eigenvalues of J can reveal two possible behaviors.

2.1) If J is diagonal and similar to matrix $J = \begin{bmatrix} \lambda & 0 \\ 0 & \lambda \end{bmatrix}$, then the

equilibrium point is called a stellar node which is asymptotically stable if $\lambda < 0$ and unstable if $\lambda > 0$ (see Figure 2.4a,b).

2.2) If J is not diagonal, then it is not similar to a diagonal matrix. The equilibrium point is called an asymptotically stable one tangent node if $\lambda < 0$ and an unstable one tangent node if $\lambda > 0$ (see Figure 2.5a,b).

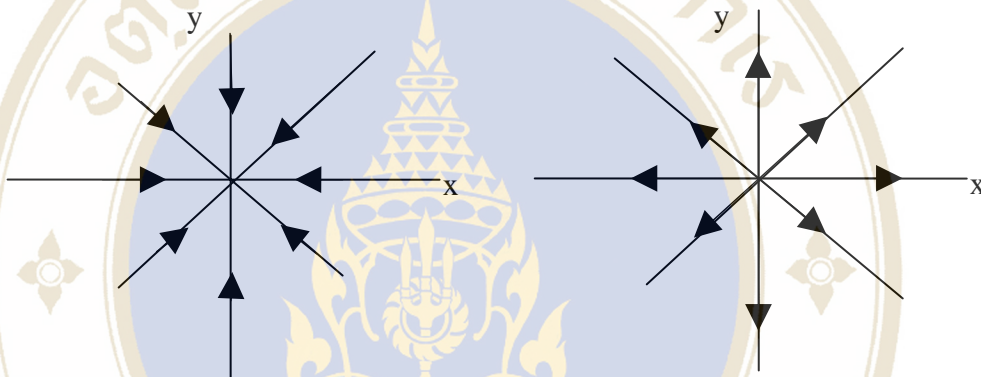


Figure 2.4a Stable.

Figure 2.4b Unstable.

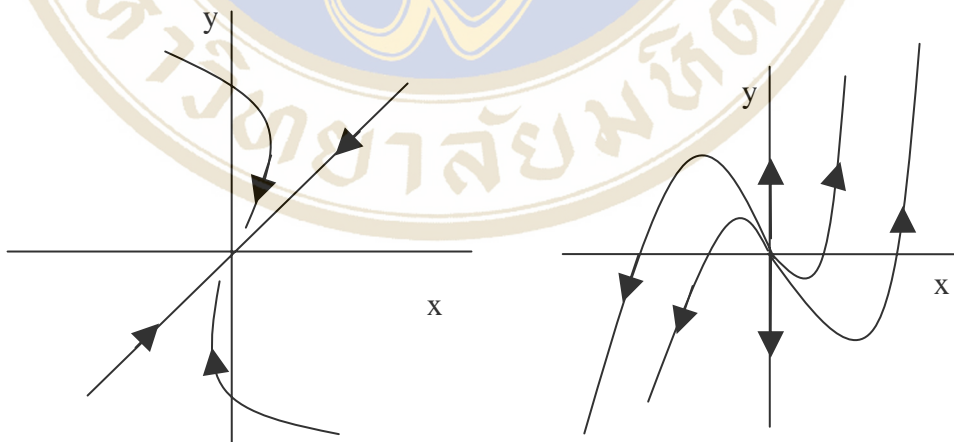


Figure 2.5a Stable one-tangent node.

Figure 2.5b Unstable one-tangent node.

Case 3: The eigenvalues of J are complex conjugate.

It is necessary and sufficient that the discriminant term is negative and then

$$\lambda_{1,2} = \frac{a \pm i\sqrt{4b - a^2}}{2}. \tag{2.13}$$

There are six possible behaviors described as follows.

- 3.1) If $a^2 < 4b$ and $a > 0$, then the equilibrium point will be an unstable spiral node (see Figure 2.6a).
- 3.2) If $a^2 < 4b$ and $a = 0$, the equilibrium point will be a neutral center for a linear system, but for a nonlinear system, the stability is not known.
- 3.3) If $a^2 < 4b$ and $a < 0$, then the equilibrium point will be a stable spiral node (see Figure 2.6b).

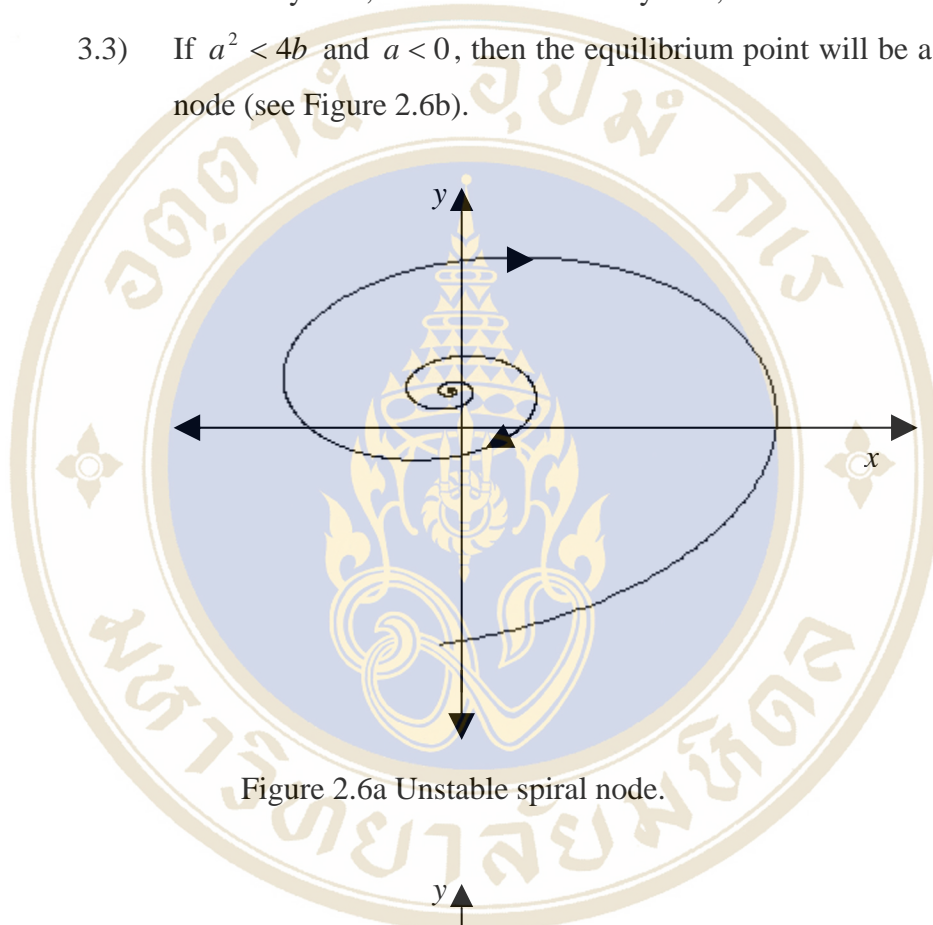


Figure 2.6a Unstable spiral node.

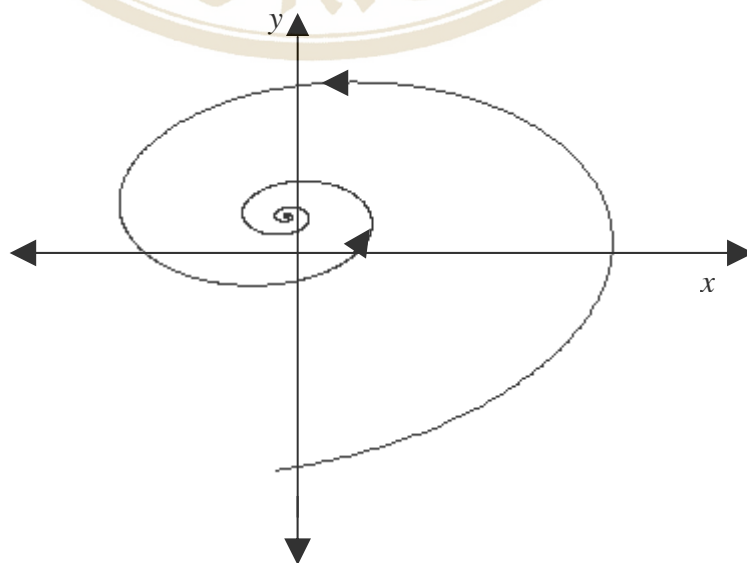


Figure 2.6b Stable spiral node.

For nonlinear systems, limit cycles can also exist. In the phase-plane plots a limit cycle is any simple oriented closed curve trajectory that does not contain singular points (points have been calling steady states and at which the phase flow is stagnant). The curve must be closed so that a point moving along the cycle will return to its starting position at fixed time intervals and thus execute periodic motion. What distinguishes a limit cycle from the cycles that surround a neutral center is the fact that it represents the limiting behavior of adjacent trajectories; point nearby will approach the limit cycle either for $t \rightarrow +\infty$ or for $t \rightarrow -\infty$ [23].

If the trajectories close to the limit cycle are spirals that gradually approach the limit cycle as $t \rightarrow \infty$, then the cycle is said to be stable (see Figure 2.7).

If the trajectories close to the limit cycle are spirals that move away from the limit cycle as $t \rightarrow \infty$, then the limit cycle is said to be unstable (see Figure 2.8).

If the spirals approach the limit cycle from one side as $t \rightarrow \infty$, and recede from it on the other side, then the limit cycle is called semi-stable (see Figure 2.9).

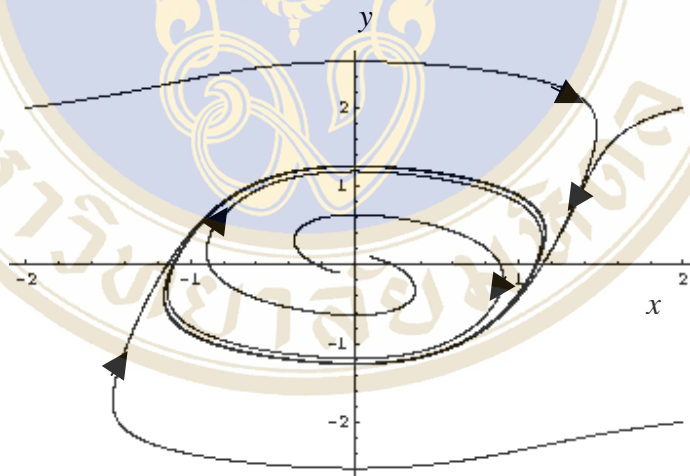


Figure 2.7 Stable limit cycle.

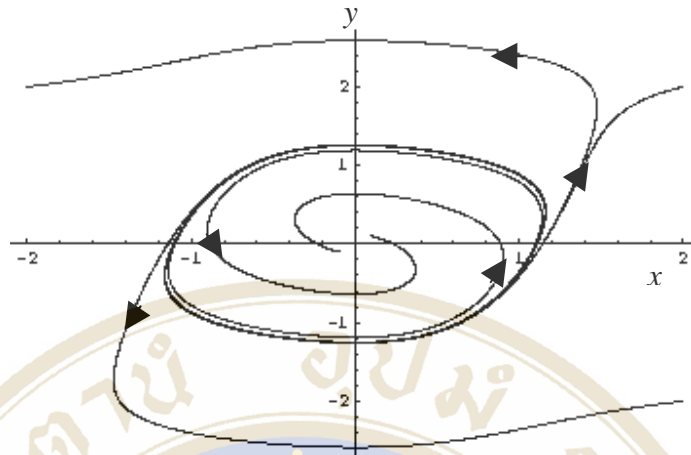


Figure 2.8 Unstable limit cycle.

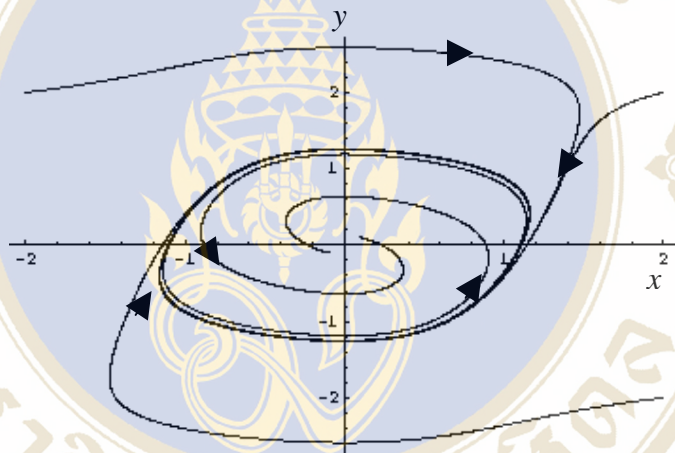


Figure 2.9 Semi-stable limit cycle.

Hyperbolic Equilibria in Three-Dimensional Space [24]

The Jacobian matrix of a three-dimensional system has 3 nonzero eigenvalues, one of which must be real and the other two can be either both real or complex-conjugate. Depending on the types and signs of the eigenvalues, there are a few interesting cases illustrated in Figure 2.10. A hyperbolic equilibrium can be

- 1) node when all eigenvalues are real and have the same sign; the node is stable (unstable) when the eigenvalues are negative (positive);
- 2) saddle when all eigenvalues are real and at least one of them is positive and at least one is negative; Saddles are always unstable;

3) focus-node when it has one real eigenvalue and a pair of complex-conjugate eigenvalues, and all eigenvalues have real parts of the same sign; The equilibrium is stable (unstable) when the sign is negative (positive);

4) saddle-focus when it has one real eigenvalue with the sign opposite to the sign of the real part of a pair of complex-conjugate eigenvalues; this type of equilibrium is always unstable.

Notice that nodes and focus-nodes change stability when time is reversed (i.e. when t is replaced by $-t$), whereas saddles and saddle-foci are unstable regardless of the direction of time [24].

Nonhyperbolic Equilibria in Three-Dimensional Space [24]

There are many more types of non-hyperbolic equilibria, i.e. those that have at least one eigenvalue with zero real part, since the phase portrait in a small neighborhood of such equilibria also depends on the nonlinear terms of $f(x)$. Most of these equilibria do not have names or are named after the type of the bifurcation in which they play a role. Three most common examples are depicted in Figure 2.11.

1) The center equilibrium typically occurs in linear systems with a pair of pure-imaginary eigenvalues or in Hamiltonian systems. The neighborhood of the equilibrium is foliated by periodic orbits. Centers are neutrally stable but not asymptotically stable. (A pair of pure-imaginary eigenvalues also occurs in Andronov-Hopf bifurcation; due to the nonlinear terms, the neighborhood of such an equilibrium is not foliated by periodic orbits, but it looks like a focus.)

2) The saddle-node equilibrium occurs in nonlinear systems with one zero eigenvalue when the system undergoes the saddle-node bifurcation, where a saddle and a node approach each other, coalesce into a single equilibrium (depicted in the figure), and then disappear. Saddle-nodes are always unstable. In the theory of homoclinic bifurcations in R^2 , $n > 2$, a saddle-saddle equilibrium is a saddle-node with both positive and negative eigenvalues.

3) The Bogdanov-Takens equilibrium occurs in nonlinear systems with two zero eigenvalues, typically when the system undergoes the Bogdanov-Takens bifurcation. It is also an unstable equilibrium.

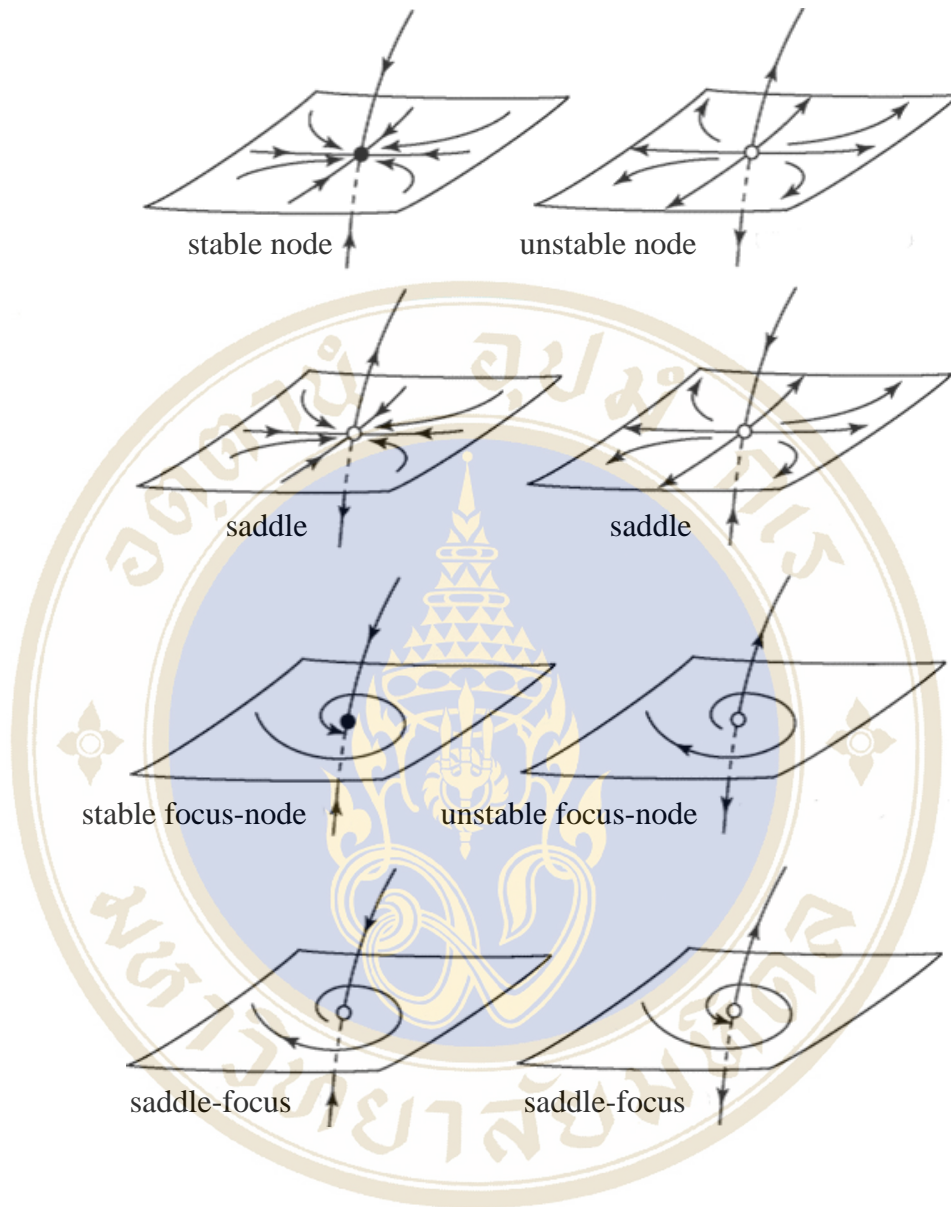


Figure 2.10 Examples of hyperbolic equilibria in R^3 [24].

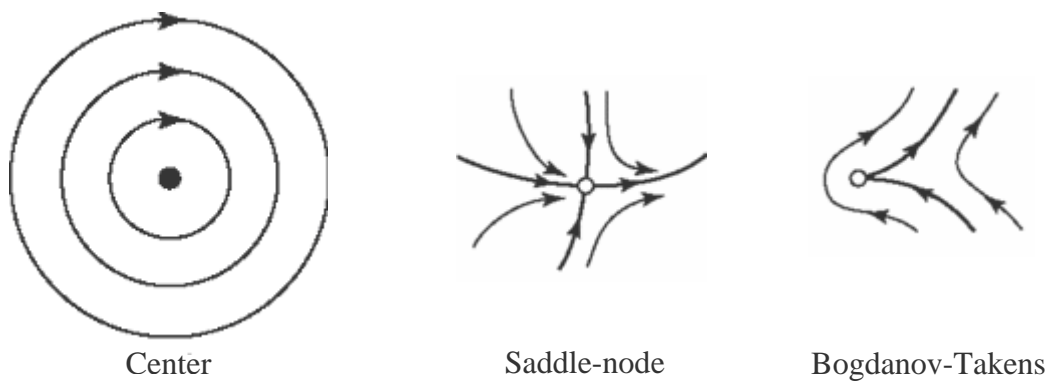


Figure 2.11 Examples of non-hyperbolic equilibria in R^2 [24].

The previous notions of stability are local in nature. They concern only the behavior of solutions near the fixed point. Even if such solutions remain bounded for all time, other solutions may exist globally. However a Liapunov function approach is a useful method to consider the global stability.

2.2 Liapunov Function

Let $V(u)$ be a scalar continuous function defined in Ω , i.e. $V \in [\Omega, R]$, and $V(0) = 0$. For this function we need the following:

Definition 2.7 $V(u)$ is said to be positive definite in Ω if and only if $V(u) > 0$ for $u \neq 0, u \in \Omega$ [25].

Definition 2.8 $V(u)$ is said to be negative definite in Ω if and only if $-V(u)$ is positive definite in Ω [25].

Theorem 2.1 Let $x^* \in \Omega$ be an equilibrium point for $x' = f(x)$. Let $V : U \rightarrow R$ be a continuous function defined on a neighborhood of x and differentiable on $U - x^*$, such that $V(x^*) = 0$ and $V(x) > 0$ if $x \neq x^*$. Then, if

- (a) $\dot{V} \leq 0$ in $U - x^*$, then x^* is stable. However, if
- (b) $\dot{V} < 0$ in $U - x^*$, then x^* is asymptotically stable. [16]

2.3 Local and Global Maxima and Minima [26]

Definition 2.9 Let $D \rightarrow R^n$ and $f : D \rightarrow R$. The point $\mathbf{a} \in D$ is said to be:

- 1) a local maximum if $f(\mathbf{x}) \leq f(\mathbf{a})$ for all points \mathbf{x} sufficiently close to \mathbf{a} ;
- 2) a local minimum if $f(\mathbf{x}) \geq f(\mathbf{a})$ for all points \mathbf{x} sufficiently close to \mathbf{a} ;
- 3) a global (or absolute) maximum if $f(\mathbf{x}) \leq f(\mathbf{a})$ for all points $\mathbf{x} \in D$;
- 4) a global (or absolute) minimum if $f(\mathbf{x}) \geq f(\mathbf{a})$ for all points $\mathbf{x} \in D$;
- 5) a local or global extremum if it is a local or global maximum or minimum.

Definition 2.10 Let $D \rightarrow R^n$ and $f : D \rightarrow R$. The point $\mathbf{a} \in D$ is said to be a stationary point if $\nabla f(\mathbf{a}) = 0$ and a singular point if ∇f does not exist at \mathbf{a} .

Definition 2.11 A stationary point \mathbf{a} which is neither a local maximum nor minimum is called a saddle point.

Theorem 2.2 If f has a relative extremum at a point (x_0, y_0) and if the first-order partial derivatives of f exist at this point then, $f_x(x_0, y_0) = 0$ and $f_y(x_0, y_0) = 0$.

Proof Assume that f has a relative maximum at (x_0, y_0) and that both partial derivatives of f exist at (x_0, y_0) .

$$G(x) = f(x, y_0) \quad (2.14)$$

has a relative maximum at $x = x_0$ and

$$H(y) = f(x_0, y) \quad (2.15)$$

has a relative maximum at $y = y_0$. It follows from these results that

$$G'(x_0) = f_x(x_0, y_0) = 0 \text{ and } H'(y_0) = f_y(x_0, y_0) = 0$$

The proof for a relative minimum is similar.

Definition 2.12 If $f : R^2 \rightarrow R$ is a function of two variables such that all second order partial derivatives exist at the point (a, b) , then the Hessian matrix of f at (a, b) is the matrix

$$H = \begin{bmatrix} f_{xx} & f_{xy} \\ f_{yx} & f_{yy} \end{bmatrix} \quad (2.16)$$

where the derivatives are evaluated at (a, b) .

Theorem 2.3 Suppose that $f : R^2 \rightarrow R$ is a sufficiently smooth function of two variables with a critical point at (a, b) and H is the Hessian of f at (a, b) . If $\det(H) \neq 0$, then (a, b) is:

- 1) a local maximum if $0 > f_{xx}$ and $0 < \det(H) = f_{xx}f_{yy} - f_{xy}^2$;
- 2) a local minimum if $0 < f_{xx}$ and $0 < \det(H) = f_{xx}f_{yy} - f_{xy}^2$;
- 3) a saddle point if neither of the above hold

where the partial derivatives are evaluated at (a, b) . Then (a, b) can be either a local extremum or saddle point [26].

Periodic phenomena or oscillations are observed in many naturally occurring systems. The appearance of a limit cycle which can occur when an equilibrium point becomes unstable as some parameter is varied is called a Hopf bifurcation. The Hopf

bifurcation is the door that opens from the small room of an equilibrium state to the large hall of the periodic solution [27].

2.4 Hopf Bifurcation Theorem

Theorem 2.4 Hopf Bifurcation for the Case $n = 2$ [23, 27, 28]

Consider a system of two equations that contains a parameter γ

$$\frac{dx}{dt} = f(x, y; \gamma) \quad (2.17a)$$

$$\frac{dy}{dt} = g(x, y; \gamma). \quad (2.17b)$$

The usual differentiability and continuity assumptions are made about f and g as functions of x , y , and γ . Suppose that for each value of γ the equations admit a steady state whose value may depend on γ , this is $(x^*(\gamma), y^*(\gamma))$. Consider the Jacobian matrix evaluated at the parameter-dependent steady state:

$$J(\gamma) = \begin{bmatrix} \frac{\partial f}{\partial x} & \frac{\partial f}{\partial y} \\ \frac{\partial g}{\partial x} & \frac{\partial g}{\partial y} \end{bmatrix}_{(x^*, y^*)} \quad (2.18)$$

Suppose eigenvalues of this matrix are $\lambda(\gamma) = a(\gamma) \pm b(\gamma)i$. Also suppose that there is a value γ^* , called the bifurcation value, such that $a(\gamma^*) = 0$, $b(\gamma^*) \neq 0$, and as γ is varied through γ^* , the real parts of the eigenvalues change signs ($da/d\gamma \neq 0$ at $\gamma = \gamma^*$).

Given these hypotheses, the following possibilities arise:

1) At the value $\gamma = \gamma^*$ a center is created at the steady state, and thus infinitely many neutrally stable concentric closed orbits surround the point (x^*, y^*) .

2) There is a range of γ values such that $\gamma^* < \gamma < c$ for which a single closed orbit (a limit cycle) surrounds (x^*, y^*) . As γ is varied, the diameter of the limit cycle changes in proportion to $|\gamma - \gamma^*|^{1/2}$. There are no other closed orbits near (x^*, y^*) . Since the limit cycle exists for γ values above γ^* , this phenomenon is known as a

supercritical bifurcation (see Figure 2.12). If $\gamma = \gamma^*$ is an asymptotically stable point, then the limit cycle is asymptotically stable for $\gamma^* < \gamma < c$.

3) There is a range of values such that $d < \gamma < \gamma^*$ for which a conclusion similar to case 2 holds. (The limit cycle exists for values below γ^* , and this is termed a subcritical bifurcation.) (see Figure 2.13). In this case, $\gamma = \gamma^*$ is an unstable equilibrium point.

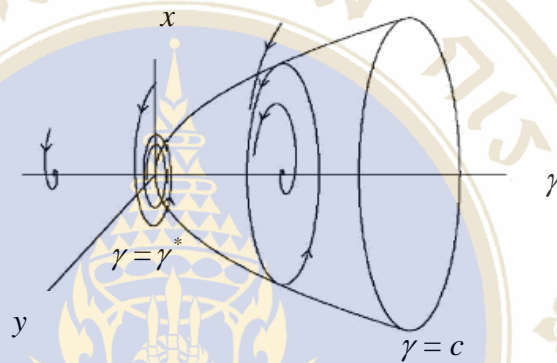


Figure 2.12 Supercritical bifurcation: as γ increases from small values through γ^* and up to $\gamma = c$, the steady state changes from a stable node to an unstable node. A stable limit cycle appears at γ^* , and its diameter grows as indicated by the parabolic envelope.

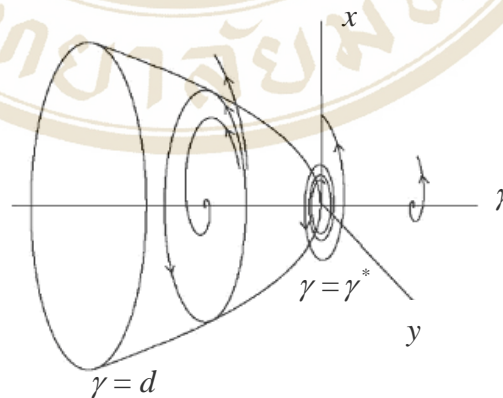


Figure 2.13 Subcritical bifurcation: as γ decreases from values above γ^* and down to $\gamma = d$, the steady state changes from an unstable node to a stable node. An unstable limit cycle appears at γ^* , and its diameter grows as indicated by the parabolic envelope.

Theorem 2.5 Hopf Bifurcation for the Case $n > 2$

Consider a system of n equations in n variables,

$$\frac{dX}{dt} = F(X, \gamma) \quad (2.19)$$

where

$$X = (x_1, x_2, \dots, x_n)$$

$$F = (f_1(X; \gamma), f_2(X; \gamma), \dots, f_n(X; \gamma))$$

with the appropriate smoothness assumptions on f_i which are functions of the variables and a parameter γ . If X^* is a steady state of this system and linearization about this point yields n eigenvalues

$$\lambda_1, \lambda_2, \dots, \lambda_{n-2}, a + bi, a - bi,$$

where eigenvalues λ_1 through λ_{n-2} have negative real parts and λ_{n-1}, λ_n (precisely these two) are complex conjugates that cross the imaginary axis when γ varies through some critical value, then the theorem still predicts closed (limit-cycle) trajectories. The extension of this theorem to arbitrary dimensions depend in large part on another important theorem (called the center manifold theorem), which ensures that close to the steady state the interesting events take place on a plane-like subset of R^n (mathematically called a two-dimensional manifold).

CHAPTER III

MODEL ANALYSIS I

According to William Mitsch *et al.* [29], wetlands are effective nitrogen sinks because of the high level of denitrification that has occurred in their soils. Nitrogen transformations in wetland and riparian soils, surface water, and groundwater involve several microbiological processes, some of which favor these systems as sinks for nitrogen. They have explained that ammonium-nitrogen (NH_4^+) is the primary form of mineralized nitrogen in most flooded wetland soils and is often the primary initial form of nitrogen fertilizer. As shown in Figure 3.1, NH_4^+ can be absorbed by plants through their root systems or by anaerobic microorganisms and converted back to organic matter. It can also be immobilized through ion exchange onto negatively charged soil particles. Because of anaerobic conditions in wetland soils, NH_4^+ would normally be restricted from further oxidation and would build up to excessive levels were it not for the thin oxidized layer at the surface of many wetland soils. The gradient between high concentrations of NH_4^+ in the reduced soils and low concentrations in the oxidized surface layer causes the ammonium to diffuse upward, albeit very slowly, to the oxidized layer. The NH_4^+ then is oxidized by a restricted number of chemoautotrophic bacteria through the process of nitrification to nitrate-nitrogen (NO_3^-).

Unlike NH_4^+ , NO_3^- is a negative ion, therefore it is not subject to immobilization by the negatively charged soil particles. Consequently, it is thus much more mobile in solution. This is why it discharges so readily from agricultural fields if it is not assimilated immediately by plants or microbes. Denitrification is carried out by certain microorganisms in anaerobic conditions with NO_3^- as the terminal electron acceptor.

It results in the loss of NO_3^- as it is converted to gaseous nitrous oxide (N_2O) and molecular nitrogen (N_2) as visualized in Figure 3.1 [29].

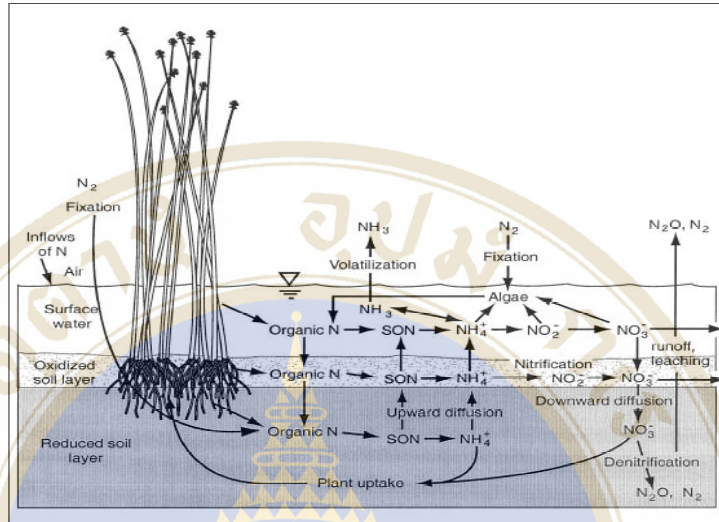


Figure 3.1 Nitrogen transformations in wetlands.

The mangrove forests are generally nutrient limited with nitrogen [30]. Therefore, after wastewater polluted by nutrient flows into the constructed wetland, not only dissolved nitrogen concentration in water drops but this accumulated nutrient also helps mangrove trees to make protein, to grow and to reproduce (see Figure 3.2).

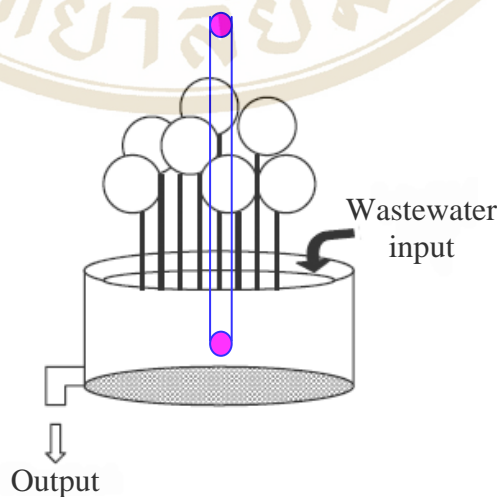


Figure 3.2 A pond for the experiment of constructed wetland.

3.1 Two-Dimensional Model: Constant Input

We begin with a rather simple system of two ordinary differential equations that describe the change of mangrove biomass and the change of total nitrogen (TN) in the soil and water. TN is a measure of all the various forms of dissolved organic and inorganic (i.e. ammonium, nitrite, and nitrate) nitrogen that is used to determine water and sediment quality. Table 3.1 shows our variables and parameters including their meaning and their dimension.

For biological processes, each parameter must be positive while each variable must be non-negative.

Table 3.1 Definition of variables and parameters for model I.

Quantity	Symbol	Dimension
Mangrove biomass concentration	T	mg / ha
TN concentration in the source	N	mg / ha
TN uptake rate	β	$(mg / ha)^{-1}(month)^{-1}$
Litter fall rate	σ	$month^{-1}$
TN input rate	Q	$(mg / ha)(month)^{-1}$
TN loss rate in the source	ϕ	$month^{-1}$

As illustrated in Figure 3.3, there are two separate compartments. The first compartment is the mangrove biomass. The second compartment is the TN concentration in wastewater and soil solution and is the source of TN for the plants. Plants absorb the TN from the source and transform it into biomass.

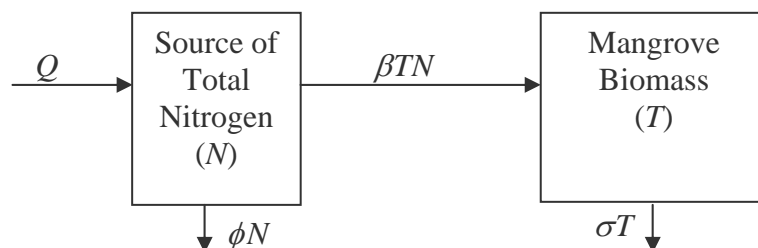


Figure 3.3 Flow chart for the transformation of total nitrogen for model I.

Our constructed wetland pond is based on the assumptions that the nutrient (TN) is non-reproducing, the input rate of TN concentration is a constant, “ Q ”, and we assume that there is perfect mixing in our pond so that TN is removed in proportion to its concentration. “ ϕN ” represents the loss function of TN through leaching or evaporation. “ βNT ” represents the TN uptake function for plants and also the conversion rate of TN to biomass. Finally, “ σT ” represents the rate of litter fall. This litter fall will not return to the pond again because of a filter placed over the pond. Therefore we can develop a model as follows,

$$\frac{dT}{dt} = \beta NT - \sigma T \tag{3.1a}$$

$$\frac{dN}{dt} = Q - \beta NT - \phi N . \tag{3.1b}$$

After introducing non-dimensionalization

$$x = \frac{T}{Q}, y = \frac{N}{Q}, m = \beta Q, \tau = t,$$

we can reduce system (3.1) to

$$\frac{dx}{d\tau} = mxy - \sigma x \tag{3.2a}$$

$$\frac{dy}{d\tau} = 1 - mxy - \phi y . \tag{3.2b}$$

For convenience, we will still use the meaning of the original variables for the dimensionless variables.

The Steady State Solutions

The steady state (time-independent) solutions are obtained by setting $\frac{dx}{d\tau} = 0$ and

$\frac{dy}{d\tau} = 0$. Therefore the conditions for a steady state solution are:

$$mxy - \sigma x = 0 \tag{3.3a}$$

$$1 - mxy - \phi y = 0 \tag{3.3b}$$

From equation (3.3a); we obtain $x_1^* = 0$ or $y_2^* = \frac{\sigma}{m}$.

Substituting $x_1^* = 0$ into equation (3.3b), we find $y_1^* = \frac{1}{\phi}$.

Substituting $y_2^* = \frac{\sigma}{m}$ into equation (3.3b), we get $x_2^* = \frac{1}{m} \left(\frac{m}{\sigma} - \phi \right)$.

Another name for steady state solution is equilibrium solution or equilibrium point. Therefore there are two steady state solutions for this system, namely:

1) the washout of only mangrove biomass solution: $E_1^* = (x_1^*, y_1^*) = (0, \frac{1}{\phi})$ and

2) the coexistence of mangrove biomass and TN concentration solution:

$$E_2^* = (x_2^*, y_2^*) = \left(\frac{1}{m} \left(\frac{m}{\sigma} - \phi \right), \frac{\sigma}{m} \right), \text{ provided that } \frac{m}{\sigma} \neq \phi.$$

Note that if $\frac{m}{\sigma} = \phi$ then the two equilibria coincide.

The availability of nitrogen in our constructed wetland depends mainly on the external TN concentration supply and the TN concentration loss. When the system loses TN concentration too fast, the availability of TN concentration is low. Then each plant is not able to absorb adequate TN. Thus plants die out. After the washout of mangrove, the added nitrogen will partially remain in the soil pores as shown in the first equilibrium. However, if the TN loss rate is sufficiently low, the availability of TN increases and leads to mangrove survival. The balance between mangrove biomass and TN concentration occurs in the second equilibrium.

Lemma 3.1 If the inequality

$$\frac{m}{\sigma} > \phi \tag{3.4}$$

holds, then the system (3.2a,b) has a non-negative equilibrium solution

$$E_2^* = (x_2^*, y_2^*) = \left(\frac{1}{m} \left(\frac{m}{\sigma} - \phi \right), \frac{\sigma}{m} \right)$$

Lemma 3.1 indicates that if the inequality (3.4) holds, then the equilibrium E_2^* exists. However, if the inequality (3.4) fails, the equilibrium E_2^* does not exist because biomass has no meaning when its sign is negative.

3.1.1 Local Stability Analysis

The local stability of each steady state is determined by linearizing equations (3.2a,b) about the steady state and examining the eigenvalues of the resulting Jacobian matrix.

Theorem 3.1 If the inequalities

$$\phi + \sigma + mx^* - my^* > 0 \tag{3.5}$$

and

$$\sigma mx^* - \phi my^* + \sigma\phi > 0 \tag{3.6}$$

hold, then a steady state solution (x^*, y^*) of equations (3.3a,b) will be stable.

Proof

From system (3.2a,b), the Jacobian matrix is evaluated at an equilibrium (x^*, y^*)

$$J_{(x^*, y^*)} = \begin{bmatrix} my^* - \sigma & mx^* \\ -my^* & -mx^* - \phi \end{bmatrix}. \tag{3.7}$$

The eigenvalues can be found by solving the following characteristic equation.

$$\det(J - \lambda I) = 0. \tag{3.8}$$

Therefore, $(my^* - \sigma - \lambda)(-mx^* - \phi - \lambda) + m^2 x^* y^* = 0,$

or
$$\lambda^2 + \lambda(\phi + \sigma + mx^* - my^*) + (\sigma mx^* - \phi my^* + \sigma\phi) = 0. \tag{3.9}$$

This leads to

$$\lambda_{1,2} = \frac{-(\phi + \sigma + mx^* - my^*) \pm \sqrt{(\phi + \sigma + mx^* - my^*)^2 - 4(\sigma mx^* - \phi my^* + \sigma\phi)}}{2} \tag{3.10}$$

If the inequalities 3.5 and 3.6 hold, both eigenvalues are negative. Consequently, the equilibrium (x^*, y^*) is stable.

Theorem 3.2

- 1) The equilibrium point E_1^* is unstable if $\frac{m}{\sigma} > \phi$ and stable if $\frac{m}{\sigma} < \phi$.
- 2) The equilibrium point E_2^* is stable if $\frac{m}{\sigma} > \phi$ and unstable if $\frac{m}{\sigma} < \phi$. However, E_2^* has no biological meaning if $\frac{m}{\sigma} < \phi$.

Proof

Firstly, the Jacobian matrix at $E_1^* = (x_1^*, y_1^*) = (0, \frac{1}{\phi})$ is

$$J_{(0, \frac{1}{\phi})} = \begin{bmatrix} \frac{m}{\phi} - \sigma & 0 \\ -\frac{m}{\phi} & -\phi \end{bmatrix}. \quad (3.11)$$

Therefore, the eigenvalues of the lower diagonal matrix are $\lambda_{1,2} = -\phi, \frac{m}{\phi} - \sigma$, respectively. The eigenvalue λ_1 is negative. Consider for λ_2 :

If $\frac{m}{\sigma} > \phi$, the eigenvalue λ_2 is positive and therefore the equilibrium point E_1^* is unstable.

If $\frac{m}{\sigma} < \phi$, the eigenvalue λ_2 is negative. Therefore, the equilibrium point E_1^* is stable because both eigenvalues are negative. Figures 3.4-5 show the results of numerical solution of the dimensionless model equations (3.2a,b) for mangrove biomass and TN concentration for parameters $m = 0.05$, $\sigma = 0.5$, $\phi = 1$ for which the equilibrium point E_1^* is stable. It can be seen that the solution converges to this steady state solution $(0, \frac{1}{\phi}) = (0, 1)$.

Secondly, the Jacobian matrix at $E_2^* = (x_2^*, y_2^*) = (\frac{1}{m}(\frac{m}{\sigma} - \phi), \frac{\sigma}{m})$ is

$$J_{(\frac{1}{m}(\frac{m}{\sigma} - \phi), \frac{\sigma}{m})} = \begin{bmatrix} 0 & \frac{m}{\sigma} - \phi \\ -\sigma & -\frac{m}{\sigma} \end{bmatrix}. \quad (3.12)$$

Therefore, the corresponding characteristic equation is

$$\det(J - \lambda I)_{(\frac{1}{m}(\frac{m}{\sigma} - \phi), \frac{\sigma}{m})} = \lambda^2 + \frac{m}{\sigma} \lambda + (m - \sigma\phi) = 0. \quad (3.13)$$

Then the eigenvalues are

$$\lambda_{3,4} = \frac{-\frac{m}{\sigma} \pm \sqrt{\left(\frac{m}{\sigma}\right)^2 - 4m + 4\sigma\phi}}{2}, \text{ respectively.} \quad (3.14)$$

If $\left(\frac{m}{\sigma}\right)^2 - 4m + 4\sigma\phi > 0$, then the eigenvalues are real. We consider two cases.

Case 1: The inequality $\frac{m}{\sigma} > \phi$ holds.

The eigenvalues are
$$\lambda_{3,4} = \frac{-\frac{m}{\sigma} \pm \sqrt{\left(\frac{m}{\sigma}\right)^2 - 4m + 4\sigma\phi}}{2}.$$

The inequality $\frac{m}{\sigma} > \phi$ leads to $m > \sigma\phi$ and $\frac{m}{\sigma} > 0$. Obviously, for all positive

parameters $\frac{m}{\sigma} > \sqrt{\left(\frac{m}{\sigma}\right)^2 - 4(m - \sigma\phi)}$ and thus all eigenvalues are negative and the

equilibrium point $E_2^* (x_2^*, y_2^*) = \left(\frac{1}{m}\left(\frac{m}{\sigma} - \phi\right), \frac{\sigma}{m}\right)$ is stable. Figures 3.6-7 show the

results of a numerical solution of the dimensionless model equations (3.2a,b) for parameter values $m = 0.6, \sigma = 0.5, \phi = 1$ for which the equilibrium point E_2^* is

stable. It can be seen that the mangrove biomass concentration and TN concentration

tend toward the equilibrium point $E_2^* = \left(\frac{1}{m}\left(\frac{m}{\sigma} - \phi\right), \frac{\sigma}{m}\right) = (0.33, 0.83)$.

Case 2: The inequality (3.4) reverses, i.e. $\frac{m}{\sigma} < \phi$.

The eigenvalues are
$$\lambda_{3,4} = \frac{-\frac{m}{\sigma} \pm \sqrt{\left(\frac{m}{\sigma}\right)^2 - 4m + 4\sigma\phi}}{2}.$$

From the inequality $\frac{m}{\sigma} < \phi$, we obtain $m < \sigma\phi$ and since m, σ and ϕ are positive

$$-\frac{m}{\sigma} + \sqrt{\left(\frac{m}{\sigma}\right)^2 - 4(m - \sigma\phi)} \text{ is positive,}$$

while
$$-\frac{m}{\sigma} - \sqrt{\left(\frac{m}{\sigma}\right)^2 - 4(m - \sigma\phi)} \text{ is negative.}$$

Therefore the equilibrium $E_2^*(x^*, y^*) = \left(\frac{1}{m} \left(\frac{m}{\sigma} - \phi \right), \frac{\sigma}{m} \right)$ is unstable.

If $\left(\frac{m}{\sigma} \right)^2 - 4m + 4\sigma\phi < 0$, complex eigenvalues exist. Since the parameters m and σ are positive, the real parts of all eigenvalues are negative, and therefore the equilibrium point is stable.

Concerning the equilibrium E_2^* , if the initial point does not start exactly at E_2^* , and the condition for complex eigenvalues is satisfied then the solution trajectory will spiral toward to E_2^* as time progresses. Figures 3.8-9 show the results of a numerical solution of the dimensionless model equations (3.2a,b) for parameter values $m = 0.05$, $\sigma = 0.5$, $\phi = 0.001$ for which the equilibrium point E_2^* is stable. It can be seen that the mangrove biomass concentration and TN concentration tend toward the equilibrium point $E_2^* = \left(\frac{1}{m} \left(\frac{m}{\sigma} - \phi \right), \frac{\sigma}{m} \right) = (1.98, 10)$.

Remark 3.1 The eigenvalues of the Jacobian for the equilibrium $E_1^*(x_1^*, y_1^*) = \left(0, \frac{1}{\phi} \right)$ are $\lambda_{1,2} = -\phi, \frac{m}{\phi} - \sigma$ respectively. Since both eigenvalues are real it is impossible to obtain a periodic solution. Therefore a Hopf bifurcation cannot exist at E_1^* .

Remark 3.2

The eigenvalues of the Jacobian for the equilibrium point E_2^* can be complex and therefore oscillating solutions can exist. However, the real part of the complex eigenvalues $-\frac{m}{\sigma} \neq 0$ and therefore a Hopf bifurcation cannot exist at E_2^* .

Therefore, the system lacks a required condition for the Hopf bifurcation Theorem and a limit cycle cannot occur for this system through Hopf bifurcation at an equilibrium point.

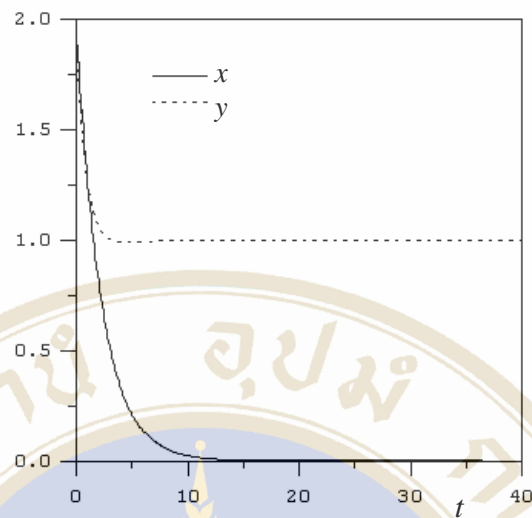


Figure 3.4 Numerical solution of the dimensionless model equations (3.2a,b) for mangrove biomass and TN concentration for parameters $m = 0.05$, $\sigma = 0.5$, $\phi = 1$.

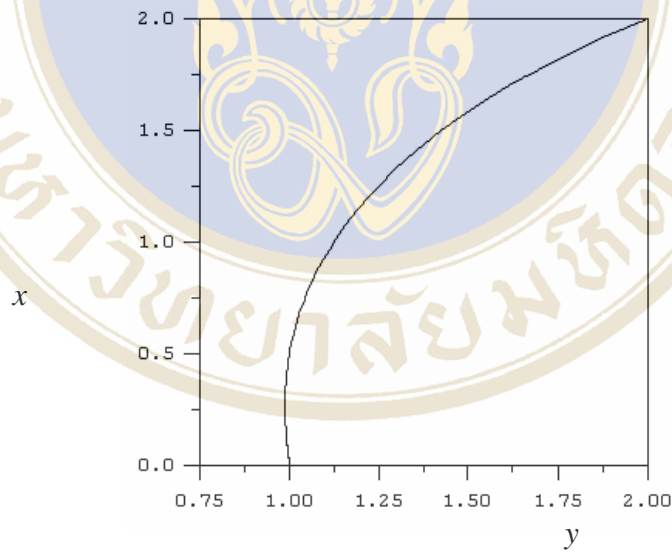


Figure 3.5 Phase plane plot of the dimensionless model equations (3.2a,b) for the solution for mangrove biomass and the TN concentration for parameters $m = 0.05$, $\sigma = 0.5$, $\phi = 1$.

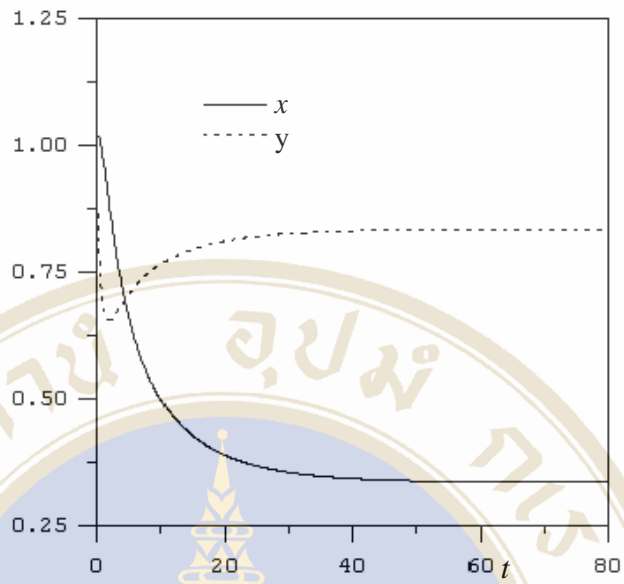


Figure 3.6 Numerical solution of the dimensionless model equations (3.2a,b) for mangrove biomass and TN concentration for parameters $m = 0.6$, $\sigma = 0.5$, $\phi = 1$.

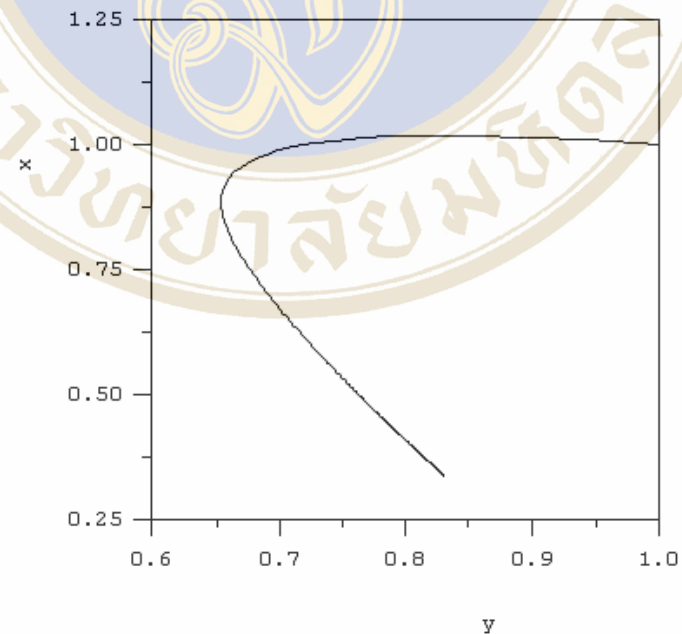


Figure 3.7 Phase plane plot of the dimensionless model equations (3.2a,b) for the solution for mangrove biomass and the TN concentration for parameters $m = 0.6$, $\sigma = 0.5$, $\phi = 1$.

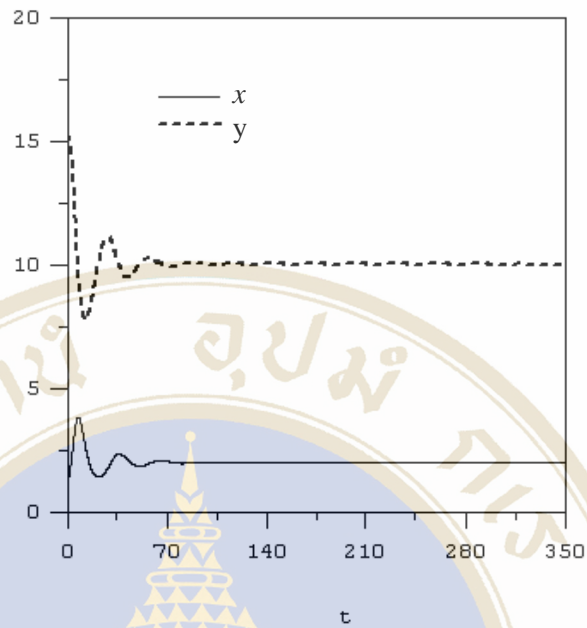


Figure 3.8 Numerical solution of the dimensionless model equations (3.2a,b) for mangrove biomass and TN concentration for parameters $m = 0.05$, $\sigma = 0.5$, $\phi = 0.001$.

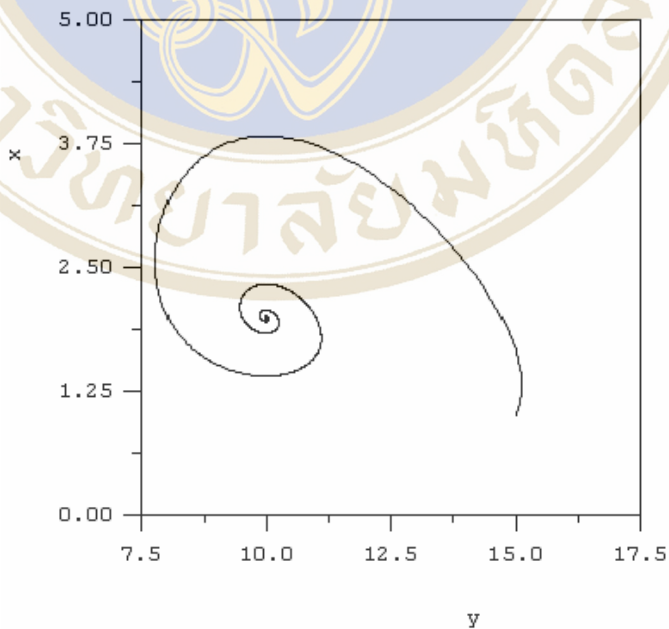


Figure 3.9 Phase plane plot of the dimensionless model equations (3.2a,b) for the solution for mangrove biomass and the TN concentration for parameters $m = 0.05$, $\sigma = 0.5$, $\phi = 0.001$.

Suppose we have an equilibrium E^* . If we want to determine whether or not it is stable there are two possible approaches. One approach is to use linearization about the equilibrium point. This is often called Liapunov's first method. We have used this approach in the earlier sections of this chapter. The linearization method is a local test as the linear approximations used only apply close to the equilibrium point. The second approach is a global test that we will now discuss.

3.1.2 Global Stability Analysis

The global test is often called Liapunov's second method and involves finding a Liapunov function [27]. It is sufficient to find a neighborhood U of E^* for which orbits starting in U remain in U for all positive times. One possibility is to show that the vector field is either tangent to the boundary of U or pointing inward toward E^* for all neighborhoods of E^* inside U . One method for proving this is to construct a Liapunov function.

It is widely recognized that analysis of global stability and/or domains of attraction of the equilibrium points is essential for a full understanding of the stability and persistence of ecological systems [15]. The difficulty of this approach is how to construct a Liapunov function.

The Liapunov Function

Definition 3.1 [16] A function $f(x, y)$ is positive definite relative to the point $E^* = (x^*, y^*)$ in the set O if $f(x^*, y^*) = 0$, and $f(x, y) > 0$, for all $(x, y) \in O$, $(x, y) \neq (x^*, y^*)$. A function $f(x, y)$ is negative definite, if $-f(x, y)$ is positive definite.

Suppose the system of differential equation system is

$$\frac{dx}{dt} = F(x, y) \quad (3.15a)$$

$$\frac{dy}{dt} = G(x, y). \quad (3.15b)$$

Theorem 3.3 Let $E^* = (x^*, y^*) \in O$ be an equilibrium for the system (3.15a,b). Let $V:U \rightarrow R$ be a continuous function defined on a neighborhood of (x^*, y^*) , differentiable on $U - (x^*, y^*)$, such that $V(x^*, y^*) = 0$ and $V(x, y) > 0$ if $(x, y) \neq (x^*, y^*)$ Then, if

- (a) $\dot{V} \leq 0$ in $U - (x^*, y^*)$ then (x^*, y^*) is stable. However, if
- (b) $\dot{V} < 0$ in $U - (x^*, y^*)$, then (x^*, y^*) is asymptotically stable.

Harrison [15] studied a general model for a predator-prey interaction

$$\frac{dH}{dt} = a(H) - f(H)b(P) \tag{3.16a}$$

$$\frac{dP}{dt} = n(H)g(P) + c(P), \tag{3.16b}$$

where H is a prey density and P is a predator density. He found the equilibrium points and also constructed a Liapunov function for the model .

Firstly, he assumed that $f(H)$, $n(H)$, and $b(P)$ are all nondecreasing functions, that there exist positive equilibrium densities H^* and p^* and that $f(H)$ and $g(P)$ are positive over intervals containing H^* and P^* . His Liapunov function is

$$V(H, P) = \int_{H^*}^H \frac{n(x) - n(H^*)}{f(x)} dx + \int_{P^*}^P \frac{b(x) - b(P^*)}{g(x)} dx \tag{3.17}$$

where $[n(H) - n(H^*)][H - H^*] > 0$ for $H \neq H^*$, and $[b(P) - b(P^*)][P - P^*] > 0$ for $P \neq P^*$.

Our system (3.2a,b)

$$\frac{dx}{d\tau} = mxy - \sigma x = (my - \sigma)x$$

$$\frac{dy}{d\tau} = 1 - mxy - \phi y = 1 - (mx + \phi)y$$

looks similar to the Harrison predator-prey model. We can modify his approach in order to construct our own Liapunov function. Comparing our model to Harrison’s model, we get

$$a(H) \equiv 1, n(H) \equiv my - \sigma, f(H) \equiv y, g(P) \equiv x, b(P) \equiv mx + \phi, c(P) \equiv 0.$$

Lemma 3.2 Assume that $[my - \sigma - (my^* - \sigma)][y - y^*] > 0$ for $y \neq y^*$ and $[mx + \phi - (mx^* + \phi)][x - x^*] > 0$ for $x \neq x^*$. The Liapunov function is

$$V(x, y) = (x - x^*) + x^* \ln\left(\frac{x^*}{x}\right) + (y - y^*) + y^* \ln\left(\frac{y^*}{y}\right).$$

Proof

$$U(x, y) = \int_{y^*}^y \frac{(ms - \sigma) - (my^* - \sigma)}{s} ds + \int_{x^*}^x \frac{(ms + \phi) - (mx^* + \phi)}{s} ds \quad (3.18)$$

$$\text{Then, } U(x, y) = \int_{y^*}^y \left(m - \frac{my^*}{s}\right) ds + \int_{x^*}^x \left(m - \frac{mx^*}{s}\right) ds \quad (3.19)$$

$$\begin{aligned} &= m s \left|_{y^*}^y - m y^* \ln s \right|_{y^*}^y + m s \left|_{x^*}^x - m x^* \ln s \right|_{x^*}^x \\ &= m(y - y^*) - m y^* \ln\left(\frac{y}{y^*}\right) + m(x - x^*) - m x^* \ln\left(\frac{x}{x^*}\right) \\ &= m(x - x^*) + m x^* \ln\left(\frac{x^*}{x}\right) + m(y - y^*) + m y^* \ln\left(\frac{y^*}{y}\right) \\ &= m \left[(x - x^*) + x^* \ln\left(\frac{x^*}{x}\right) + (y - y^*) + y^* \ln\left(\frac{y^*}{y}\right) \right]. \end{aligned} \quad (3.20)$$

Since m is positive, we define a Liapunov function

$$V(x, y) = (x - x^*) + x^* \ln\left(\frac{x^*}{x}\right) + (y - y^*) + y^* \ln\left(\frac{y^*}{y}\right). \quad (3.21)$$

The Liapunov function (3.21) is called Volterra's Liapunov function. It can be easily verified that $V(x, y)$ is zero at the equilibrium point.

Lemma 3.3 $V(x, y)$ is positive definite in O .

Proof The relation $x > \ln(1+x) > \frac{x}{(1+x)}$, for $x > -1$ is useful for this proof and it is

illustrated in Figure 3.10

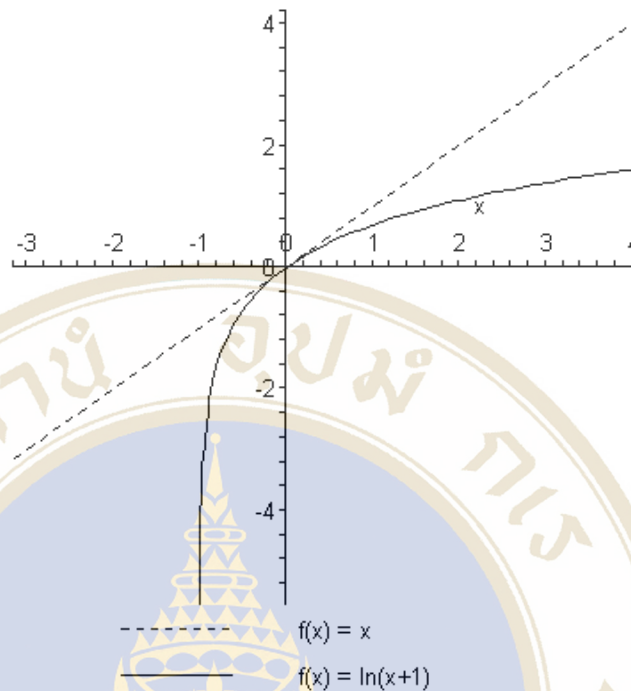


Figure 3.10 Graph of $f(x) = x$ and $f(x) = \ln(x+1)$.

According to $V(x, y) = (x - x^*) + x^* \ln\left(\frac{x}{x^*}\right) + (y - y^*) + y^* \ln\left(\frac{y}{y^*}\right)$, we can rewrite $V(x, y)$ as a linear combination of the functions $V_1(x)$ and $V_2(y)$ as follows

$$V(x, y) = V_1(x) + V_2(y), \tag{3.22}$$

where
$$V_1(x) = (x - x^*) + x^* \ln\left(\frac{x}{x^*}\right) \tag{3.23}$$

and
$$V_2(y) = (y - y^*) + y^* \ln\left(\frac{y}{y^*}\right). \tag{3.24}$$

Let $u_1 = x - x^*$.

Firstly, consider $V_1(x) = u_1 + x^* \ln\left(\frac{x}{u_1 + x^*}\right)$ (3.25)

where $V_1(x) = u_1 - x^* \ln\left(\frac{u_1 + x^*}{x^*}\right)$ because $\ln\left(\frac{1}{x}\right) = -\ln x$. Obviously,

$$V_1(x) = u_1 - x^* \ln \left(\frac{u_1}{x^*} + 1 \right) \quad (3.26)$$

and $V_1(x) = x^* \left(\frac{u_1}{x^*} - \ln \left(\frac{u_1}{x^*} + 1 \right) \right)$ where x^* is a positive number.

Finally, $\frac{u_1}{x^*} - \ln \left(\frac{u_1}{x^*} + 1 \right) > 0$ because $\frac{u_1}{x^*} > -1$.

Therefore, $V_1(x) = (x - x^*) + x^* \ln \left(\frac{x^*}{x} \right)$ is positive definite.

Similarly it can be proved that $V_2(y) = (y - y^*) + y^* \ln \left(\frac{y^*}{y} \right)$ is also positive definite.

Finally we can conclude that $V(x, y) = (x - x^*) + x^* \ln \left(\frac{x^*}{x} \right) + (y - y^*) + y^* \ln \left(\frac{y^*}{y} \right)$ is positive definite.

Lemma 3.4 $\dot{V}(x, y)$ is negative definite in O .

Proof We attempt to show that $\dot{V}(x, y) = \frac{\partial V}{\partial x} \dot{x} + \frac{\partial V}{\partial y} \dot{y}$ is negative definite relative to E^* in the set O . Consider $\dot{V}(x, y)$ for our system. We have

$$\frac{\partial V}{\partial x} \dot{x} + \frac{\partial V}{\partial y} \dot{y} = \left(1 - \frac{x^*}{x} \right) (mxy - \sigma x) + \left(1 - \frac{y^*}{y} \right) (1 - mxy - \phi y) \quad (3.27)$$

For the second equilibrium point $(x_2^*, y_2^*) = \left(\frac{1}{m} \left(\frac{m}{\sigma} - \phi \right), \frac{\sigma}{m} \right)$, we obtain

$$\dot{V}(x, y) = 2 - \frac{my}{\sigma} - \frac{\sigma}{my}. \quad (3.28)$$

The y value of the stable equilibrium E_2^* is $y^* = \frac{\sigma}{m}$. After substituting $y^* = \frac{\sigma}{m}$ into

equation (3.28), we find that $\dot{V}(x, y) = 0$. Therefore, if we can show that $\dot{V}(x, \frac{\sigma}{m})$ is the

absolute maximum value of $\dot{V}(x, y)$ then $\dot{V}(x, y)$ will be negative definite. Firstly we find the derivative of $\dot{V}(x, y)$ with respect to y and obtain

$$\frac{d(\dot{V}(x, y))}{dy} = -\frac{m}{\sigma} + \frac{\sigma}{my^2}. \tag{3.29}$$

We then set it equal to zero in order to find the critical point:

$$-\frac{m}{\sigma} + \frac{\sigma}{my^2} = 0. \tag{3.30}$$

There are two critical points, namely $\frac{\sigma}{m}, -\frac{\sigma}{m}$. However, $-\frac{\sigma}{m}$ is out of our interest domain. Therefore $y_c = \frac{\sigma}{m}$ is only critical point of our model.

By the second derivative test, $\frac{d^2(\dot{V}(x, y))}{dy^2} = -\frac{2\sigma}{my^3} < 0$, so the critical point is the relative maximum. Thus $\dot{V}(x, y) = 2 - \frac{my}{\sigma} - \frac{\sigma}{my}$ is negative definite. The graph of $\dot{V}(x, y)$ is shown in Figure 3.11.

Therefore, $V(x, y) = (x - x^*) + x^* \ln\left(\frac{x}{x^*}\right) + (y - y^*) + y^* \ln\left(\frac{y}{y^*}\right)$ is a suitable Liapunov function for model I, showing that the equilibrium point E_2^* is also globally stable.

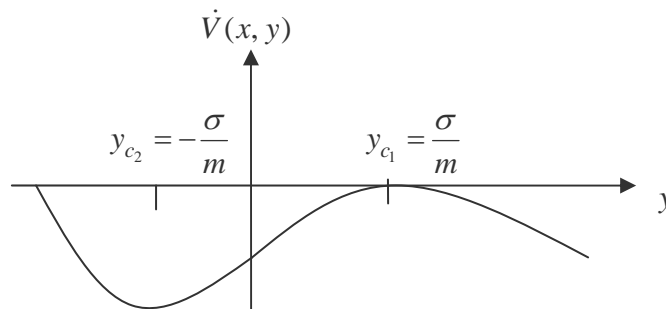


Figure 3.11 The sketch of the curve $\dot{V}(x, y)$.

We have shown that our first model has two equilibrium points. For one range of parameter values one of the points will be asymptotically stable and for the remaining range of parameter values the second point will be asymptotically stable. Therefore for all parameter values there will be one stable equilibrium point. Therefore the conditions for a Hopf bifurcation cannot occur and a limit cycle cannot occur through a Hopf bifurcation. We will now examine a second model in which the TN source is periodic. This periodic source model is more likely to be realistic because of the occurrence of tides and seasons in the real world.

3.2 Two-Dimensional Model: Periodic Input

A real mangrove forest is open to the sea and therefore the tides cause a periodic change in the water flow in the forest. We will assume that the change is represented by a cosine function.

We modify equation (3.1b) by replacing the source term Q by a periodic function. The modified equations are:

$$\frac{dT}{dt} = \beta NT - \sigma T \quad (3.31a)$$

$$\frac{dN}{dt} = Q \left(\frac{1 + \cos \omega t}{2} \right) - \beta NT - \phi N. \quad (3.31b)$$

The model system (3.31) can be non-dimensionalised by substituting

$$x = \frac{2T}{Q}, \quad y = \frac{2N}{Q},$$

and we obtain

$$\frac{dx}{dt} = \frac{\beta Q}{2} xy - \sigma x \quad (3.32a)$$

$$\frac{dy}{dt} = (1 + \cos \omega t) - \frac{\beta Q}{2} xy - \phi y. \quad (3.32b)$$

Let $\sigma = \phi$.

If we combine equations (3.32a,b) the nonlinear xy terms cancel and we obtain the linear equation;

$$\frac{d(x+y)}{dt} = (1 + \cos \omega t) - \sigma(x+y) \quad (3.33)$$

Then letting $(x + y) = s$, we obtain the first order linear equation

$$\frac{ds}{dt} + \sigma s = (1 + \cos \omega t) \tag{3.34}$$

which can be solved by the integrating factor method.

The integrating factor is $u(t) = e^{\int \sigma dt} = e^{\sigma t}$, and therefore the solution is:

$$s(t) = e^{-\sigma t} \left[\int_0^t e^{\sigma \tau} (1 + \cos \omega \tau) d\tau + C \right]. \tag{3.35}$$

Let $\Phi(t) = \int_0^t e^{\sigma \tau} (1 + \cos \omega \tau) d\tau$. (3.36)

$$s(t) = \frac{1}{e^{\sigma t}} [\Phi(t) + C]. \tag{3.37}$$

At $t = 0$, $s(0) = C$. Consider

$$\Phi(t) = \int_0^t e^{\sigma \tau} d\tau + \int_0^t e^{\sigma \tau} \cos \omega \tau d\tau. \tag{3.38}$$

Complex numbers are useful for solving the above equation. We use Euler's formula

$z = re^{i\theta} = r(\cos \theta + i \sin \theta)$. Starting with $e^{\sigma t} \cos \omega t = \operatorname{Re} e^{(\sigma+i\omega)t}$, and then

$$\int_0^t e^{\sigma \tau} \cos \omega \tau d\tau = \operatorname{Re} \int_0^t e^{(\sigma+i\omega)\tau} d\tau \tag{3.39}$$

$$\begin{aligned} &= \operatorname{Re} \left. \frac{e^{(\sigma+i\omega)\tau}}{\sigma+i\omega} \right|_0^t \\ &= \operatorname{Re} \left. \frac{(\sigma-i\omega)e^{(\sigma+i\omega)\tau}}{\sigma^2+\omega^2} \right|_0^t \\ &= \left. \frac{e^{\sigma \tau} (\sigma \cos \omega \tau + \omega \sin \omega \tau)}{\sigma^2 + \omega^2} \right|_0^t \\ &= \frac{e^{\sigma t} (\sigma \cos \omega t + \omega \sin \omega t) - \sigma}{\sigma^2 + \omega^2}. \end{aligned} \tag{3.40}$$

From (3.35), $s(t) = e^{-\sigma t} \left[\int_0^t e^{\sigma \tau} (1 + \cos \omega \tau) d\tau + C \right]$ and therefore from (3.40)

$$s(t) = \frac{1 - e^{-\sigma t}}{\sigma} + \frac{(\sigma \cos \omega t + \omega \sin \omega t) - \sigma e^{-\sigma t}}{\sigma^2 + \omega^2} + s(0)e^{-\sigma t} \tag{3.41}$$

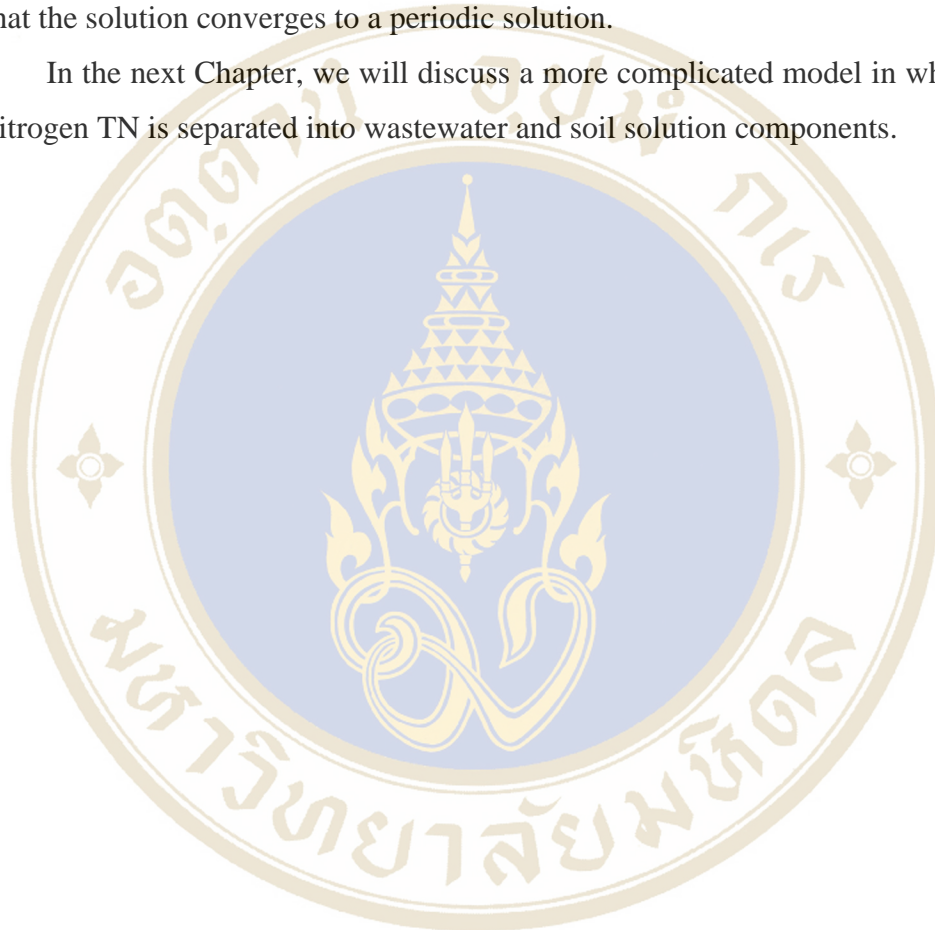
For large t , the exponential terms tend to zero and the solution becomes

$$s(t) = \frac{1}{\sigma} + \frac{(\sigma \cos \omega t + \omega \sin \omega t)}{\sigma^2 + \omega^2} \tag{3.42}$$

which is a periodic solution . Therefore, mangrove has adaptation to its surrounding environment.

Figures 3.12-15 show the results of a numerical solution of the dimensionless model equations (3.32a,b) for parameter values $\frac{\beta Q}{2} = 10$, $\sigma = \phi = 1$. It can be seen that the solution converges to a periodic solution.

In the next Chapter, we will discuss a more complicated model in which the total nitrogen TN is separated into wastewater and soil solution components.



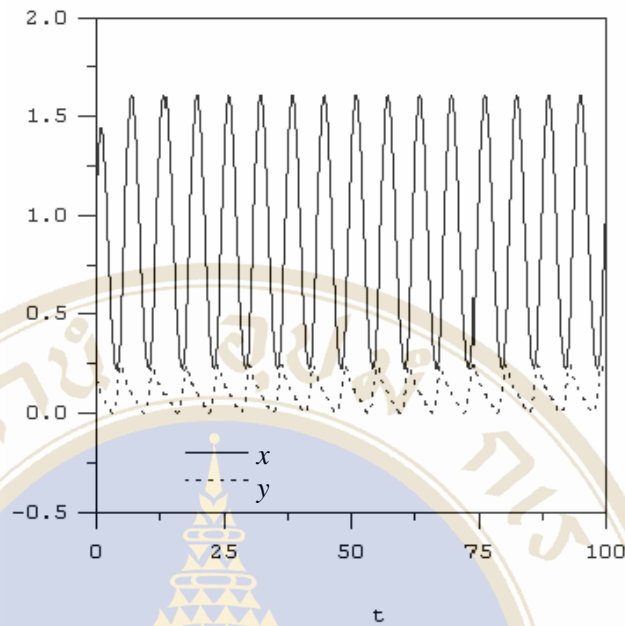


Figure 3.12 Numerical solution of the dimensionless model equations (3.32a,b) for mangrove biomass and TN concentration for the parameters $\frac{\beta Q}{2} = 10$, $\sigma = \phi = 1$.

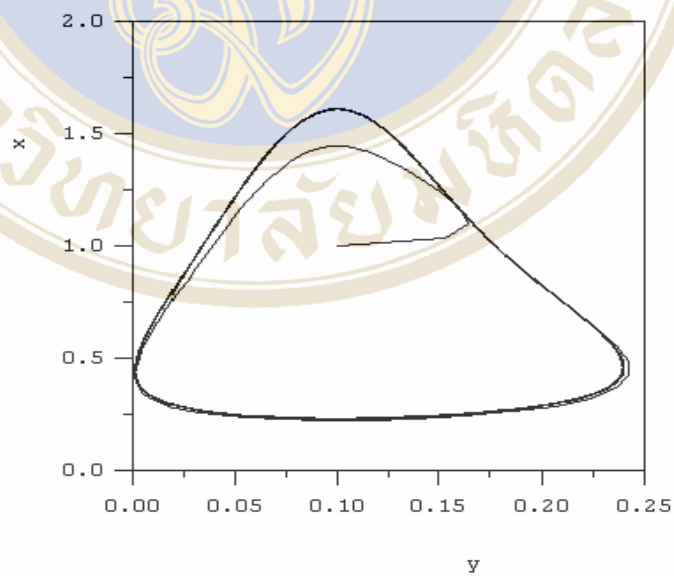


Figure 3.13 Phase plane plot of the solution of the dimensionless model equations (3.32a,b) for mangrove biomass and the TN for parameters are $\frac{\beta Q}{2} = 10$, $\sigma = \phi = 1$.

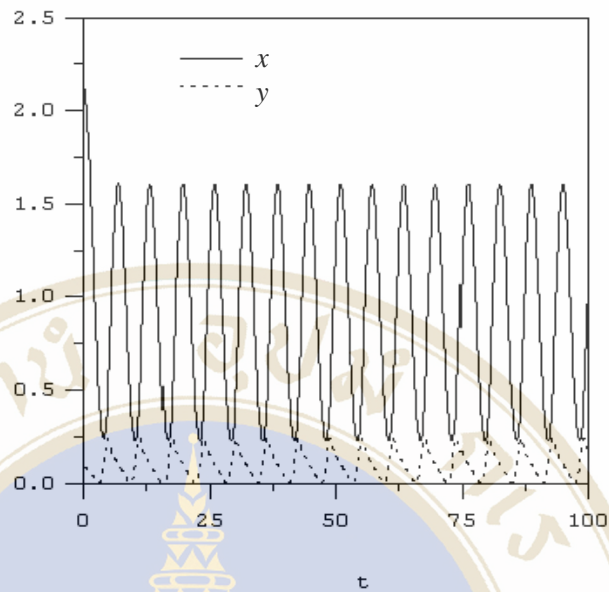


Figure 3.14 Numerical solution of the dimensionless model equations (3.32a,b) for mangrove biomass and TN concentration for the parameters $\frac{\beta Q}{2} = 10$, $\sigma = \phi = 1$.

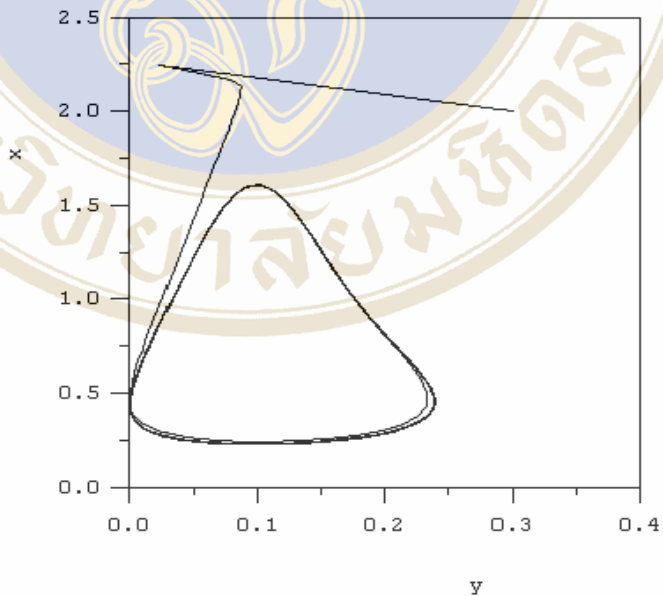


Figure 3.15 Phase plane plot of the solution of the dimensionless model equations (3.32a,b) for mangrove biomass and the TN for parameters are $\frac{\beta Q}{2} = 10$, $\sigma = \phi = 1$.

CHAPTER IV

MODEL ANALYSIS II

In the two-dimensional models discussed in the previous chapter, the system variables consist of the concentration of mangrove biomass and the combined concentration of the TN in wastewater and soil solution. In this chapter, we separate the TN into two parts. The first part is the TN concentration in the wastewater and the second is TN concentration in the soil solution. The mangrove can uptake TN separately from the wastewater and the soil solution because the mangrove has roots both in the water and in the soil. We consider two separate models. In the first model the uptake function is assumed to be a linear function and in the second model the uptake function is assumed to be the nonlinear Monod function.

4.1 Three-Dimensional Model: Linear Uptake Function

Table 4.1 Definition of variables and parameters for model III.

Quantity	Symbol	Dimension
Mangrove biomass concentration	T	mg / ha
TN concentration in wastewater	W	mg / ha
TN concentration in soil solution	S	mg / ha
TN uptake rate	β	$(mg / ha)^{-1}(month)^{-1}$
Litter fall rate	σ	$month^{-1}$
TN input rate	Q	$(mg / ha)(month)^{-1}$
TN loss rate in wastewater	α	$month^{-1}$
TN exchange rate between wastewater to soil solution	γ	$month^{-1}$
TN loss rate in soil solution	ϕ	$month^{-1}$

The system of three ordinary differential equations contains the rate of change of the following: mangrove biomass, TN concentration in wastewater, and TN concentration in soil solution, through time. Table 4.1 gives the definitions, meaning and dimensions of the variables and parameters. For biological processes, each parameter must be positive while each variable must be non-negative.

We attempt to create a model representing the constructed wetland pond that is composed of three interacting components, i.e. the concentration of biomass (T), TN concentration in wastewater (W), and TN concentration in soil solution (S). Their relationships are visualized in Figure 4.1 which is simplified from Figure 3.1.

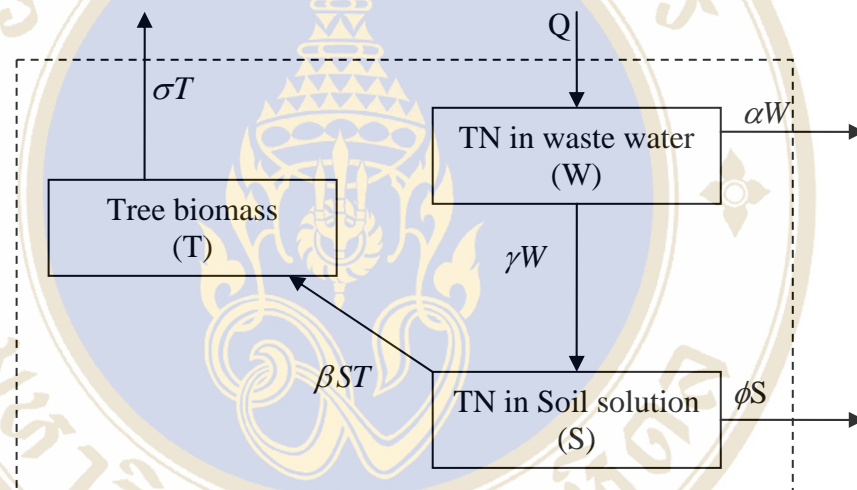


Figure 4.1 The flow chart for the transformation of total nitrogen for model III.

The model is constructed under the same assumptions as before, namely that the nutrient (TN) is nonreproducing and there is perfect mixing in our pond. There is a filter protecting our pond from litter fall. The input rate of TN concentration is a constant, “ Q ”. “ γW ” is the TN exchange rate between wastewater and soil solution. “ αW ” is the loss function of TN in wastewater through runoff or evaporation. “ βST ” is the TN uptake function for plants and also the conversion rate of TN to biomass. “ ϕS ” is the loss function of TN in soil solution through leaching or denitrification. “ σT ” is the rate of litter fall.

A first attempt at writing the rate of change of mangrove biomass concentration in an equation might be

$$\frac{dT}{dt} = fT - \sigma T$$

where f is the growth rate of plants and σ is the litter fall rate. Generally, the growth rate of the population depends on nutrient availability, so that $f = f(S)$. Here, we choose a linear function, i.e.

$$f(S) = \beta S.$$

Therefore, we arrive at the following model:

$$\frac{dT}{dt} = \beta ST - \sigma T \tag{4.1a}$$

$$\frac{dW}{dt} = Q - (\gamma + \alpha)W \tag{4.1b}$$

$$\frac{dS}{dt} = \gamma W - \beta ST - \phi S. \tag{4.1c}$$

A dimensionless system can be obtained by introducing the new variables and parameters

$$x = \frac{T}{Q}, y = \frac{W}{Q}, z = \frac{S}{Q}, m = \beta Q.$$

The transformed non-dimensionalized version of equations (4.1a-c) is given by

$$\frac{dx}{dt} = mxz - \sigma x \tag{4.2a}$$

$$\frac{dy}{dt} = 1 - \gamma y - \alpha y \tag{4.2b}$$

$$\frac{dz}{dt} = \gamma y - mxz - \phi z \tag{4.2c}$$

For convenience, we will use the meaning of the original variables for the dimensionless variables.

The Steady State Solution

From above system, its steady state solutions are obtained by setting

$$\frac{dx}{dt} = 0, \frac{dy}{dt} = 0, \frac{dz}{dt} = 0.$$

Therefore,

$$mxz - \sigma x = 0, \quad (4.3a)$$

$$1 - \gamma y - \alpha y = 0, \quad (4.3b)$$

$$\gamma y - mxz - \phi z = 0. \quad (4.3c)$$

From equation (4.3a); we obtain $x_1^* = 0$ or $z_2^* = \frac{\sigma}{m}$.

From equation (4.3b); we obtain $y_{1,2}^* = \frac{1}{\alpha + \gamma}$.

Then substituting $x_1^* = 0$ and $y_1^* = \frac{1}{\alpha + \gamma}$ into equation (4.3c), we get $z_1^* = \frac{\gamma}{\phi(\alpha + \gamma)}$,

and substituting $z_2^* = \frac{\sigma}{m}$ and $y_2^* = \frac{1}{\alpha + \gamma}$ into equation (4.3c), we get

$$x_2^* = \frac{1}{\sigma} \left(\frac{\gamma}{\alpha + \gamma} - \frac{\phi\sigma}{m} \right).$$

There are two equilibria for this system, namely:

1) the washout only mangrove biomass: $E_1^* = (x_1^*, y_1^*, z_1^*) = \left(0, \frac{1}{\alpha + \gamma}, \frac{\gamma}{\phi(\alpha + \gamma)} \right)$

and

2) the coexistence of mangrove biomass and TN concentration in both wastewater and soil solution: $E_2^* = (x_2^*, y_2^*, z_2^*) = \left(\frac{1}{\sigma} \left(\frac{\gamma}{\alpha + \gamma} - \frac{\phi\sigma}{m} \right), \frac{1}{\alpha + \gamma}, \frac{\sigma}{m} \right)$,

provided that $\frac{\gamma}{\alpha + \gamma} \neq \frac{\phi\sigma}{m}$.

Note that if $\frac{\gamma}{\alpha + \gamma} = \frac{\phi\sigma}{m}$ then the two equilibria coincide.

Lemma 4.1 If the inequality

$$\frac{m\gamma}{\alpha + \gamma} > \phi\sigma \quad (4.4)$$

holds, then the system that is composed of equations (4.2a-c) has a non-negative equilibrium solution

$$E_2^* = (x_2^*, y_2^*, z_2^*) = \left(\frac{1}{\sigma} \left(\frac{\gamma}{\alpha + \gamma} - \frac{\phi\sigma}{m} \right), \frac{1}{\alpha + \gamma}, \frac{\sigma}{m} \right).$$

Lemma 4.1 indicates that if the inequality (4.4) holds, then equilibrium E_2^* exists. However, if the inequality (4.4) fails, the equilibrium E_2^* does not exist because biomass has no meaning when its sign is negative.

4.1.1 Local Stability Analysis

The local stability of each equilibrium point is determined by linearizing equations (4.2a-c) about the steady state and examining the eigenvalues of the resulting Jacobian matrix.

Theorem 4.1 If the inequalities

$$\sigma - mz^* + mx^* + \phi > 0 \tag{4.5}$$

and

$$\sigma mx^* - \phi mz^* + \phi\sigma > 0 \tag{4.6}$$

hold, then steady state (x^*, y^*, z^*) of the equations (4.3a-c) will be stable.

Proof

From system (4.2a-c), the Jacobian matrix is evaluated at an equilibrium point (x^*, y^*, z^*)

$$J_{(x^*, y^*, z^*)} = \begin{bmatrix} mz^* - \sigma & 0 & mx^* \\ 0 & -(\alpha + \gamma) & 0 \\ -mz^* & \gamma & -mx^* - \phi \end{bmatrix}. \tag{4.7}$$

The eigenvalues can be found by solving the following characteristic equation

$$\det(J - \lambda I) = 0. \tag{4.8}$$

Therefore, $(mz^* - \sigma - \lambda)(-(\alpha + \gamma) - \lambda)(-mx^* - \phi - \lambda) - m^2 x^* z^* (\alpha + \gamma + \lambda) = 0$,

$$0 = -(\alpha + \gamma) - \lambda \left[(mz^* - \sigma - \lambda)(-mx^* - \phi - \lambda) + m^2 x^* z^* \right], \tag{4.9}$$

$$0 = -(\alpha + \gamma) - \lambda \left[\lambda^2 + \lambda(\sigma - mz^* + mx^* + \phi) + (\sigma mx^* - \phi mz^* + \phi\sigma) \right], \tag{4.10}$$

The eigenvalues are

$$\lambda_1 = -(\alpha + \gamma), \text{ and} \tag{4.11}$$

$$\lambda_{2,3} = \frac{-(\sigma - mz^* + mx^* + \phi) \pm \sqrt{(\sigma - mz^* + mx^* + \phi)^2 - 4(\sigma mx^* - \phi mz^* + \phi\sigma)}}{2}. \tag{4.12}$$

Obviously, λ_1 is negative.

Therefore, if the inequalities (4.5) and (4.6) hold, all eigenvalues are negative. It means that the equilibrium (x^*, y^*, z^*) is stable.

Theorem 4.2

- 1) The equilibrium point E_1^* is unstable if $\frac{m\gamma}{\alpha + \gamma} > \phi\sigma$ and stable if $\frac{m\gamma}{\alpha + \gamma} < \phi\sigma$.
- 2) The equilibrium point E_2^* is stable if $\frac{m\gamma}{\alpha + \gamma} < \phi\sigma$ and unstable if $\frac{m\gamma}{\alpha + \gamma} > \phi\sigma$.

However, E_2^* has no biological meaning if $\frac{m\gamma}{\alpha + \gamma} < \phi\sigma$.

Proof Using the equation (4.12),

$$\lambda_{2,3} = \frac{-(\sigma - mz^* + mx^* + \phi) \pm \sqrt{(\sigma - mz^* + mx^* + \phi)^2 - 4(\sigma mx^* - \phi mz^* + \phi\sigma)}}{2}.$$

- 1) For the first equilibrium $E_1^* (x_1^*, y_1^*, z_1^*) = (0, \frac{1}{(\alpha + \gamma)}, \frac{\gamma}{\phi(\alpha + \gamma)})$.

Case 1: The inequality $\frac{m\gamma}{\alpha + \gamma} > \phi\sigma$ holds.

The corresponding eigenvalues can be obtained by substitute E_1^* into equation (4.12).

$$\text{Therefore, } \lambda_{2,3} = \frac{-(\sigma + \phi - \frac{m\gamma}{\phi(\alpha + \gamma)}) \pm \sqrt{(\sigma + \phi - \frac{m\gamma}{\phi(\alpha + \gamma)})^2 - 4(\phi\sigma - \frac{m\gamma}{\alpha + \gamma})}}{2}. \quad (4.13)$$

Thus the term $(\sigma + \phi - \frac{m\gamma}{\phi(\alpha + \gamma)})^2 - 4(\phi\sigma - \frac{m\gamma}{\alpha + \gamma})$ is positive.

The inequality $\frac{m\gamma}{\alpha + \gamma} > \sigma\phi$, leads to $\frac{m\gamma}{\phi(\alpha + \gamma)} > \sigma$ and $\frac{m\gamma}{\alpha + \gamma} - \sigma\phi > 0$.

Therefore, one eigenvalues is positive and other are negative. Consequently, E_1^* is unstable.

Case 2: The inequality (4.4) reverses, i.e. $\frac{m\gamma}{\alpha + \gamma} < \phi\sigma$.

The corresponding eigenvalues are

$$\lambda_{2,3} = \frac{-(\sigma + \phi - \frac{m\gamma}{\phi(\alpha + \gamma)}) \pm \sqrt{(\sigma + \phi - \frac{m\gamma}{\phi(\alpha + \gamma)})^2 - 4(\phi\sigma - \frac{m\gamma}{\alpha + \gamma})}}{2}.$$

All eigenvalues are negative because $\frac{m\gamma}{\alpha + \gamma} < \phi\sigma$. Therefore, the equilibrium point

$E_1^* (x_1^*, y_1^*, z_1^*) = (0, \frac{1}{\alpha + \gamma}, \frac{\gamma}{\phi(\alpha + \gamma)})$ is stable. Figure 4.2-4 show the result of a

numerical solution of the dimensionless model equations (4.2a-c) for parameter values $m = 0.05$, $\sigma = 1$, $\gamma = 0.5$, $\alpha = 0.5$, $\phi = 2$ for which the equilibrium point E_1^* is stable.

It can be seen that the mangrove biomass concentration, TN concentration in wastewater and soil solution tend toward the equilibrium point $E_1^* =$

$$(0, \frac{1}{\alpha + \gamma}, \frac{\gamma}{\phi(\alpha + \gamma)}) = (0, 1, 0.25).$$

2) For the equilibrium point, $E_2^* (x_2^*, y_2^*, z_2^*) = (\frac{1}{\sigma} (\frac{\gamma}{\alpha + \gamma} - \frac{\phi\sigma}{m}), \frac{1}{\alpha + \gamma}, \frac{\sigma}{m})$.

Case 1: The inequality $\frac{m\gamma}{\alpha + \gamma} > \phi\sigma$ holds.

The corresponding eigenvalues are

$$\lambda_{2,3} = \frac{-\left(\frac{m}{\sigma} \left(\frac{\gamma}{\alpha + \gamma} - \frac{\phi\sigma}{m}\right) + \phi\right) \pm \sqrt{\left(\frac{m}{\sigma} \left(\frac{\gamma}{\alpha + \gamma} - \frac{\phi\sigma}{m}\right) + \phi\right)^2 - 4m \left(\frac{\gamma}{\alpha + \gamma} - \frac{\phi\sigma}{m}\right)}}{2}$$

$$\text{or } \lambda_{2,3} = \frac{-\left(\frac{m\gamma}{\sigma(\alpha + \gamma)}\right) \pm \sqrt{\left(\frac{m\gamma}{\sigma(\alpha + \gamma)}\right)^2 - 4\left(\frac{m\gamma}{\alpha + \gamma} - \phi\sigma\right)}}{2}. \tag{4.14}$$

All eigenvalues are negative because $\frac{m\gamma}{\alpha + \gamma} > \phi\sigma$. Thus the second equilibrium is

stable. Figure 4.5-7 show the results of numerical solution of the dimensionless model equations (4.2a-c) for mangrove biomass concentration, TN concentration in wastewater and soil solution for parameters $m = 5$, $\sigma = 1$, $\gamma = 0.5$, $\alpha = 0.5$, $\phi = 0.1$ which is the equilibrium point E_2^* is stable. It can be seen that the mangrove biomass

concentration, TN concentration in wastewater and soil solution tend toward the

equilibrium point $E_2^* = \left(\frac{1}{\sigma} \left(\frac{\gamma}{\alpha + \gamma} - \frac{\phi\sigma}{m} \right), \frac{1}{\alpha + \gamma}, \frac{\sigma}{m} \right) = (0.48, 1, 0.2)$.

Case 2: The inequality (4.4) reverses, i.e. $\frac{m\gamma}{\alpha + \gamma} < \phi\sigma$.

The corresponding eigenvalues are

$$\lambda_{2,3} = \frac{-\left(\frac{m\gamma}{\sigma(\alpha + \gamma)}\right) \pm \sqrt{\left(\frac{m\gamma}{\sigma(\alpha + \gamma)}\right)^2 - 4\left(\frac{m\gamma}{\alpha + \gamma} - \phi\sigma\right)}}{2}.$$

We can conclude that $E_2^* (x_2^*, y_2^*, z_2^*) = \left(\frac{1}{\sigma} \left(\frac{\gamma}{\alpha + \gamma} - \frac{\phi\sigma}{m} \right), \frac{1}{\alpha + \gamma}, \frac{\sigma}{m} \right)$ is unstable

because the inequality $\frac{m\gamma}{\alpha + \gamma} < \phi\sigma$ leads to one positive and one negative eigenvalues.

Oscillations occur when the second and third eigenvalues are complex numbers i.e.

$$\left(\frac{m\gamma}{\sigma(\alpha + \gamma)}\right)^2 - 4\left(\frac{m\gamma}{\alpha + \gamma} - \phi\sigma\right) < 0$$

since the parameters m, γ, α and σ are positive, the real parts of all eigenvalues are negative, and therefore the equilibrium point is stable. Finally, the equilibrium point, E_2^* is asymptotic stable.

Figure 4.8-10 show the results of numerical solution of the dimensionless model equations (4.2a-c) for mangrove biomass concentration, TN concentration in wastewater and soil solution for parameters $m = 0.05$, $\sigma = 0.5$, $\gamma = 0.4$, $\alpha = 0.1$, $\phi = 0.001$ for which the equilibrium point E_2^* is asymptotically stable. It can be seen that the mangrove biomass concentration, TN concentration in wastewater and soil solution tend toward the equilibrium point $E_2^* = \left(\frac{1}{\sigma} \left(\frac{\gamma}{\alpha + \gamma} - \frac{\phi\sigma}{m} \right), \frac{1}{\alpha + \gamma}, \frac{\sigma}{m} \right) = (1.58, 2, 10)$.

Lemma 4.2

It is impossible for the eigenvalues ($\lambda_{2,3}$) to be purely imaginary.

Proof

Let real part $\phi + \frac{\gamma m - \phi \sigma (\alpha + \gamma)}{\sigma (\alpha + \gamma)} = 0$. It is impossible because ϕ and $\frac{\gamma m - \phi \sigma (\alpha + \gamma)}{\sigma (\alpha + \gamma)}$ are strictly positive. Therefore a Hopf bifurcation cannot exist at any equilibrium point.

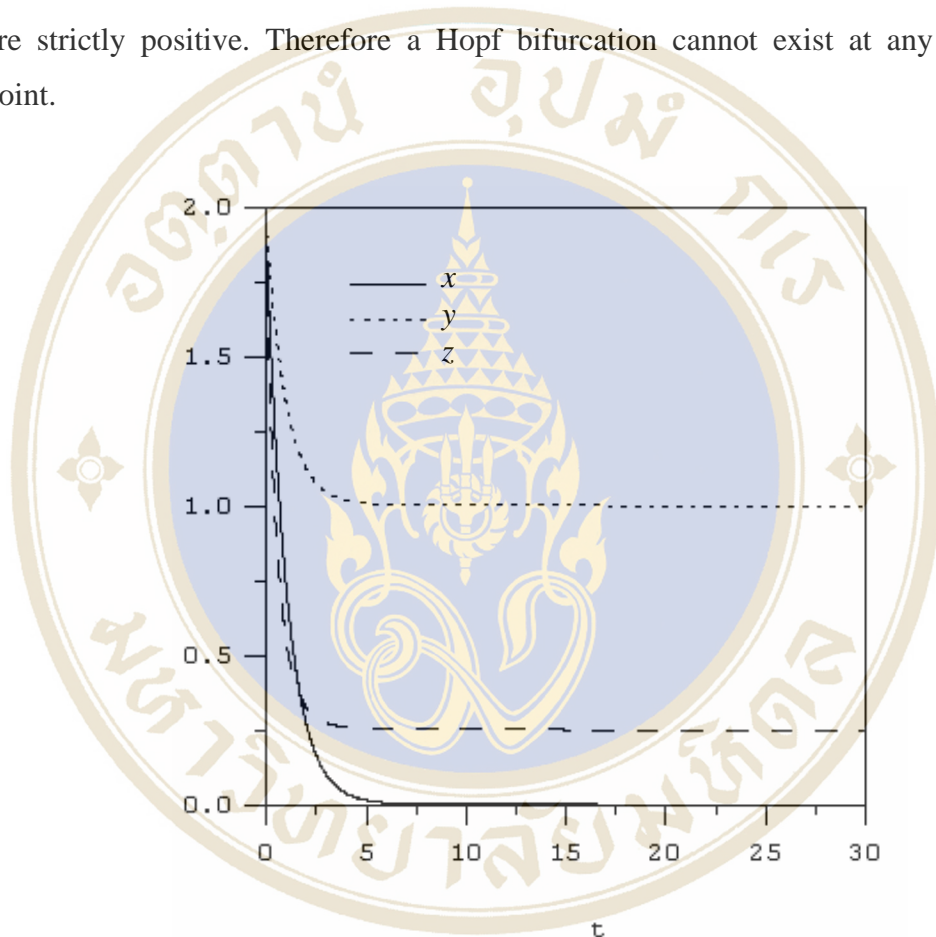


Figure 4.2 Numerical solution of the dimensionless model equations (4.2a-c) for parameters $m = 0.05$, $\sigma = 1$, $\gamma = 0.5$, $\alpha = 0.5$, $\phi = 2$.

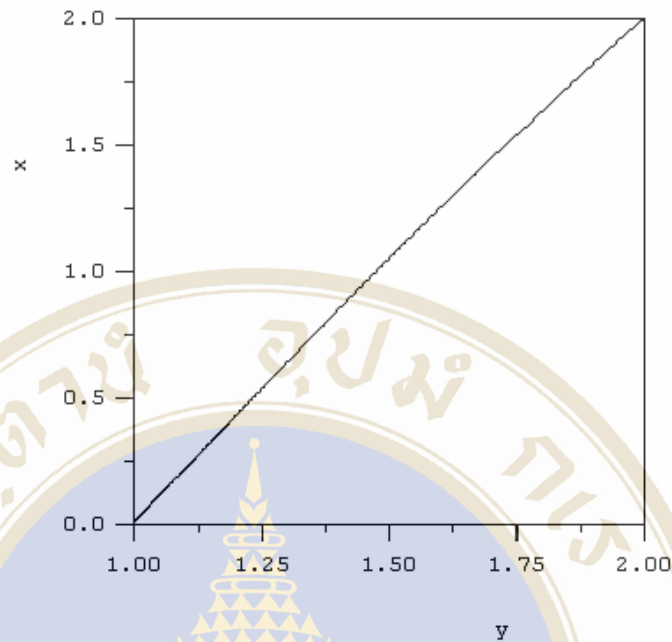


Figure 4.3 Phase plane plot of the dimensionless model equations (4.2a-c) for TN concentration in wastewater and concentration of mangrove biomass for parameters $m = 0.05$, $\sigma = 1$, $\gamma = 0.5$, $\alpha = 0.5$, $\phi = 2$.

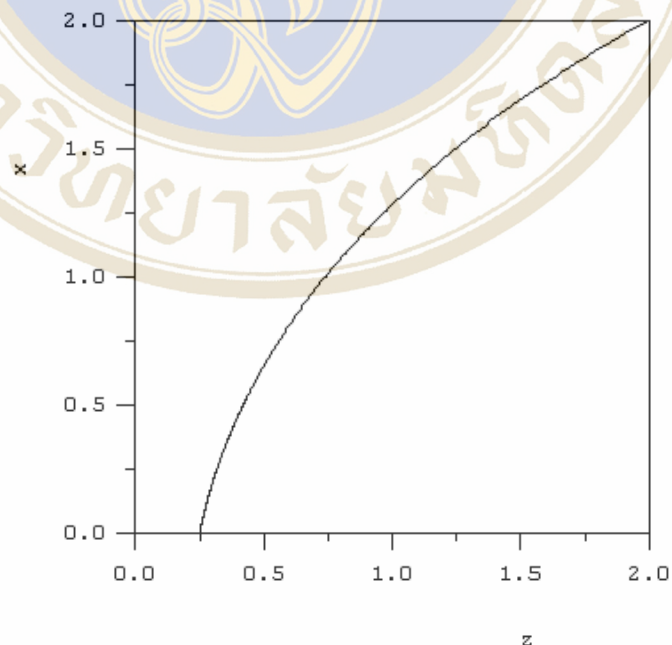


Figure 4.4 Phase plane plot of the dimensionless model equations (4.2a-c) for TN concentration in soil solution and concentration of mangrove biomass for parameters $m = 0.05$, $\sigma = 1$, $\gamma = 0.5$, $\alpha = 0.5$, $\phi = 2$.

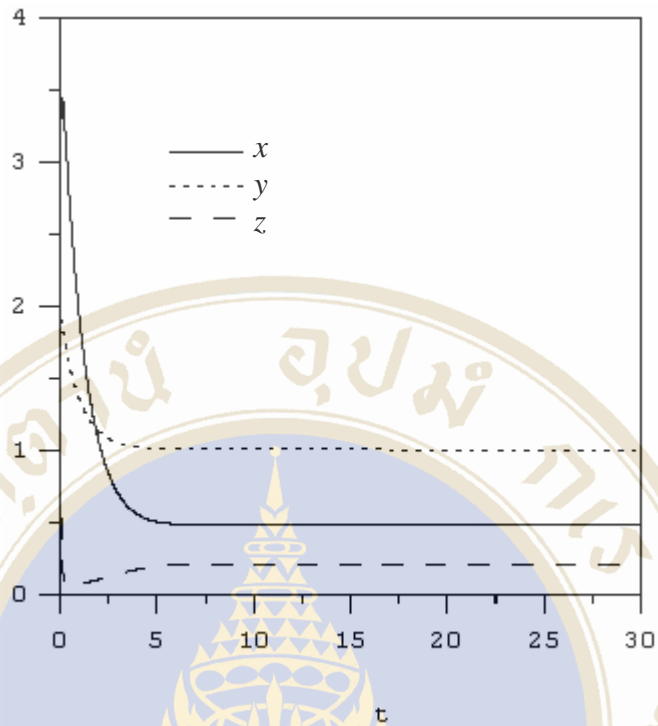


Figure 4.5 Numerical solution of the dimensionless model equations (4.2a-c) for mangrove biomass concentration, TN concentration in wastewater and soil solution for parameters $m = 5$, $\sigma = 1$, $\gamma = 0.5$, $\alpha = 0.5$, $\phi = 0.1$.

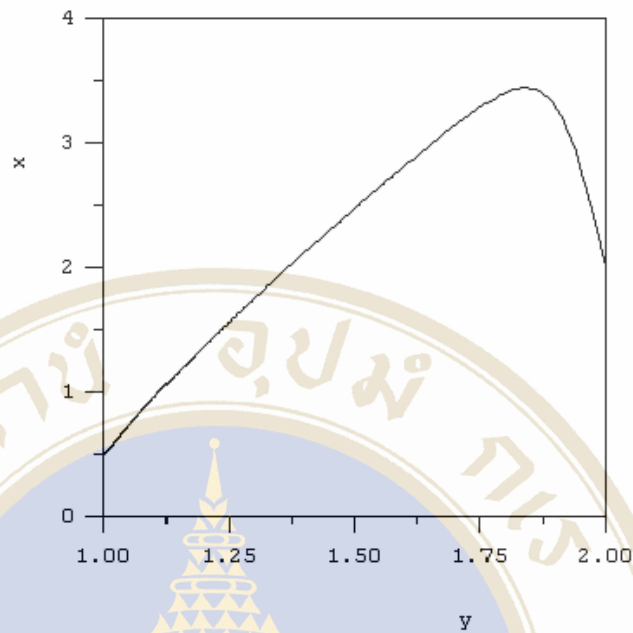


Figure 4.6 Phase plane plot of the dimensionless model equations (4.2a-c) for TN concentration in wastewater and concentration of mangrove biomass for parameters $m = 5$, $\sigma = 1$, $\gamma = 0.5$, $\alpha = 0.5$, $\phi = 0.1$.

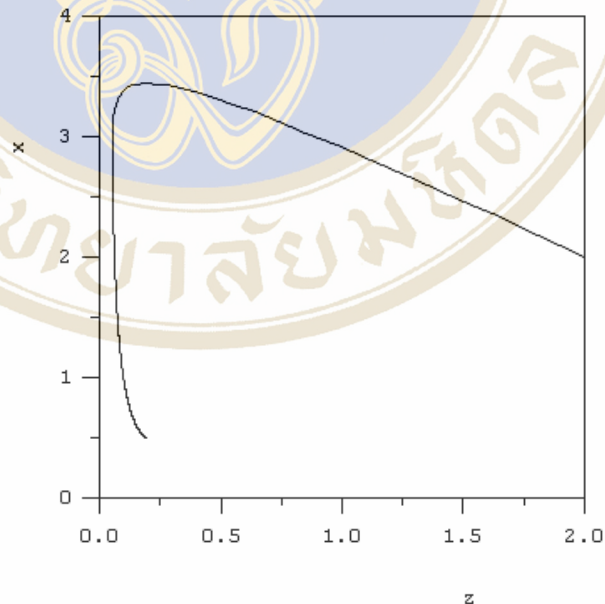


Figure 4.7 Phase plane plot of the dimensionless model equations (4.2a-c) for TN concentration in soil solution and concentration of mangrove biomass for parameters $m = 5$, $\sigma = 1$, $\gamma = 0.5$, $\alpha = 0.5$, $\phi = 0.1$.

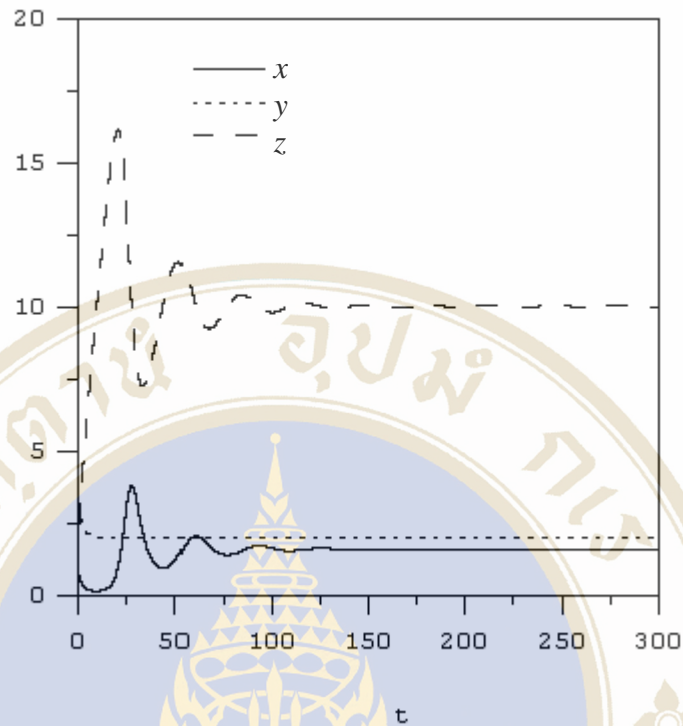


Figure 4.8 Numerical solution of the dimensionless model equations (4.2a-c) for mangrove biomass concentration, TN concentration in wastewater and soil solution for parameters $m = 0.05$, $\sigma = 0.5$, $\gamma = 0.4$, $\alpha = 0.1$, $\phi = 0.001$.

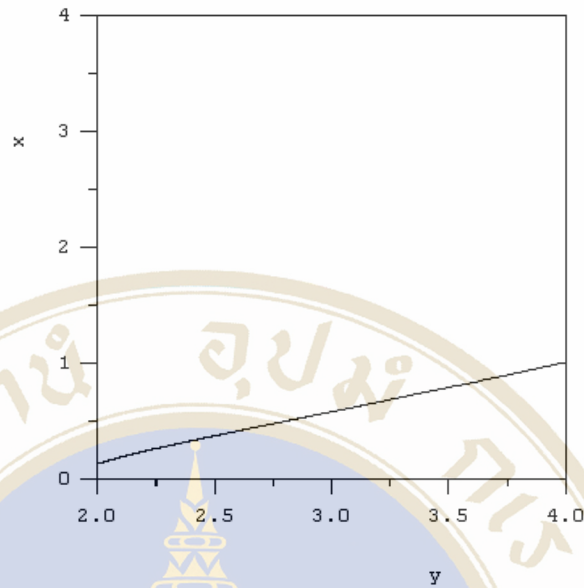


Figure 4.9 Phase plane plot of the dimensionless model equations (4.2a-c) for TN concentration in wastewater and concentration of mangrove biomass for parameters $m = 0.05$, $\sigma = 0.5$, $\gamma = 0.4$, $\alpha = 0.1$, $\phi = 0.001$.

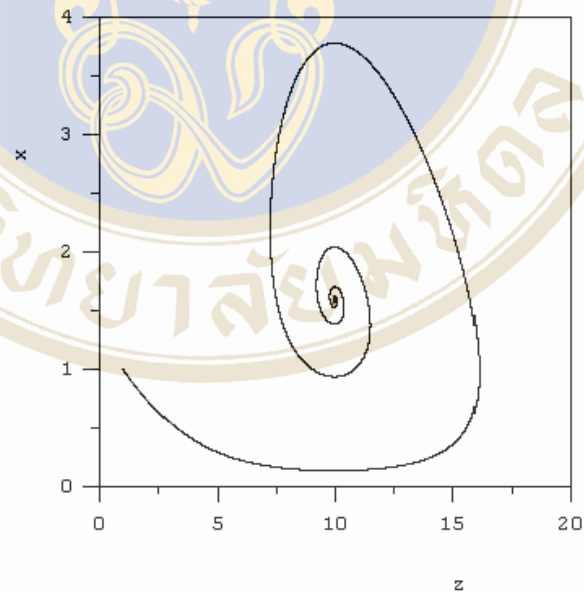


Figure 4.10 Phase plane plot of the dimensionless model equations (4.2a-c) for TN concentration in soil solution and concentration of mangrove biomass for parameters $m = 0.05$, $\sigma = 0.5$, $\gamma = 0.4$, $\alpha = 0.1$, $\phi = 0.001$.

The local stability has already been analyzed. Next, the global stability will be discussed.

4.1.2 Global Stability Analysis

The global stability of the system (4.1a-c), can be analyzed by looking at the equivalent dimensionless system (4.2a-c).

The Liapunov function for the two-dimensional system (3.21) can be expanded to the three-dimensions system as follows,

$$V(x, y, z) = (x - x^*) + x^* \ln\left(\frac{x}{x^*}\right) + (y - y^*) + y^* \ln\left(\frac{y}{y^*}\right) + (z - z^*) + z^* \ln\left(\frac{z}{z^*}\right). \quad (4.15)$$

We now check that $V(x, y, z)$ satisfies the conditions stated in Theorem 3.4 for a Liapunov function.

Lemma 4.3 $V(x^*, y^*, z^*) = 0$.

Proof
$$V(x^*, y^*, z^*) = (x^* - x^*) + x^* \ln\left(\frac{x^*}{x^*}\right) + (y^* - y^*) + y^* \ln\left(\frac{y^*}{y^*}\right) + (z^* - z^*) + z^* \ln\left(\frac{z^*}{z^*}\right) = 0.$$

Lemma 4.4 $V(x, y, z)$ is positive definite in O .

Proof The proof is similar to the proof of Lemma 3.3.

The final condition is that \dot{V} is zero at the equilibrium point and negative definite in a region surrounding the equilibrium point. \dot{V} can be calculated by

$$\dot{V}(x, y, z) = \frac{\partial V}{\partial x} \dot{x} + \frac{\partial V}{\partial y} \dot{y} + \frac{\partial V}{\partial z} \dot{z}. \quad (4.16)$$

Since
$$\frac{\partial V}{\partial x} \dot{x} = \left(1 - \frac{x^*}{x}\right) (mxz - \sigma x), \quad (4.17)$$

$$\frac{\partial V}{\partial y} \dot{y} = \left(1 - \frac{y^*}{y}\right) (1 - \gamma y - \alpha y), \quad (4.18)$$

$$\frac{\partial V}{\partial z} \dot{z} = \left(1 - \frac{z^*}{z}\right) (\gamma y - mxz - \phi z). \quad (4.19)$$

$$\dot{V} = \left(1 - \frac{x^*}{x}\right) (mxz - \sigma x) + \left(1 - \frac{y^*}{y}\right) (1 - \gamma y - \alpha y) + \left(1 - \frac{z^*}{z}\right) (\gamma y - mxz - \phi z). \quad (4.20)$$

Thus
$$\dot{V}(x, y, z) = 2 + \frac{\gamma}{(\alpha + \gamma)} - \alpha y - \frac{1}{(\alpha + \gamma)y} - \frac{\sigma \gamma y}{mz} - \frac{m \gamma z}{\sigma(\alpha + \gamma)}. \quad (4.21)$$

Lemma 4.5 $\dot{V}(x, y, z) = 0$ at equilibrium point E_2^* .

The equilibrium point is $E_2^* = \left(\frac{1}{\sigma} \left(\frac{\gamma}{\alpha + \gamma} - \frac{\phi\sigma}{m} \right), \frac{1}{\alpha + \gamma}, \frac{\sigma}{m} \right)$.

$$\begin{aligned} \dot{V}(x, y, z) &= 2 + \frac{\gamma}{(\alpha + \gamma)} - \alpha y - \frac{1}{(\alpha + \gamma)y} - \frac{\sigma\gamma y}{mz} - \frac{m\gamma z}{\sigma(\alpha + \gamma)} \\ &= 2 + \frac{\gamma}{(\alpha + \gamma)} - \frac{\alpha}{(\alpha + \gamma)} - \frac{(\alpha + \gamma)}{(\alpha + \gamma)} - \frac{m\sigma\gamma}{m\sigma(\alpha + \gamma)} - \frac{m\gamma\sigma}{\sigma m(\alpha + \gamma)} \\ &= 0. \end{aligned}$$

Lemma 4.6 $\dot{V}(x, y, z)$ is negative definite in O .

Proof $\dot{V}(x, y, z) = 2 + \frac{\gamma}{(\alpha + \gamma)} - \alpha y - \frac{1}{(\alpha + \gamma)y} - \frac{\sigma\gamma y}{mz} - \frac{m\gamma z}{\sigma(\alpha + \gamma)}$.

Obviously, $\dot{V}(x, y, z)$ depends only on two variables y and z . Thus we can suppose that $\dot{V}(x, y, z) = f(y, z)$. Then

$$f_y(y, z) = -\alpha + \frac{1}{(\alpha + \gamma)y^2} - \frac{\sigma\gamma}{mz}, \quad (4.22)$$

$$f_z(y, z) = \frac{\sigma\gamma y}{mz^2} - \frac{m\gamma}{\sigma(\alpha + \gamma)}. \quad (4.23)$$

To obtain a stationary point, equations (4.22) and (4.23) should equal to zero, i.e.

$$\begin{aligned} \frac{1}{(\alpha + \gamma)y^2} &= \frac{\sigma\gamma}{mz} + \alpha, \\ mz &= (\sigma\gamma + \alpha mz)(\alpha + \gamma)y^2. \end{aligned} \quad (4.24)$$

Setting equation (4.23) equal to zero; $y = \frac{m^2 z^2}{\sigma^2(\alpha + \gamma)}$, or

$$y^2 = \frac{m^4 z^4}{\sigma^4(\alpha + \gamma)^2}. \quad (4.25)$$

Substituting condition (4.25) into equation (4.24); we obtain

$$mz = (\sigma\gamma + \alpha mz)(\alpha + \gamma) \left(\frac{m^4 z^4}{\sigma^4(\alpha + \gamma)^2} \right), \quad (4.26)$$

$$1 = (\sigma\gamma + \alpha mz) \left(\frac{m^3 z^3}{\sigma^4(\alpha + \gamma)} \right),$$

$$\sigma^4(\alpha + \gamma) = m^3 z^3 (\sigma\gamma + \alpha m z), \tag{4.27}$$

$$\alpha m^4 z^4 + \sigma\gamma m^3 z^3 - \sigma^4(\alpha + \gamma) = 0. \tag{4.28}$$

Suppose
$$g(z) = \alpha m^4 z^4 + \sigma\gamma m^3 z^3 - \sigma^4(\alpha + \gamma). \tag{4.29}$$

Then zeros of $g(z) = 0$ imply stationary points of $f(y, z)$. The graph of $g(z)$ can easily be obtained by elementary calculus to be as shown in Figure 4.11.

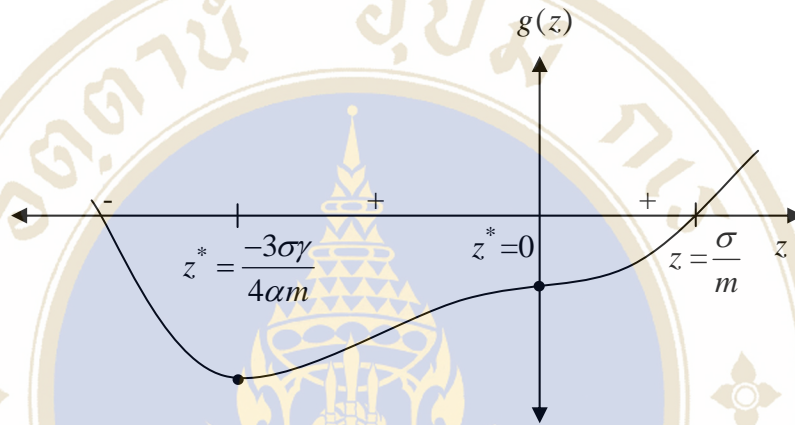


Figure 4.11 Plot of $g(z)$.

From Figure 4.11, there are two zeros of $g(z) = 0$ as well as turning points of $f(y, z)$. However, biological variables and parameters should be positive. Thus $\{z | z \geq 0\}$ is our domain of interest O . Consequently, $z = \frac{\sigma}{m}$ becomes the only turning point of $f(y, z)$ in O . The only stationary point of interest is $(x^*, y^*, z^*) = \left(\frac{1}{\sigma} \left(\frac{\gamma}{(\alpha + \gamma)} - \frac{\phi\sigma}{m}\right), \frac{1}{\alpha + \gamma}, \frac{\sigma}{m}\right)$.

To check $\dot{V}(x^*, y^*, z^*)$ is local maximum, we look at the Hessian matrix at (x^*, y^*, z^*) . The Hessian matrix is a function of y, z only and is

$$H = \begin{bmatrix} \frac{\partial^2 \dot{V}}{\partial y^2} & \frac{\partial^2 \dot{V}}{\partial y \partial z} \\ \frac{\partial^2 \dot{V}}{\partial z \partial y} & \frac{\partial^2 \dot{V}}{\partial z^2} \end{bmatrix}_{(y^*, z^*)} = \begin{bmatrix} -2(\alpha + \gamma)^2 & \frac{m\gamma}{\sigma} \\ \frac{m\gamma}{\sigma} & \frac{-2m^2\gamma}{\sigma^2(\alpha + \gamma)} \end{bmatrix}$$

Consequently, $\det(H)$ is $\frac{\gamma m^2}{\sigma^2}(4\alpha + 3\gamma) > 0$ and $\frac{\partial^2 \dot{V}}{\partial y^2} = -\frac{2}{(\alpha + \gamma)y^3} < 0$. As state above, (y^*, z^*) is the only stationary point in O . Therefore, (y^*, z^*) is global maximum in O . So we can conclude that $\dot{V}(x, y, z)$ is negative definite in O . The Figure 4.12 shows the plot of $\dot{V}(x, y, z)$.

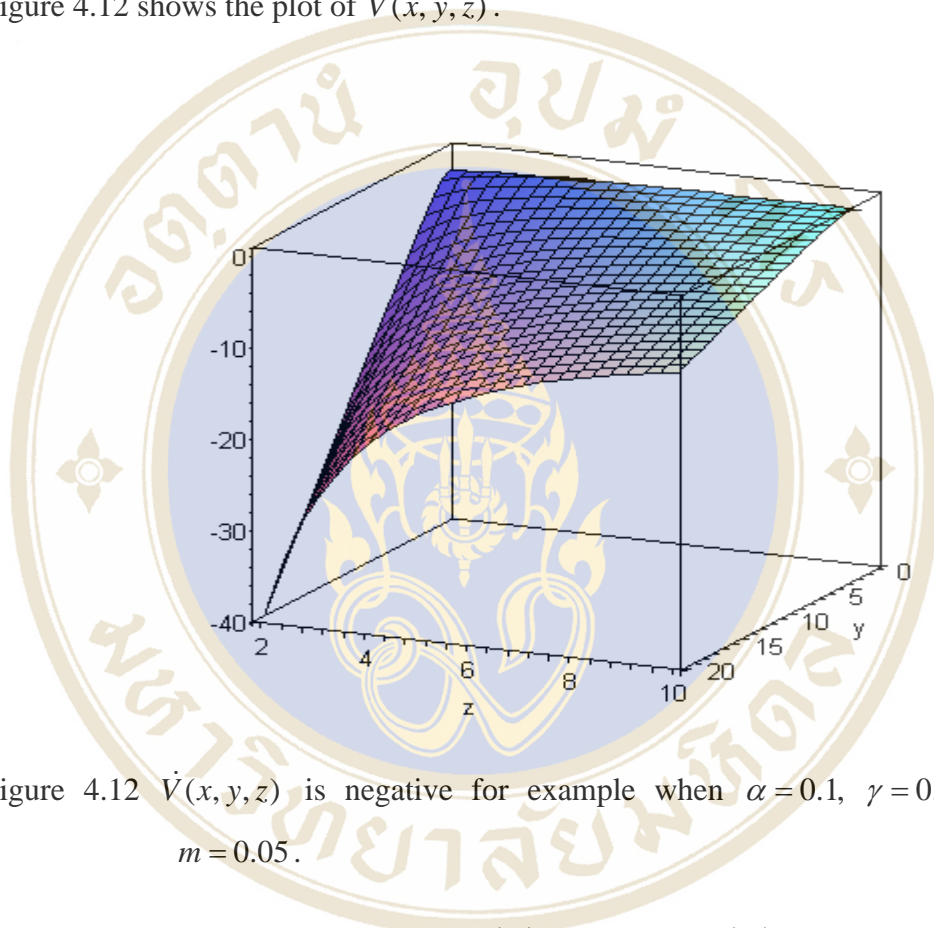


Figure 4.12 $\dot{V}(x, y, z)$ is negative for example when $\alpha = 0.1$, $\gamma = 0.4$, $\sigma = 0.5$, $m = 0.05$.

Therefore, $V(x, y, z) = (x - x^*) + x^* \ln\left(\frac{x}{x^*}\right) + (y - y^*) + y^* \ln\left(\frac{y}{y^*}\right) + (z - z^*) + z^* \ln\left(\frac{z}{z^*}\right)$ is a suitable Liapunov function for model III, showing that the equilibrium point E_2^* is also globally stable.

4.2 Three-Dimensional Model: Monod Uptake Function (Limiting Growth)

All of the previous models fail to show oscillatory behavior in mangrove biomass and TN concentration in wastewater and soil solution. Huang, X. and Zhu, Lemin [17] used a Monod uptake function and a quadratic yield function and proved that a limit cycle existed in their model. Here we have used the Monod function and chosen the simplest possible linear yield function, i.e. $Y(S) = C + DS$. We will show that our model permits the existence of a limit cycle.

We assume that the mangrove biomass growth rate and the TN concentration in soil solution sorption rate are proportional to each other. We write this in differential form as

$$\frac{dT}{dt} = -Y(S) \frac{dS}{dt} . \tag{4.30}$$

The yield function Y is dimensionless, and the minus sign accounts for the fact that an increase in mangrove biomass is related to a decrease in soil TN concentration. Then assuming a linear function for Y we obtain:

$$\frac{dT}{dt} = -(C + DS) \frac{dS}{dt}$$

or

$$\frac{dS}{dt} = -\frac{1}{(C + DS)} \frac{dT}{dt}$$

For the uptake term in the biomass equation we assume that

$$\frac{dT}{dt} = f(S)T \tag{4.31}$$

where the uptake rate function $f(S) = \frac{\beta S}{k + S}$. This function is usually called the Monod model or the Michaelis-Menten model. β is the maximum possible value of uptake $f(S)$ at infinite TN concentration in soil solution and k is called a saturation or Michaelis-Menten constant and it is equal to the value of S for which $\beta(S)$ is one-half its maximum value.

The remaining parameters of the model are the same as those in the system (4.2a-c). Table 4.2 gives the definition, meaning and dimensions of all variables and parameters in the model.

Table 4.2 Definition of variables and parameters for model IV.

Quantity	Symbol	Dimension
Mangrove biomass concentration	T	mg / ha
TN concentration in wastewater	W	mg / ha
TN concentration in soil solution	S	mg / ha
Litter fall rate	σ	$month^{-1}$
TN input rate	Q	$(mg / ha)(month)^{-1}$
TN loss rate in wastewater	α	$month^{-1}$
TN exchange rate between wastewater and soil solution	γ	$month^{-1}$
TN loss rate in soil solution	ϕ	$month^{-1}$

The model with a variable yield coefficient leads to the following set of ordinary differential equations:

$$\frac{dT}{dt} = f(S)T - \sigma T \quad (4.32a)$$

$$\frac{dW}{dt} = Q - (\alpha + \gamma)W \quad (4.32b)$$

$$\frac{dS}{dt} = \gamma W - \frac{1}{C + DS} f(S)T - \phi S. \quad (4.32c)$$

Performing the standard scaling for the system, we let $x = \frac{T}{Q}$, $y = \frac{W}{Q}$, $z = \frac{S}{Q}$, $E = \frac{k}{Q}$.

The equations above can be expressed in dimensionless form:

$$\frac{dx}{dt} = \frac{\beta xz}{(E + z)} - \sigma x \quad (4.33a)$$

$$\frac{dy}{dt} = 1 - (\alpha + \gamma)y \quad (4.33b)$$

$$\frac{dz}{dt} = \gamma y - \frac{1}{C + DQz} \frac{\beta xz}{(E + z)} - \phi z. \quad (4.33c)$$

The region of biological interest is $R_+^3 = \{(x, y, z) | x \geq 0, 0 \leq y \leq 1, z \geq 0\}$.

The Steady State Solution

The steady state solution is

$$\frac{\beta xz}{(E+z)} - \sigma x = 0, \quad (4.34a)$$

$$1 - (\alpha + \gamma)y = 0, \quad (4.34b)$$

$$\gamma y - \frac{1}{C + DQz} \frac{\beta xz}{(E+z)} - \phi z = 0. \quad (4.34c)$$

From equation (4.34a), we obtain either $x_1^* = 0$ or $\frac{\beta z_1^*}{E + z_1^*} = \sigma$, i.e. $z_1^* = \frac{E\sigma}{\beta - \sigma}$.

From equation (4.34b), we obtain $y_{1,2}^* = \frac{1}{\Omega}$, where $\Omega = \alpha + \gamma$.

Then substituting $y_1^* = \frac{1}{\Omega}$ and $x_1^* = 0$ into equation (4.34c), we obtain $z_1^* = \frac{\gamma}{\Omega\phi}$.

Therefore one equilibrium point is $E_1^* = (x_1^*, y_1^*, z_1^*) = (0, \frac{1}{\Omega}, \frac{\gamma}{\Omega\phi})$.

Substituting $z_2^* = \frac{E\sigma}{\beta - \sigma}$ and $y_2^* = \frac{1}{\Omega}$ into equation (4.34c), we obtain

$$x_2^* = \frac{(\gamma - \Omega\phi z_2^*)(C + DQz_2^*)}{\Omega\sigma}.$$

Therefore a second equilibrium point is

$$E_2^* = (x_2^*, y_2^*, z_2^*) = \left(\frac{(\gamma - \Omega\phi z_2^*)(C + DQz_2^*)}{\Omega\sigma}, \frac{1}{\Omega}, \frac{E\sigma}{\beta - \sigma} \right).$$

Therefore there are two steady state solutions or equilibrium points for the system, namely;

1) the washout only mangrove biomass: $E_1^* = (x_1^*, y_1^*, z_1^*) = (0, \frac{1}{\Omega}, \frac{\gamma}{\Omega\phi})$ and

2) the coexistence of mangrove biomass and TN concentration:

$$E_2^* = (x_2^*, y_2^*, z_2^*) = \left(\frac{(\gamma - \Omega\phi z_2^*)(C + DQz_2^*)}{\Omega\sigma}, \frac{1}{\Omega}, \frac{E\sigma}{\beta - \sigma} \right).$$

Lemma 4.7 If the inequalities $\beta > \sigma$ and $\gamma > \Omega\phi z_2^*$ hold

the inequality $\frac{\gamma}{\Omega\phi} > z_2^*$ implies

$$\frac{\gamma}{\Omega\phi} > \frac{E\sigma}{\beta - \sigma}. \quad (4.35)$$

Therefore, the system of equations (4.33a-c) has a non-negative equilibrium $E_2^*(x_2^*, y_2^*, z_2^*)$.

4.2.1 The Local Stability Analysis

The Jacobian matrix of the system (4.33a-c) is

$$\begin{bmatrix} \frac{\beta z^*}{E+z^*} - \sigma & 0 & \frac{\beta E x^*}{(E+z)^2} \\ 0 & -\Omega & 0 \\ \frac{\beta z^*}{(C+DQz^*)(E+z^*)} & \gamma & -\phi - \frac{\beta x^*(CE+DQ(z^*)^2)}{(C+DQz^*)^2(E+z^*)^2} \end{bmatrix} \quad (4.36)$$

The corresponding eigenvalues can be found by solving the following characteristic equation

$$\det(J - \lambda I) = 0. \quad (4.37)$$

Theorem 4.3

The equilibrium point E_1^* is stable if $\frac{\beta\gamma}{E\Omega\phi + \gamma} < \sigma$ and unstable if $\frac{\beta\gamma}{E\Omega\phi + \gamma} > \sigma$.

Proof

The Jacobian matrix at $E_1^* = (x_1^*, y_1^*, z_1^*) = (0, \frac{1}{\Omega}, \frac{\gamma}{\Omega\phi})$

$$\begin{bmatrix} \frac{\beta\gamma}{\Omega\phi} - \sigma - \lambda & 0 & 0 \\ E + \frac{\gamma}{\Omega\phi} & -\Omega - \lambda & 0 \\ \frac{\beta\gamma}{\Omega\phi} & \gamma & -\phi - \lambda \\ (C + \frac{DQ\gamma}{\Omega\phi})(E + \frac{\gamma}{\Omega\phi}) & & \end{bmatrix}. \quad (4.38)$$

Then the characteristic equation is $\left(\frac{\beta\gamma}{E\Omega\phi+\gamma}-\sigma-\lambda\right)(-\Omega-\lambda)(-\phi-\lambda)=0$. (4.39)

Therefore, the eigenvalues are $\lambda_1 = -\Omega, -\phi$ and $\lambda_2 = \frac{\beta\gamma}{E\Omega\phi+\gamma}-\sigma$. Obviously λ_1 is negative. Thus the equilibrium point will be stable if λ_2 is negative, i.e.

$\frac{\beta\gamma}{E\Omega\phi+\gamma} < \sigma$. If $\frac{\beta\gamma}{E\Omega\phi+\gamma} > \sigma$, then the equilibrium point will be unstable.

Theorem 4.4

The equilibrium E_2^* is stable if $\phi + \frac{\beta(\gamma + \Omega\phi z_2^*)(CE - DQz_2^{*2})}{\Omega\sigma(C + DQz_2^*)(E + z_2^*)^2} > 0$ and unstable if $\phi + \frac{\beta(\gamma + \Omega\phi z_2^*)(CE - DQz_2^{*2})}{\Omega\sigma(C + DQz_2^*)(E + z_2^*)^2} < 0$. (4.40)

Proof

The Jacobian Matrix at $E_2^* = (x_2^*, y_2^*, z_2^*) = \left(\frac{(\gamma - \Omega\phi z_2^*)(C + Dz_2^*)}{\Omega\sigma}, \frac{1}{\Omega}, \frac{E\sigma}{\beta - \sigma}\right)$ is

$$\begin{bmatrix} \frac{\beta z_2^*}{E + z_2^*} - \sigma - \lambda & 0 & \frac{\beta E x_2^*}{(E + z_2^*)^2} \\ 0 & -\Omega - \lambda & 0 \\ -\frac{\beta z_2^*}{(C + DQz_2^*)(E + z_2^*)} & \gamma & -\phi - \frac{\beta x_2^* (CE + DQ(z_2^*)^2)}{(C + DQz_2^*)^2 (E + z_2^*)^2} - \lambda \end{bmatrix}. \quad (4.41)$$

The characteristic equation is

$$(-\Omega - \lambda) \left[\lambda^2 + \lambda \left(\phi + \frac{\beta x_2^* (CE - DQz_2^{*2})}{(C + DQz_2^*)^2 (E + z_2^*)^2} \right) + \frac{\beta^2 E x_2^* z_2^*}{(C + DQz_2^*)(E + z_2^*)^3} \right] = 0. \quad (4.42)$$

Therefore, the eigenvalues are $-\Omega$ and $\lambda_{1,2}$ which are roots of

$$\lambda^2 + \lambda \left(\phi + \frac{\beta x_2^* (CE - DQz_2^{*2})}{(C + DQz_2^*)^2 (E + z_2^*)^2} \right) + \frac{\beta^2 E x_2^* z_2^*}{(C + DQz_2^*)(E + z_2^*)^3} = 0. \quad (4.43)$$

If $\phi + \frac{\beta x_2^* (CE - DQz_2^{*2})}{(C + DQz_2^*)^2 (E + z_2^*)^2} > 0$, then the sum of eigenvalues is negative. Now, the

determinant for the two eigenvalues is the constant term in equation (4.43). The determinant is greater than zero, and therefore both eigenvalues must be negative.

Therefore all three of the eigenvalues of the Jacobian J are negative and the equilibrium point E_2^* is stable.

However, if $\phi + \frac{\beta x_2^*(CE - DQz_2^{*2})}{(C + DQz_2^*)^2(E + z_2^*)^2} < 0$, then at least one eigenvalue has a

positive real part and the equilibrium is unstable.

We now look for the range of parameter values for which the equilibrium point E_2^* is stable.

Consider

$$\phi + \frac{\beta x_2^*(CE - DQz_2^{*2})}{(C + DQz_2^*)^2(E + z_2^*)^2} > 0. \quad (4.44)$$

Substituting the value of x_2^* , we obtain $\phi + \frac{\beta \left(\frac{\gamma}{\Omega} - \phi z_2^* \right) (CE - DQz_2^{*2})}{\sigma(C + DQz_2^*)(E + z_2^*)^2} > 0$,

$$\frac{\beta(\gamma - \Omega\phi z_2^*)(CE - DQz_2^{*2})}{\Omega\sigma(C + DQz_2^*)(E + z_2^*)^2} > -\phi,$$

$$\beta(\gamma - \Omega\phi z_2^*)(CE - DQz_2^{*2}) > -\phi\Omega\sigma(C + DQz_2^*)(E + z_2^*)^2,$$

$$\frac{D}{C} < \left(\frac{\beta E(\gamma - \phi\Omega z_2^*) + \phi\sigma\Omega(E + z_2^*)^2}{\beta Qz_2^{*2}(\gamma - \phi\Omega z_2^*) - \phi\sigma\Omega Qz_2^*(E + z_2^*)^2} \right) \quad (4.45)$$

and

$$\beta Qz_2^{*2}(\gamma - \phi\Omega z_2^*) - \phi\sigma\Omega Qz_2^*(E + z_2^*)^2 > 0.$$

The equilibrium $E_2^* = (x_2^*, y_2^*, z_2^*) = \left(\frac{(\gamma - \Omega\phi z_2^*)(C + Dz_2^*)}{\Omega\sigma}, \frac{1}{\Omega}, \frac{E\sigma}{\beta - \sigma} \right)$ is stable.

Theorem 4.5 Let $R = \left(\frac{\beta E(\gamma - \phi\Omega z_2^*) + \phi\sigma\Omega(E + z_2^*)^2}{\beta Qz_2^{*2}(\gamma - \phi\Omega z_2^*) - \phi\sigma\Omega Qz_2^*(E + z_2^*)^2} \right)$. (4.46)

The system (4.33) undergoes a Hopf bifurcation at $\frac{D}{C} = R$.

Proof

Consider at the real part of the eigenvalues of the Jacobian matrix (4.41)

$$\phi + \frac{\beta x_2^*(CE - DQz_2^{*2})}{(C + DQz_2^*)^2(E + z_2^*)} = \phi + \frac{\beta(\gamma - \Omega\phi z_2^*)\left(E - \frac{D}{C}Qz_2^{*2}\right)}{\Omega\sigma(E + z_2^*)^2\left(1 + \frac{D}{C}Qz_2^*\right)}. \quad (4.47)$$

We will not consider for $\frac{\beta^2 Ex_2^* z_2^*}{(C + DQz_2^*)(E + z_2^*)^3}$ because it is positive.

Let $F = \phi + \frac{\beta(\gamma - \Omega\phi z_2^*)\left(E - \frac{D}{C}Qz_2^{*2}\right)}{\Omega\sigma(E + z_2^*)^2\left(1 + \frac{D}{C}Qz_2^*\right)}$ and $\frac{D}{C} = \mu$. Then (4.48)

$$\frac{dF}{d\mu} = -\frac{Q\beta z_2^*(\gamma - \Omega\phi z_2^*)}{\Omega\sigma(E + z_2^*)(1 + \mu Qz_2^*)^2} \neq 0$$

and

$$\frac{dF}{d\mu} = -\frac{Q\beta z_2^*(\gamma - \Omega\phi z_2^*)}{\Omega\sigma(E + z_2^*)(1 + \mu Qz_2^*)^2} \text{ at } \mu = R.$$

We get $\left. \frac{dF}{d\mu} \right|_{\mu=R} = -\frac{[\beta Qz_2^{*2}(\gamma - \Omega\phi z_2^*) - Q\phi\sigma\Omega z_2^*(E + z_2^*)^2]^2}{\beta\sigma Q\Omega z_2^*(E + z_2^*)^3(\gamma - \Omega\phi z_2^*)}$.

The function F is decreasing at $\mu = R$.

Therefore

- 1) The equilibrium point E_2^* is unstable if $\mu > R$.
- 2) The equilibrium point E_2^* is asymptotically stable if $\mu < R$.
- 3) There exists a stable supercritical limit cycle or an unstable subcritical limit cycle depending on the stability of the equilibrium point at $\mu = R$.

Figure 4.13-15 show the result of numerical solution of the dimensionless model equations (4.33a-c) for parameters $\beta = 2, \sigma = 1, E = 1, Q = 1, \Omega = 3, \gamma = 1, \phi = 0.1, C = 0.8, D = 1$, which all solutions of x, y and z tend toward the equilibrium point at

$$E_2^* = (x_2^*, y_2^*, z_2^*) = \left(\frac{(\gamma - \Omega\phi z_2^*)(C + Dz_2^*)}{\Omega\sigma}, \frac{1}{\Omega}, \frac{E\sigma}{\beta - \sigma} \right) = (0.42, 0.33, 1).$$

Figure 4.16-18 show the result of numerical solution of the dimensionless model equations (4.33a-c) for parameters $\beta = 2, \sigma = 1, E = 1, Q = 1, \Omega = 3, \gamma = 1, \phi = 0.1, C = 0.076923077, D = 1$. The value of D/C is approximately equal to R .

Figure 4.19-21 show the result of numerical solution of the dimensionless model equations (4.33a-c) for parameters $\beta = 2$, $\sigma = 1$, $E = 1$, $Q = 1$, $\Omega = 3$, $\gamma = 1$, $\phi = 0.1$, $C = 0.001$, $D = 1$. The value of D/C is greater than R . There exists at least one limit cycle.

The numerical solutions in Figure 4.16-18, 4.19-21 suggest the existence of a stable supercritical limit cycle.



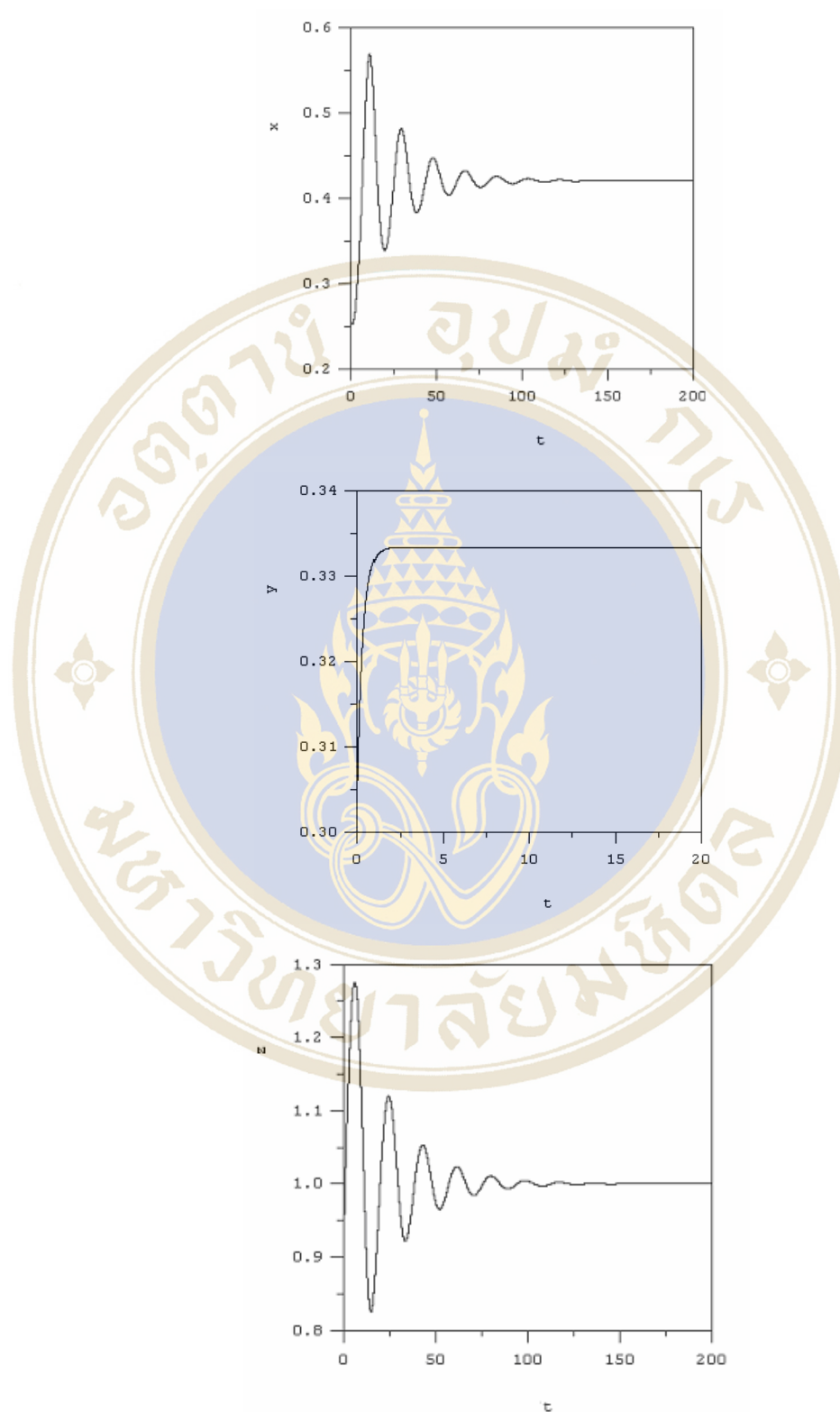


Figure 4.13 Numerical solution of the dimensionless model equations (4.33a-c) for parameters $\beta = 2$, $\sigma = 1$, $E = 1$, $Q = 1$, $\Omega = 3$, $\gamma = 1$, $\phi = 0.1$, $C = 0.8$, $D = 1$.

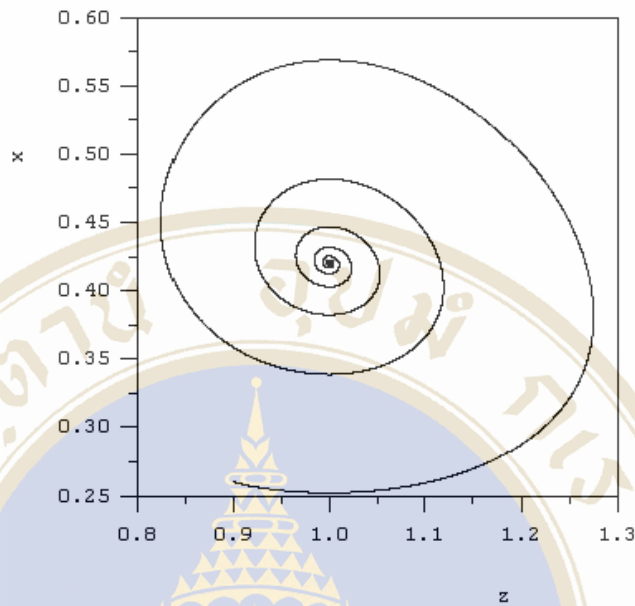


Figure 4.14 Phase plane plot for the solution of the dimensionless model equations (4.33a-c) for parameter $\beta = 2$, $\sigma = 1$, $E = 1$, $Q = 1$, $\Omega = 3$, $\gamma = 1$, $\phi = 0.1$, $C = 0.8$, $D = 1$.

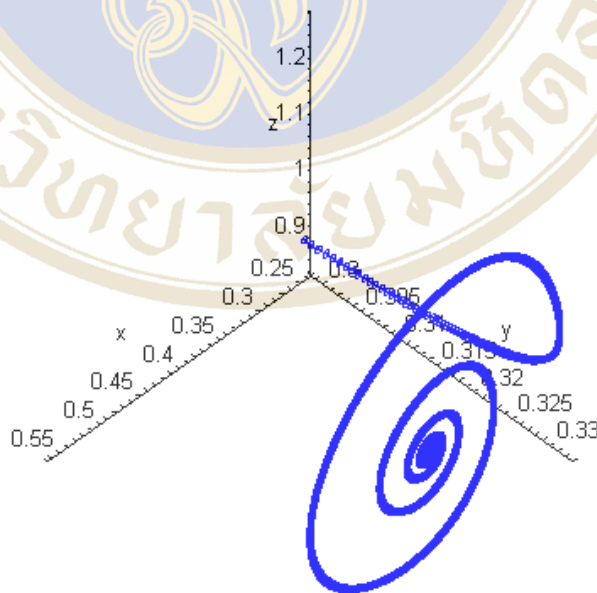


Figure 4.15 Numerical solution of the dimensionless model equations (4.33a-c) in three-dimensions for parameter $\beta = 2$, $\sigma = 1$, $E = 1$, $Q = 1$, $\Omega = 3$, $\gamma = 1$, $\phi = 0.1$, $C = 0.8$, $D = 1$.

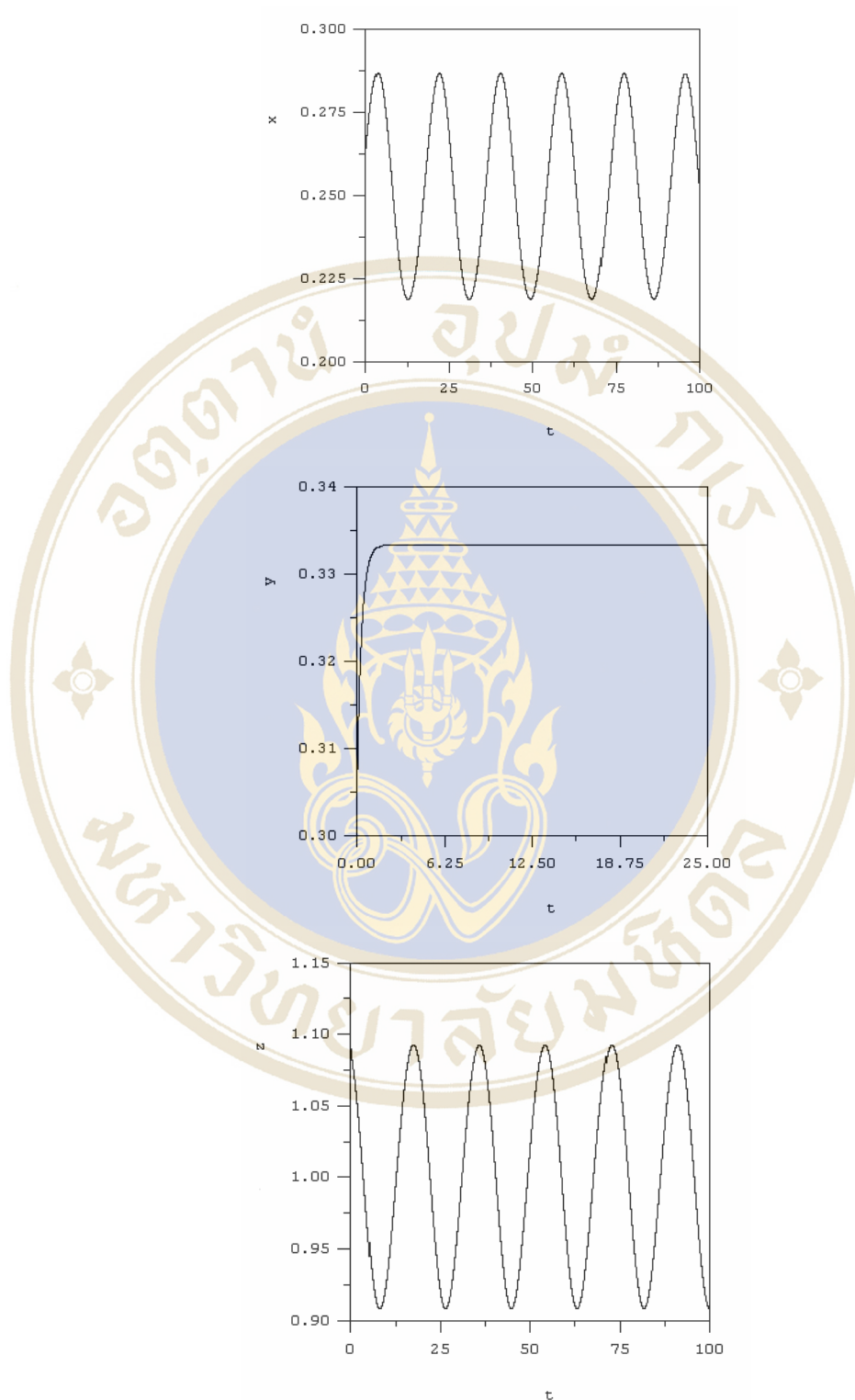


Figure 4.16 Numerical solution of the dimensionless model equations (4.33a-c) for parameters $\beta = 2$, $\sigma = 1$, $E = 1$, $Q = 1$, $\Omega = 3$, $\gamma = 1$, $\phi = 0.1$, $C = 0.076923077$, $D = 1$.

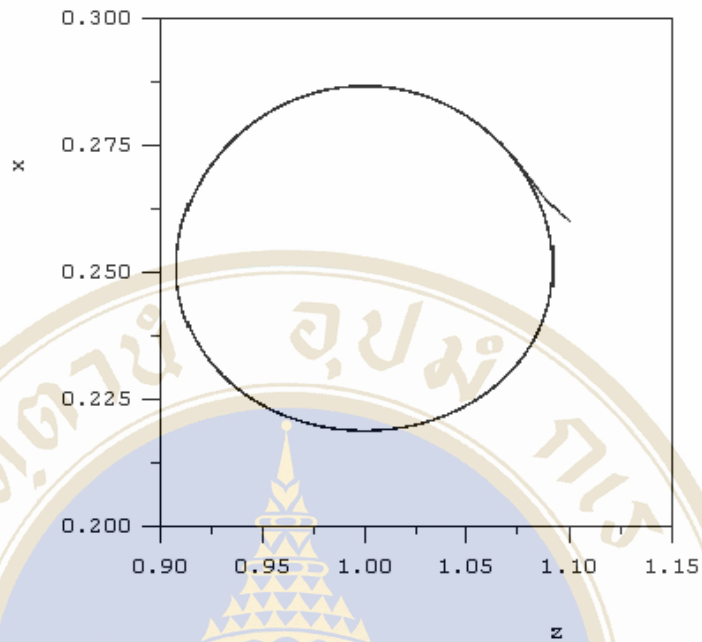


Figure 4.17 Phase plane plot for the solution of the dimensionless model equations (4.33a-c) for parameter are $\beta = 2$, $\sigma = 1$, $E = 1$, $Q = 1$, $\Omega = 3$, $\gamma = 1$, $\phi = 0.1$, $C = 0.076923077$, $D = 1$.

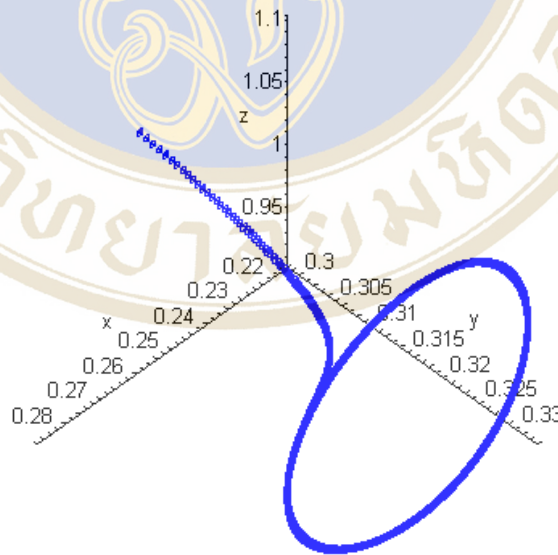


Figure 4.18 Numerical solution of the dimensionless model equations (4.33a-c) in three-dimensions for parameter are $\beta = 2$, $\sigma = 1$, $E = 1$, $Q = 1$, $\Omega = 3$, $\gamma = 1$, $\phi = 0.1$, $C = 0.076923077$, $D = 1$.

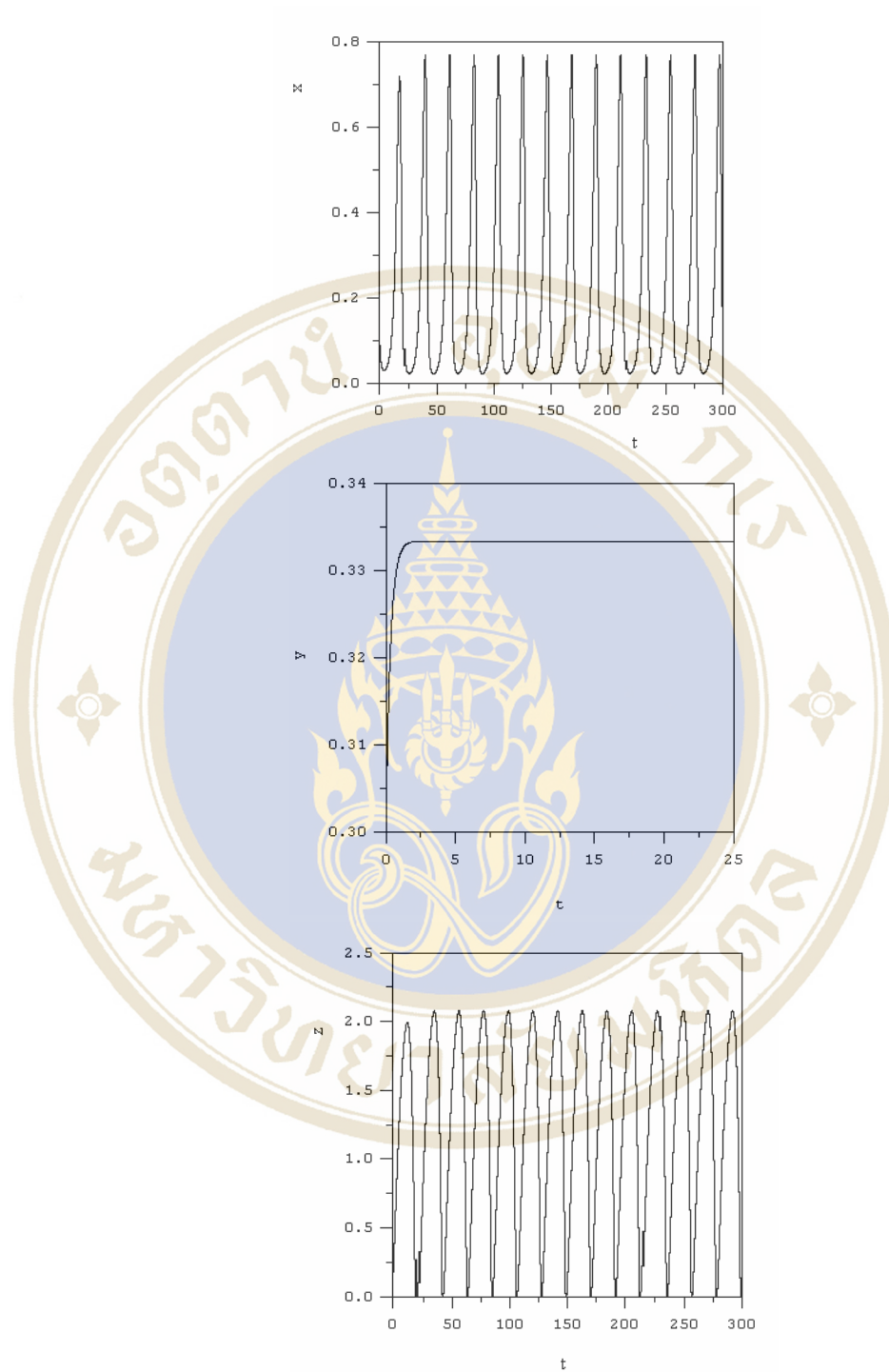


Figure 4.19 Numerical solution of the dimensionless model equations (4.33a-c) for parameters are $\beta=2$, $\sigma=1$, $E=1$, $Q=1$, $\Omega=3$, $\gamma=1$, $\phi=0.1$, $C=0.001$, $D=1$.

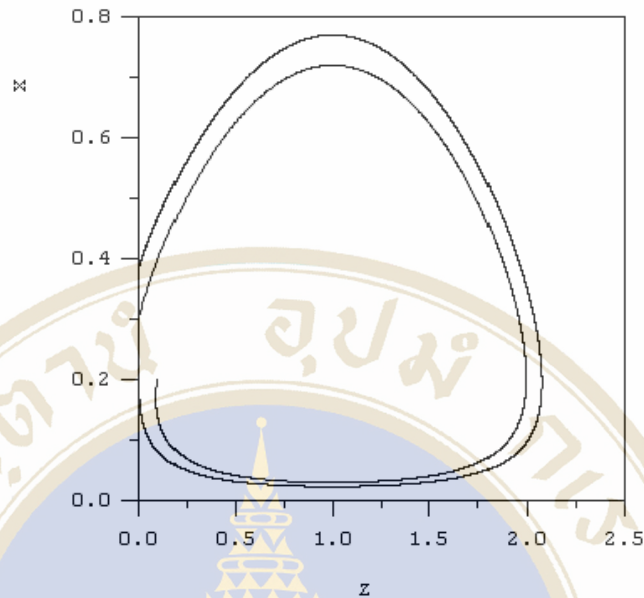


Figure 4.20 Phase plane plot of the dimensionless model equations (4.33a-c) for parameters are $\beta=2$, $\sigma=1$, $E=1$, $Q=1$, $\Omega=3$, $\gamma=1$, $\phi=0.1$, $C=0.001$, $D=1$.

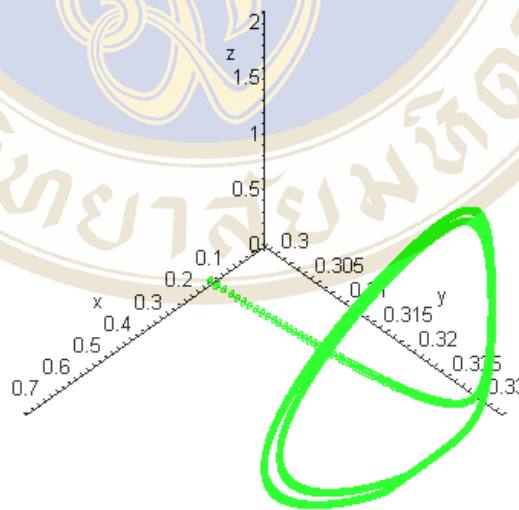


Figure 4.21 Numerical solution of the dimensionless model equations (4.33a-c) in three-dimensions for parameter are $\beta=2$, $\sigma=1$, $E=1$, $Q=1$, $\Omega=3$, $\gamma=1$, $\phi=0.1$, $C=0.001$, $D=1$.

CHAPTER V

CONCLUSIONS AND DISCUSSION

In this thesis we have developed four models for the interaction between mangrove biomass and total nitrogen (TN) concentration in a constructed wetland. The first two of these models are two-dimensional models and the last two are three-dimensional models. The two-dimensional models (models I and II) are discussed in Chapter III and the three-dimensional models (models III and IV) are discussed in Chapter IV.

In the two-dimensional models, the variables are the mangrove biomass concentration and the combined total nitrogen concentration in the TN source. The TN source consists of the TN in the wastewater and the TN in the soil solution. In model I, the wastewater input to the wetland is assumed to be constant while in model II the wastewater input is assumed to be a periodic function of time.

For model I, the existence of steady state solutions is determined and the local and the global stabilities of the steady state solutions are analyzed. There are two possible steady state solutions. One certainly exists, but the other exists only when the ratio of uptake rate m to litter fall rate σ is greater than the TN leaching rate ϕ , i.e. if

$\frac{m}{\sigma} > \phi$. If $\frac{m}{\sigma} < \phi$, only one equilibrium exists in which the mangrove biomass is zero

and the TN is nonzero. This solution is also asymptotically stable for $\frac{m}{\sigma} < \phi$. For

$\frac{m}{\sigma} > \phi$, this first equilibrium solution becomes unstable and a new equilibrium

solution appears in which both the mangrove biomass and the TN are positive. This positive equilibrium solution is asymptotically stable for all values of m, σ, ϕ such that

$\frac{m}{\sigma} > \phi$. We have found that the eigenvalues of the linearized model about the positive

equilibrium point can be either real or complex and that the real parts of the

eigenvalues are always negative. For the real case, trajectories will approach the equilibrium point monotonically, and for the complex case, trajectories will spiral inwards towards the equilibrium point. We have also shown that the positive equilibrium solution is globally stable by constructing a Liapunov function. We have also shown for model I that a limit cycle cannot arise through a Hopf bifurcation from an equilibrium solution. We have also obtained numerical solutions for model I and shown that the types of solutions agree with the results of the linearized analysis.

A biological interpretation of the above results is as follows. Nitrogen is an essential part of amino acids and nucleic acids, both of which are essential to all life. The availability of nitrogen in our constructed wetland depends mainly on the external TN concentration supply on and the TN concentration loss. When the system loses TN too fast, the availability of TN is low. Then each plant is not capable of absorbing the adequate TN. Thus plants die out. After the washout of mangrove, the added nitrogen will partially remain in the source such as in soil pores. However, if the TN loss rate is sufficiently low, the availability of TN increases and leads to mangrove survival. Consequently, the balance between mangrove biomass and TN concentration give a stable positive steady state for the wetland.

Model II is similar to model I except that the TN input to the wetland is taken to be a periodic function rather than a constant. This assumption could be more realistic because mangrove forests are usually in coastal regions where freshwater and sea water are mixed by ocean tides and the amount of freshwater in the river also depends on the seasons. The explicit solution in this case is a periodic solution with the periods given by the daily period of the tides and the annual period of the seasons. We have found that both mangrove biomass concentration and total nitrogen concentration are related and that sustainable behavior is possible.

In Chapter IV, there are two theoretical models using three variables and a yield coefficient. These models describe the relationship between the mangrove biomass concentration and total nitrogen concentration in the source, here, separated into wastewater and soil solutions components. The notion of yield [31] dates from the beginning of continuous bacterial culture, and is for example defined by Monod as the ratio K of the amount of bacterial substance formed per amount of limiting nutrient utilized. He notes that if the growth is expressed as “standard” cell concentration, then

$1/K$ represents the amount of limiting nutrient used in the formation of a “standard” cell. In our studied models, the yield has a slightly different meaning. It is the ratio between the amount of TN concentration in soil solution taken up and the resulting mangrove biomass. Under the assumption of constant yield as in the model III, mathematical model predicts that there can be no sustained oscillations [31]. Since such oscillation has been observed in some experiments [32], it is useful to find model that reproduces these oscillation. The explicit form of the yield function is not yet known exactly [31]. However, we can assume that the yield is a function of the TN concentration in soil solution for model IV. One of the important differences that occur when the yield is not constant is that the variable yield term can lead to uptake and growth terms that have different monotonicity properties. Therefore, careful attention to the interpretation of the yield term is necessary [33] so that it can be correctly placed in the model equations. The different interpretations of yield can lead to different forms for the yield functions and different ways to include the yield terms. Moreover, modeling the yield as a function of nutrient concentration could also provide an indirect way of modeling storage of nutrient.

For model III, we assume that the mangroves can absorb TN only from the soil and that the uptake function from the soil is a linear function of TN concentration in the soil. We find that the solutions for model III are similar to the solutions for model I. As for model III, there are two possible steady state solutions. One always exists but the second one exists only when $\frac{m\gamma}{\alpha + \gamma} > \phi\sigma$. If $\frac{m\gamma}{\alpha + \gamma} < \phi\sigma$ only one equilibrium

exists in which the mangrove biomass is zero and the TN is nonzero. This solution is also asymptotically stable for $\frac{m\gamma}{\alpha + \gamma} < \phi\sigma$. For $\frac{m\gamma}{\alpha + \gamma} > \phi\sigma$ this first equilibrium solution becomes unstable and a new equilibrium solution appears in which both the mangrove biomass and the TN are positive. This positive equilibrium solution is asymptotically stable for all values of m, σ, ϕ such that $\frac{m\gamma}{\alpha + \gamma} > \phi\sigma$. We have found

that the eigenvalues of the linearized model about the positive equilibrium point can be either real or complex and that the real parts of the eigenvalues are always negative. We have also shown that the positive equilibrium solution is globally stable by

constructing a Liapunov function. We have also shown for model III that a limit cycle cannot arise through a Hopf bifurcation from an equilibrium solution. We have also obtained numerical solutions for model III and shown that the types of solutions agree with the results of the linearized analysis.

The biological interpretation of model III is similar to the interpretation for model I. The only significant difference is that the uptake rate m from wastewater and soil of model I is replaced by the uptake rate m from the soil only.

In model IV, we modify model III by including the restriction that a plant will not grow to unlimited size even with abundant nutrients. We model this restriction by using a Monod function for the uptake function from the soil. This means that the mangrove uptake function reaches an upper bound as the TN soil concentration increases. We also include a linear yield function in the model. This term means that as the soil concentration increases the relative contribution of the mangroves to the rate of change of TN in the soil decreases. Again, there are two possible steady state solutions. One certainly exists but another exists only when $\frac{\gamma}{\Omega\phi} > z_2^*$, where γ is TN exchange rate between wastewater to soil solution, Ω is TN loss rate in wastewater and soil solution, ϕ is TN loss rate in soil solution, and z_2^* is the value of TN concentration in soil solution at the equilibrium point. Each steady state solution in model IV has stability properties similar to those in models I and III. As stated for model I, the general criterion for the existence of steady state solutions with nonzero mangrove biomass is that the leaching rate plus nitrogen demands of the mangroves can be equal to the total nitrogen input into the wetland. If this is not possible, then the mangroves cannot exist.

However, an important difference in the behavior of the model IV solution is that a Hopf bifurcation exists and therefore a limit cycle exists in this model. We have found that the bifurcation point depends on the ratio (D/C) , where the yield function is taken as $(C+DS)$, with S the TN concentration in soil solution. If (D/C) is greater than a specific value, the condition for a steady state mangrove biomass requires a decreasing TN soil concentration and the condition for a steady state TN soil concentration requires an increasing mangrove biomass and a limit cycle can occur.

Dicussion

The models discussed in this thesis are an approximation to the real behavior of mangrove forests. Generally, the biomass production not only depends on the TN concentration but also on other factors such as light, acidity (pH), dissolved oxygen (*DO*), etc.

For further study, new systems can be developed in many ways depending on each point of view. For example, after the plant consumes nutrient, it take some time to transform it into biomass. Therefore, a delay model is likely to be more realistic.

For systems in which the rate of changes of variables are different in magnitude (i.e. if the equations are stiff), the numerical solution method used in this thesis is not likely to give accurate solutions and special stiff solvers will be required.

In a real mangrove forest, there is a spatial variation. If these spatial effects were included then the model would have to be a partial differential equation model and the analysis would become extremely complicated. In this thesis we have neglected this spatial dependence and developed models based on ordinary differential equations to describe the time dependence of mangrove biomass and domestic wastewater. Therefore we expect that our model will be more applicable to constructed wetlands in which the spatial variation can be neglected rather than in real mangrove forests.

REFERENCES

1. Saymanopun P. Ability of *Rhizophora mucronata* Lamk. and *Avicennia marina* (Forsk.) Vierh. seeding for municipal sewage treatment in different mangrove soil textures. [M. Sc. Thesis in Environmental Science]. Bangkok: Graduate School, Chulalongkorn Universty ; 2000.
2. Senzia MA, Mashauri DA, and Mayo AW. Suitability of constructed wetlands and waste stabilization ponds in wastewater treatment: nitrogen transformation and removal. *Physics and Chemistry of the Earth* 2003; 28: 1117-1124.
3. MacFarlane GR, Pulkownik A, Burchett MD. Accumulation and distribution of heavy metals in the grey mangrove, *Avicennia marina* (Forsk.)Vierh.: biological indication potential. *Environmental Pollution* 2003; 123: 139-151.
4. Mangrove forests. Available from <http://www.marinebiology.co.uk/mangrove.htm>. [Accessed 10 Sep 2006].
5. Hong PN and San HT. *Mangrove of Vietnam*. Bangkok: Dyna Print; 1993.
6. นพรัตน์ บำรุงรักษ์. การปลูกป่าชายเลน. พิมพ์ครั้งที่ 1. กรุงเทพฯ : โอ.เอส.พรี้นติ้ง เฮ้าส์; 2535.
7. ศโรชา จิรชวรัตน์. โลกของพืช. พิมพ์ครั้งที่ 6. กรุงเทพฯ: สำนักพิมพ์ไทยวัฒนาพานิช จำกัด; 2547.
8. Lewis III Roy R. Ecological engineering for successful management and restoration of mangrove forests. *Ecological Engineering* 2005; 24: 403-408.
9. Campbell NA, Reece JB, Simon EJ. *Essential biology with physiology*. California: Benjamin Cummings; 2004.
10. สุวัฒน์ นิ่มรัตน์. จุลชีววิทยาของน้ำเสีย. พิมพ์ครั้งที่ 1. กรุงเทพฯ: บริษัท แอคทีฟ พรี้นท์จำกัด; 2548.

11. ศรีสม สุวรรณวงศ์. การวิเคราะห์ธาตุอาหารพืช. พิมพ์ครั้งที่ 2. กรุงเทพฯ: สำนักพิมพ์มหาวิทยาลัยเกษตรศาสตร์; 2547.
12. Nitrogen cycle. Available from <http://www.physicalgeography.net/fundamentals/9s.html> [Accessed 10 Sep 2006].
13. Vopel K and Hancock N. Marine ecosystems more than just a crab hole. *Water and Atmosphere* 2005; 13: 18-19.
14. Mangrove. Available from <http://en.wikipedia.org/wiki/Mangrove>. [Accessed 10 Aug 2006].
15. Harrison GW. Global stability of predator-prey interactions, *J. Math. Biology.* 1979; 8: 159-171.
16. Gard TC. A new Liapunov function for the simple chemostat. *Nonlinear Analysis: Real World Applications* 2002; 3: 21-226.
17. Huang X and Zhu L. A three dimensional chemostat with quadratic yield. *J. Math. Chem.* 2005; 38: 575-588.
18. Zhu L and Xuncheng H. Bifurcation in a three dimensional continuous fermentation model. *Int. J. Appl. Sc. Eng.* 2005; 3: 117-123.
19. Bai L and Wang K. A diffusive stage-structured model in a polluted environment. *Nonlinear Analysis: Real World Applications* 2006; 7: 96-108.
20. Hirsch MW. and Smale S. *Differential equations dynamical systems, and linear algebra*, Academic Press, New York, 1974.
21. Plaat O. *Ordinary differential equations*, Holden-Day, Inc, California, 1971.
22. Wiggins, S. *Introduction to applied nonlinear dynamical system system and chaos*, Springer-Verlag, California, 1990.
23. Agarwal RP. and Gupta R C. *Essentials of ordinary differential equations*, McGraw-Hill Book Company, Singapore, 1991.
24. Keshet LE. *Mathematical models in biology*, The Random House, Toronto, 1987.
25. Hyperbolic–nonhyperbolic equilibria. Available from http://www.scholarpedia.org/article/Nonhyperbolic_Equilibrium. [Accessed 4 May 2007].
26. Anton H. *Calculus with analytic geometry*. 4th ed. New York : Wiley; 1992.

27. Kaewmanee C. The effect of cannibalism on a structured predator-prey system. [M. Sc. Thesis in Applied Mathematics]. Bangkok: Faculty of Graduate Studies, Mahidol University; 2001.
28. Hopf bifurcation Available from <http://www.math.rutgers.edu/~sontag/613/hopf-exposition.pdf>. [Accessed 4 May 2007].
29. Mitsch WJ., et al. Reducing nitrogen loading to the Gulf of Mexico from the Mississippi river basin: strategies to counter a persistent ecological problem. *BioScience* 2001; 51: 373-388.
30. Chih YC, *et.al*, Nitrogen nutritional status and fate of applied N in Mangrove soils. *Bot. Bull. Acad. Sin.* 1996; 37: 191-196.
31. Butler GJ and Wolkowicz G.S.K. A mathematical model of the chemostat with a general class of functions describing nutrient uptake. *SIAM J. Appl. Math.*, 1985; 45: 138-151.
32. Hargeby A, Jonzon N and Blindow I. Does a long-term oscillation in nitrogen concentration reflect climate impact on submerged vegetation and vulnerability to state shifts in a shallow lake? *OIKOS*, 2006; 115: 334-348.
33. Arino J, Pilyugin SS. and Wolkowicz GSK. Considerations on yield, nutrient uptake, cellular growth, and competition in chemostat models. *Canadian applied math quarterly*, 2003; 11: 107-142.



APPENDIX

Computer program

Rung-Kutta-Fehlberg's method is used in this thesis. This method is one of the most popular.

```
#include<stdio.h>
#include<conio.h>
#include<math.h>
double F(double T,double X,double Y,double Z,double a,double b,double c,double d);
double G(double T,double X,double Y,double Z,double a,double b,double c,double d);
double L(double T,double X,double Y,double Z,double a,double b,double c,double d);
void main(void)
{ FILE *stream;
  int j,M;
  float A,B,H;
  double X,Y,Z,T,K[6],R[6],Q[6],a,b,c,d;
  clrscr();
  printf("\t\t SYSTEMS OF DIFFERTIAL EQUATIONS\n");
  printf("please follow this direction \n");
  printf("The equation will be from like this\n");
  printf("dx/dt = f(t,x,y)\n");
  printf("dy/dt = g(t,x,y)\n");
  printf("dx/dt = aX+bY\n");
  printf("dy/dt = cX+dY\n");
  printf("Please complete the equations\n");
  printf("Input endpoints or the interval [A,B]\nA:");
  scanf("%f",&A);
  printf("\nB:");
  scanf("%f",&B);
```

```

printf("\nInitial value of X:");
scanf("%lf",&X);
printf("\nInitial value of Y:");
scanf("%lf",&Y);
printf("\nInitial value of Z:");
scanf("%lf",&Z);
printf(" \nNumber of step:");
scanf("%d",&M);
H=0.01;
T=A;
stream = fopen("d:\\candy\\DUMMY.txt", "w+");
for(j=0;j<=M;j++)
{
fprintf(stream, "%lf ,%.7lf ,%.7lf ,%.7lf\n" ,T,X,Y,Z);
printf("T(%d)=%lf,X(%d)=%.7f ,Y(%d)=%.7f
,Z(%d)=%.7f\n",j,T,j,X,j,Y,j,Z);
K[0]=H*F(T,X,Y,Z,a,b,c,d);
R[0]=H*G(T,X,Y,Z,a,b,c,d);
Q[0]=H*L(T,X,Y,Z,a,b,c,d);
K[1]=H*F(T+(H/4),X+(K[0]/4),Y+(R[0]/4),Z+(Q[0]/4),a,b,c,d);
R[1]=H*G(T+(H/4),X+(K[0]/4),Y+(R[0]/4),Z+(Q[0]/4),a,b,c,d);
Q[1]=H*L(T+(H/4),X+(K[0]/4),Y+(R[0]/4),Z+(Q[0]/4),a,b,c,d);

K[2]=H*F(T+(H*3/8),X+(9*K[1]/32)+(3*K[0]/32),Y+(9*R[1]/32)+(3*R[0]/32),Z+
(9*Q[1]/32)+(3*Q[0]/32),a,b,c,d);

R[2]=H*G(T+(H*3/8),X+(9*K[1]/32)+(3*K[0]/32),Y+(9*R[1]/32)+(3*R[0]/32),Z+
(9*Q[1]/32)+(3*Q[0]/32),a,b,c,d);

Q[2]=H*L(T+(H*3/8),X+(9*K[1]/32)+(3*K[0]/32),Y+(9*R[1]/32)+(3*R[0]/32),Z+
(9*Q[1]/32)+(3*Q[0]/32),a,b,c,d);

```

$$\begin{aligned} K[3] &= H * F(T + (12 * H / 13), X + (1932 * K[0] / 2197) - \\ &(7200 * K[1] / 2197) + (7296 * K[2] / 2197), Y + (1932 * R[0] / 2197) - \\ &(7200 * R[1] / 2197) + (7296 * R[2] / 2197), Z + (1932 * Q[0] / 2197) - \\ &(7200 * Q[1] / 2197) + (7296 * Q[2] / 2197), a, b, c, d); \end{aligned}$$

$$\begin{aligned} R[3] &= H * G(T + (12 * H / 13), X + (1932 * K[0] / 2197) - \\ &(7200 * K[1] / 2197) + (7296 * K[2] / 2197), Y + (1932 * R[0] / 2197) - \\ &(7200 * R[1] / 2197) + (7296 * R[2] / 2197), Z + (1932 * Q[0] / 2197) - \\ &(7200 * Q[1] / 2197) + (7296 * Q[2] / 2197), a, b, c, d); \end{aligned}$$

$$\begin{aligned} Q[3] &= H * L(T + (12 * H / 13), X + (1932 * K[0] / 2197) - \\ &(7200 * K[1] / 2197) + (7296 * K[2] / 2197), Y + (1932 * R[0] / 2197) - \\ &(7200 * R[1] / 2197) + (7296 * R[2] / 2197), Z + (1932 * Q[0] / 2197) - \\ &(7200 * Q[1] / 2197) + (7296 * Q[2] / 2197), a, b, c, d); \end{aligned}$$

$$\begin{aligned} K[4] &= H * F(T + H, X + (439 * K[0] / 216) - (8 * K[1]) + (3680 * K[2] / 513) - \\ &(845 * K[3] / 4101), Y + (439 * R[0] / 216) - (8 * R[1]) + (3680 * R[2] / 513) - \\ &(845 * R[3] / 4101), Z + (439 * Q[0] / 216) - (8 * Q[1]) + (3680 * Q[2] / 513) - \\ &(845 * Q[3] / 4101), a, b, c, d); \end{aligned}$$

$$\begin{aligned} R[4] &= H * G(T + H, X + (439 * K[0] / 216) - (8 * K[1]) + (3680 * K[2] / 513) - \\ &(845 * K[3] / 4101), Y + (439 * R[0] / 216) - (8 * R[1]) + (3680 * R[2] / 513) - \\ &(845 * R[3] / 4101), Z + (439 * Q[0] / 216) - (8 * Q[1]) + (3680 * Q[2] / 513) - \\ &(845 * Q[3] / 4101), a, b, c, d); \end{aligned}$$

$$\begin{aligned} Q[4] &= H * L(T + H, X + (439 * K[0] / 216) - (8 * K[1]) + (3680 * K[2] / 513) - \\ &(845 * K[3] / 4101), Y + (439 * R[0] / 216) - (8 * R[1]) + (3680 * R[2] / 513) - \\ &(845 * R[3] / 4101), Z + (439 * Q[0] / 216) - (8 * Q[1]) + (3680 * Q[2] / 513) - \\ &(845 * Q[3] / 4101), a, b, c, d); \end{aligned}$$

$$\begin{aligned} K[5] &= H * F(T + H / 2, X - (8 * K[0] / 27) + 2 * K[1] - \\ &(3544 * K[2] / 2565) + (1859 * K[3] / 4104) - (11 * K[4] / 40), Y - (8 * R[0] / 27) + 2 * R[1] - \\ &(3544 * R[2] / 2565) + (1859 * R[3] / 4104) - (11 * R[4] / 40), Z - (8 * Q[0] / 27) + 2 * Q[1] - \\ &(3544 * Q[2] / 2565) + (1859 * Q[3] / 4104) - (11 * Q[4] / 40), a, b, c, d); \end{aligned}$$

$$\begin{aligned} R[5] &= H * G(T + H / 2, X - (8 * K[0] / 27) + 2 * K[1] - \\ &(3544 * K[2] / 2565) + (1859 * K[3] / 4104) - (11 * K[4] / 40), Y - (8 * R[0] / 27) + 2 * R[1] - \\ &(3544 * R[2] / 2565) + (1859 * R[3] / 4104) - (11 * R[4] / 40), Z - (8 * Q[0] / 27) + 2 * Q[1] - \\ &(3544 * Q[2] / 2565) + (1859 * Q[3] / 4104) - (11 * Q[4] / 40), a, b, c, d); \end{aligned}$$

```

Q[5]=H*L(T+H/2,X-(8*K[0]/27)+2*K[1]-
(3544*K[2]/2565)+(1859*K[3]/4104)-(11*K[4]/40),Y-(8*R[0]/27)+2*R[1]-
(3544*R[2]/2565)+(1859*R[3]/4104)-(11*R[4]/40),Z-(8*Q[0]/27)+2*Q[1]-
(3544*Q[2]/2565)+(1859*Q[3]/4104)-(11*Q[4]/40),a,b,c,d);
X=X+((25*K[0]/216)+(1408*K[2]/2565)+(2197*K[3]/4104)-0.2*K[4]);
Y=Y+((25*R[0]/216)+(1408*R[2]/2565)+(2197*R[3]/4104)-0.2*R[4]);
Z=Z+((25*Q[0]/216)+(1408*Q[2]/2565)+(2197*Q[3]/4104)-0.2*Q[4]);
T=A+H*(j+1);
}
fclose(stream);
getch();
}
double F(double T,double X,double Y,double Z,double a,double b,double c,double d )
{
double f;
f=(2*X*Z)/(1+Z)-X; /*for example*/
return f;
}
double G(double T,double X,double Y,double Z,double a,double b,double c,double d)
{
double g;
g=1-3*Y; /*for example*/
return g;
}
double L(double T,double X,double Y,double Z,double a,double b,double c,double d)
{
double l;
l=Y-(2*X*Z)/((0.8+Z)*(1+Z))-0.1*Z; /*for example*/
return l;
}

```

BIOGRAPHY

NAME	Ms. Wichuta Sae-jie
DATE OF BIRTH	26 December 1981
PLACE OF BIRTH	Songkhla, Thailand
INSTITUTIONS ATTENDED	Prince of Songkla University, Songkhla, 1999-2004: Bachelor of Science (Mathematics) Mahidol University, 2004-2006: Master of Science (Applied Mathematics)
SCHOLARSHIP	A scholarship under the Commission on Higher Education Staff Development Project, Thailand, December 2004-May 2005
HOME ADDRESS	9 Samantapradit Rd. Soi 2, Tambol Piman, Muang, Satun 91000 Thailand
E-MAIL	c_wichuta@hotmail.com